# ON THE ATMOSPHERIC CHEMISTRY OF $NO_2$ - $O_3$ SYSTEMS
## - a laboratory study -

# DE ATMOSFERISCHE CHEMIE VAN $NO_2$ - $O_3$ SYSTEMEN
## - een laboratorium studie -

### (met een samenvatting in het nederlands)

**Pieter Verhees**
**Wageningen**
**1986**

ISN 324231

P.W.C. VERHEES

# ON THE ATMOSPHERIC CHEMISTRY OF NO$_2$ - O$_3$ SYSTEMS
- a laboratory study -

# Proefschrift

## STELLINGEN

1. De bewering van Raes (1985), dat de snelheid van ozon afbraak aan de wand van een glazen reactievat bepaald wordt door diffusie, is onjuist, gezien de metingen van Van de Vate (1977) en die in dit proefschrift.

   Raes, F., 1985, De omzetting van $SO_2$ tot $H_2SO_4$-aerosol door ultraviolet licht en gammastraling, Proefschrift, Rijksuniversiteit Gent, blz. 46-47.

   Van de Vate, J.F., 1977, Verslag van milieu-hygiënisch onderzoek in het tweede halfjaar 1976, ECN-77-008, Petten, blz. 11-13.

   Dit proefschrift.

2. In de door Peters en Carmichael (1982) uitgevoerde modelberekeningen wordt ten onrechte verondersteld, dat de opnamesnelheid van $NO_2$ in wolken beschreven kan worden met de gas diffusiesnelheid van $NO_2$ naar de wolkendruppels.

   Peters, L.K., and Carmichael, G.R., 1982, Modeling of transport and chemical processes that affect regional and global distributions of trace species in the troposphere, In : S.E. Schwarz (Ed.) 'Trace atmospheric constituents', Wiley, New York, pp. 493-538.

3. De suggestie van Finlayson-Pitts (1983), dat de reactie tussen $NO_2$ en NaCl-aerosol bij kan dragen tot nitraatvorming in de atmosfeer, blijkt niet uit haar experimenten.

   Finlayson-Pitts, B.J., 1983, Reaction of $NO_2$ with NaCl and atmospheric implications for NOCl formation, Nature, 306, 676-677.

4. De methode, waarmee Martin et al. (1981) de invloed van $NO_x$ op de oxidatie van $SO_2$ in de waterfase bepalen, is foutief.

   Martin, L.B., Damschen, D.E., and Judeikis, H.S., 1981, The reactions of nitrogen oxides with $SO_2$ in aqueous aerosols, Atmos. Environ., 15, 191-195.

5. Voor een juist begrip van het atmosfeer chemisch gedrag van $N_2O_5$ is het noodzakelijk, dat het verloop van de $N_2O_5$ concentratie gedurende de nacht onder verschillende atmosferische omstandigheden bepaald wordt.

6. De garantie, dat een $NO_x$ monitor met een meetprincipe, gebaseerd op che-
   miluminescentie, probleemloos gebruikt kan worden in situaties met
   wisselende relatieve vochtigheid, is aan twijfel onderhevig. Meestal is
   de door de fabrikant verstrekte handleiding op dit punt ontoereikend
   danwel misleidend.

7. De inadembare fractie van het atmosferische stof wordt vaak ten onrechte
   aangeduid als de gezondheidsrelevante fractie.

   ISO/TR 7708 Air quality - Particle size fraction definitions for health-
   related sampling.

8. Bij de analyse van het zogenaamde 'sick building syndrome' wordt in
   toenemende mate de vervuiling van de binnenlucht gekarakteriseerd. Het
   verdient aanbeveling om daarbij meer aandacht te besteden aan chemische
   omzettingen in de binnenluchtatmosfeer.

9. Europees milieubeleid : 'L'enfer, c'est les Autres'. (Sartre, 1947)

   Sartre, J-P., 1947, "Huis clos', Editions Gallimard, blz. 92.

10. De algemeen verbreide opvatting, dat Albert Einstein een beslissende
    rol speelde in de ontwikkeling van de atoombom, is in strijd met de
    historische feiten.

11. De promovendus mag bij de traditionele bedankronde in zijn proefschrift
    zijn echtgenote of samenwonende partner niet onvermeld laten.

Stellingen, behorende bij het proefschrift :
"On the atmospheric chemistry of $NO_2-O_3$ systems; a laboratory study"
Pieter Verhees, Wageningen, 17 december 1986.

## VOORWOORD

Dit proefschrift is mede tot stand gekomen dankzij de financiële steun van zowel de Stichting Technische Wetenschappen als de vroegere Landelijke Stuurgroep voor Onderzoek in de Milieuhygiëne. Het onderzoek, waarvan dit proefschrift de neerslag vormt, is uitgevoerd aan de Vakgroep Luchthygiëne en -verontreiniging van de Landbouw Hogeschool te Wageningen.

Graag wil ik op deze plaats iedereen bedanken, die aan de totstandkoming van dit proefschrift heeft bijgedragen.

Eep Adema dank ik voor zijn enthousiaste begeleiding. De vrijheid, die hij mij gelaten heeft bij de uitvoering van de experimenten, stel ik zeer op prijs.

Harry ten Brink is voor mij een belangrijke steun geweest. Zijn kritische beoordeling van het proefschrift heb ik als positief ervaren.

De grote groep medewerkers van de Vakgroep Luchthygiëne en -verontreiniging wil ik bedanken. Zij hebben een werksfeer gecreëerd, waarin ik me thuis voelde. Dit geldt in het bijzonder voor mijn onvolprezen collega's en kamergenoten Jurjen Hooghiemstra en Ernest Vrins. De assistentie, gegeven door Wim Braun, Pieter Versloot, Joop Willems en Hillion Wegh, was van groot belang bij de uitvoering van het onderzoek. Reini de Wit ben ik dankbaar voor haar hulp bij de nieuwe start na de brand.

Ton Adang, Marcel Huis in 't Veld, Corry van der Mheen, Aatje Mugie, Anne Spoelstra, Rudy Tuik, Wouter Jan Veenis en Moniek Verbeek hebben als student of HTS-stagiaire delen van het experimentele werk verricht, waarvoor mijn dank.

Anke Kieffer, Tineke Hölscher en Riet Greve hebben van mijn slordig geschreven manuscript dit tekstverwerkt proefschrift gemaakt, waarvoor dank. Peter Attwood confronteerde mijn 'dutch english' met zijn 'native english' : Thanks !

Tenslotte wil ik Dinja, mijn ouders en schoonouders, verdere familie en vrienden bedanken voor hun steun, interesse en vriendschap.

Pieter Verhees
augustus 1986.

# CONTENTS

## GENERAL INTRODUCTION

### 1.1.  AIR POLLUTION AND ATMOSPHERIC CHEMISTRY

Atmospheric chemical processes play an essential role in a great number of air pollution problems, e.g. acid deposition, photochemical air pollution and the increase of the tropospheric ozone concentration at the middle latitudes of the Northern hemisphere caused by the increase of global emissions of CO and $CH_4$.

The general structure of an air pollution problem is schematically presented in Figure 1.
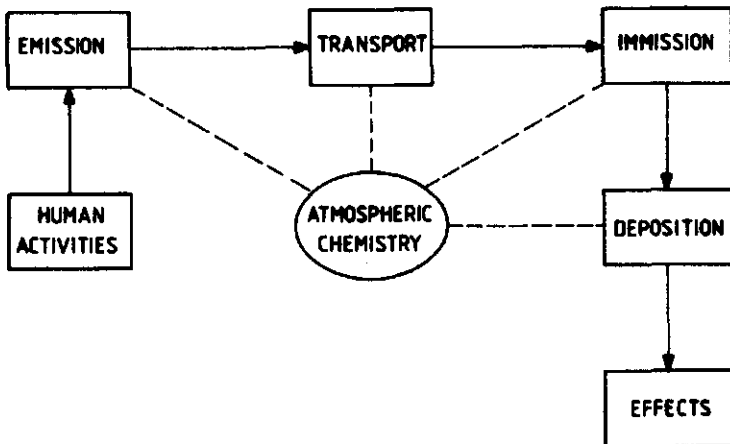
FIGURE 1.     Schematic presentation of an air pollution problem

After their emission, mostly by anthropogenic sources, air pollutants are transported in the atmosphere. During transport the air pollutants are exposed to several physical and chemical processes, e.g. the chemical formation of new atmospheric constituents, the so-called secondary air pollution. Air pollution is removed from the atmosphere by deposition processes, either direct uptake by a receiving environment or deposition via atmospheric precipitation. The final result of all these processes is the immission, which can be considered as the supply of air pollution on effect level, i.e. the distribution pattern of air pollutants in space and time. This pattern varies extensively, since it depends on emission characteristics and meteorological variables. The immission situation and the deposition processes can cause a great number of deleterious effects, thus typifying air pollution as an environmental problem.

Acid deposition is currently one of the most serious environmental problems. The combustion of fossil fuel involves the emission of the acid oxides $SO_2$ and $NO_x$. These species can be converted in sulfuric and nitric acid respectively by gas and aqueous phase chemical reactions. The deposition of all these acid substances cause a great number of effects. Well established is the acidification of many lakes accompanied with their biological exhaustion. The recent forest dieback is believed to be partly caused by either direct acid deposition or indirect via soil acidification. Another alarming effect is the deterioration of materials, e.g. the degradation of centuries old monuments. This is only a brief description of acid deposition, which lacks the detail that can be found in the numerous publications available on this subject. An entry in the scientific literature can be found in Beilke and Elshout (1983), Bubenick et al. (1983), or (in Dutch) Adema and van Ham (1983). A popular description of the problem is given in "Acidification, today and tomorrow" (Swedish Ministry of Agriculture, 1982) or (in Dutch) "Zure Regen" (VROM, 1985).

The photochemical air pollution occurs under certain meteorological circumstances after emission of $NO_x$ and hydrocarbons. A complex system of (photo)chemistry causes an immission characterized by an increased level of the ozone concentration and formation of harmful products such as formaldehyde, peroxyacetyl nitrate (PAN) or organic aerosol particles. This immission situation can cause a number of health effects, damage vegeta-

tion and reduce visibility because of the aerosol formation. The litera-
ture on this subject is recently reviewed by Besemer et al. (1984).

The recent awareness of the increase in ozone concentration at the
middle latitudes of the Northern hemisphere is an air pollution problem in
which atmospheric chemistry plays a key-role. In a $NO_x$ rich environment the
oxidation of atmospheric CO and $CH_4$ leads to the formation of $O_3$. The
emissions of CO and $CH_4$ increase annually, mainly because of activities in
the tropics such as biomass burning (CO) and rice production ($CH_4$). The
increased $O_3$ level may cause health effects. Ozone damages vegatation, thus
its increased concentration level is considered to be one of the causes of
the forest dieback. Recently, a survey on this subject is given by Crutzen
(1985).

As indicated by the above-mentioned examples, air pollution phenomena
are strongly coupled to atmospheric chemistry. The subject of this thesis,
the $NO_2$-$O_3$ system, is particularly important, since it forms an essential
part of any atmospheric chemical system. In recent years it has become
recognized that $NO_2$ and $O_3$ play a pivotal role in air pollution problems,
such as acid deposition and the production of photochemical oxidants. In
order to determine this role, it is necessary to survey the relevant
atmospheric chemical reactions.

## 1.2. A BRIEF INTRODUCTION TO ATMOSPHERIC CHEMISTRY

Atmospheric chemistry is the description of the chemical phenomena of
all the atmospheric constituents. When studying air pollution, the
atmospheric chemistry can be restricted to the description of the chemical
processes that usually take place in the troposphere. In practice, this
involves a study of many photochemical and thermochemical processes, which
can be either homogeneous gas phase reactions or heterogeneous gas-liquid,
gas-solid interactions. Since the ultimate purpose is the description of
the fate of the pollutants from source to sink and a characterization of
the immission situation, a detailed knowledge of the rates and pathways of
these atmospheric chemical processes is necessary.

Generally, there are three ways to investigate the chemistry of the
atmosphere : (1) field experiments, (2) computer modelling and (3) labora-
tory studies. By field studies direct information of the distribution in

space and time of the atmospheric constituents can be obtained. However, this information is only useful when a detailed description of the origins of the measured distribution pattern is available. Since it involves a large number of complex atmospheric processes such a description can only be made by computer simulation. The computer model mostly contains a chemical module, which summarizes the relevant atmospheric chemical reactions. In practice, the chemical module is a mathematic description of the kinetic behaviour of the included chemical species adopting a relevant set of chemical reactions. The proper reaction kinetic parameters are deduced from laboratory studies. These studies are either studies of a specific atmospheric chemical model system or a laboratory simulation of an ambient situation. Clearly, a thorough understanding of the chemistry of the atmosphere can only be obtained if the different methods of investigation are considered together.

### 1.2.1.  The formation and concentration level of oxidants

Generally, the atmosphere can be considered as an oxidizing environment since it contains almost 21 vol.% molecular oxygen. However, oxygen only plays a minor role in atmospheric oxidation. The ubiquitous ozone and its derivate the hydroxyl radical determine the oxidative power of the atmosphere, although their atmospheric concentration is extremely low compared with the concentration of molecular oxygen.

One of the key-species in atmospheric oxidation is the OH radical, which is photochemically formed. Through absorption of solar ultraviolet radiation ($\lambda < 310$ nm) $O_3$ photolizes with the production of an electronically excited oxygen atom $O(^1D)$.

$$O_3 + h\upsilon \rightarrow O_2 + O(^1D) \tag{R1}$$

The $O(^1D)$ usually relaxes to produce the ground state oxygen atom, $O(^3P)$ or reacts with water vapour with the formation of the OH radical.

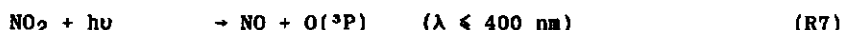$$O(^1D) + H_2O \rightarrow 2 \text{ OH} \tag{R2}$$

Next, the OH radical reacts with CO and $CH_4$ respectively. In the case of CO oxidation, another important free radical $HO_2$ is formed according to :

$$CO + OH \rightarrow CO_2 + H \tag{R3}$$

$$H + O_2 + M \rightarrow HO_2 + M \tag{R4}$$

The $HO_2$ radical reacts with $O_3$ or NO depending on the amount of NO available. If the ratio of the concentrations of NO to $O_3$ is less than $2 \times 10^{-4}$ (Crutzen, 1985) then

$$HO_2 + O_3 \rightarrow 2O_2 + OH \tag{R5}$$

If the ratio exceeds $2 \times 10^{-4}$ :

$$HO_2 + NO \rightarrow NO_2 + OH \tag{R6}$$
$$NO_2 + h\upsilon \rightarrow NO + O(^3P) \quad (\lambda \leqslant 400 \text{ nm}) \tag{R7}$$
$$O_2 + O(^3P) + M \rightarrow O_3 + M \tag{R8}$$

An M stands for any third molecule (e.g. $N_2$, $O_2$) required to make a recombination reaction take place. The net result of the CO oxidation is either an ozone destruction (R3, R4, R5) or an ozone production (R3, R4, R6, R7, R8). The OH radical initially reacts with CO (R3), and then it is regenerated (R5 or R6), indicating that it acts as a catalyst.

The $CH_4$ oxidation is far more complex. Again it is initiated by reaction with OH.

$$CH_4 + OH \rightarrow CH_3 + H_2O \tag{R9}$$
$$CH_3 + O_2 + M \rightarrow CH_3O_2 + M \tag{R10}$$

Subsequent chemical steps lead to the formation of formaldehyde, which can be further oxidized to CO and subsequently $CO_2$. The net result depends on the availability of NO. In environments in which sufficient amounts of NO are present, the oxidation of $CH_4$ to $CO_2$ yields an average net gain of about 3.7 $O_3$ molecules per $CH_4$ oxidised (Crutzen, 1973). In low NO environments oxidation of $CH_4$ to $CO_2$ leads, on the average, to a net loss of about 1.7 $O_3$ molecules.

The chemical pathway has to be extended if sufficient organic species are present. Some other formation routes for the OH radical become important (e.g. photolysis of aldehydes (Calvert and Stockwell, 1983)). Moreover, reaction sequences initiated by reaction of OH with a hydrocarbon take place. Provided sufficient NO is available, the net result of these reaction sequences is given by (R11). Once more, $NO_2$ is formed and the OH radical is conserved.

$$\overset{(O_2)}{\text{hydrocarbon} + OH + 2 NO \rightarrow \text{products} + OH + 2NO_2} \tag{R11}$$

The most important hydrocarbons are alkenes and aromatics. These hydrocarbons are converted into products such as ketones and aldehydes, which themselves are photolized or react with OH. Of special importance is the reaction acetaldehyde to form peroxyacetyl nitrate (PAN) :
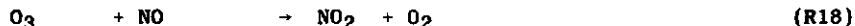
$$CH_3CHO \; + \; OH \qquad \rightarrow \quad H_2O \; + \; CH_3CO \qquad\qquad (R12)$$

$$CH_3CO \; + \; O_2 \qquad \rightarrow \quad CH_3COO_2 \qquad\qquad (R13)$$

$$CH_3COO_2 + NO_2 \qquad \rightarrow \quad CH_3 - C - O - O - NO_2 \qquad (R14)$$
$$\qquad\qquad\qquad\qquad\qquad\qquad\qquad \| $$
$$\qquad\qquad\qquad\qquad\qquad\qquad\qquad O $$
$$\qquad\qquad\qquad\qquad\qquad\qquad (PAN) $$

Several termination reactions are known which result in a loss of OH. Mutual reactions of radicals and reactions of these radicals with the 'odd electron' $NO_x$ (e.g. R14) lead to a large spectrum of organic (nitrogeneous) compounds, although most of these compounds are unstable. The most important termination reactions, resulting in the formation of relative stable watersoluble products, are :

$$HO_2 \qquad + \; HO_2 \qquad \rightarrow \quad H_2O_2 \qquad + \; O_2 \qquad\qquad (R15)$$

$$CH_3O_2 \; + \; HO_2 \qquad \rightarrow \quad CH_3COOH \quad + \; O_2 \qquad\qquad (R16)$$

$$NO_2 \qquad + \; OH + M \quad \rightarrow \quad HNO_3 \qquad + \; M \qquad\qquad (R17)$$

These products are readily removed by precipitation. The PAN formation according to the reaction sequence (R12) to (R14) is an important termination mechanism of both OH and $NO_2$. Another sink for OH radicals may be the heterogeneous process of radical scavenging.

The above-mentioned chemistry disturbs the photochemical equilibrium formed by the reactions :

$$NO_2 \qquad + \; h\upsilon \qquad \rightarrow \quad NO \quad + \; O \; (^3P) \qquad\qquad (R7)$$

$$O(^3P) \quad + \; O_2 + M \quad \rightarrow \quad O_3 \quad + \; M \qquad\qquad (R8)$$

$$O_3 \qquad + \; NO \qquad \rightarrow \quad NO_2 \; + \; O_2 \qquad\qquad (R18)$$

Since NO is converted in $NO_2$ by the CO oxidation and processes as summarized by (R11), less NO is available to react with $O_3$. This disturbance of the photostationary state leads to an increase of the $O_3$ concentration. Especially during episodes of photochemical air pollution the $O_3$ concentration can be extremely high.

It will be obvious that the concentration level of the important oxidant species ($O_3$, $HO_2$, OH) will vary in place and time to a large extent. Due to the photochemistry there will be a pronounced diurnal and seasonal variation. The OH radical concentration ($c_{OH}$) is poorly defined, both by experiment and by model studies. Until now there are no reliable methods of measurement for OH, nor there is sufficient detailed knowledge to calculate the OH concentration. In a recent review Hewitt and Harrison (1985) report a global annual mean of $c_{OH}$ : $(0.5 - 1.0) \times 10^6$ molecule/$cm^3$. In this review both atmospheric measurements and computer simulations are considered. The diurnal variation depends on the actual chemical situation, but a general feature is the absence of OH during the night. Atmospheric measurement shows, that $c_{OH}$ is below the detection limit during the night (e.g. Davis et al., 1982), model studies predict a night-time $c_{OH}$ of zero (Logan et al., 1981). The seasonal variation is also not thoroughly quantified, Hewitt and Harrison (1985) suggest that the summer concentrations are 3 - 4 times higher than those in winter.

The $HO_2$ concentration has been calculated to be two orders of magnitude higher than the OH concentration (Logan et al., 1981; Weinstock et al., 1980). Atmospheric measurements of $c_{HO_2}$ are not available. The diurnal and seasonal variation is likely to be similar to that of OH.

Ozone is present in the troposphere with an average molecular mixing ratio of about 10 to 40 ppb (1 ppb = 1 part per billion = $2.5 \times 10^{10}$ molecule/$cm^3$; at 298 K, 1 atm). In Europe the tropospheric $c_{O_3}$ levels are increasing; in Bavaria, West-Germany, a $c_{O_3}$ increasing rate of 4 % per year has been measured (Attmanspacher et al., 1984). Extreme high $O_3$ concentrations can be observed during episodes of photochemical air pollution: $c_{O_3}$ levels of 200 ppb are not uncommon.

## 1.2.2. Atmospheric $SO_2$ chemistry

The role of the oxidants can be illustrated by the oxidation of $SO_2$, which has received considerable attention. The conversion of $SO_2$ into sulfate is of great importance in atmospheric chemistry, especially in relation to the acid deposition problem. Three different formation routes for atmospheric sulfate can be distinguished : (1) gas phase oxidation, (2) aqueous phase oxidation and (3) heterogeneous oxidation at aerosol surfaces.

The homogeneous gas phase oxidation of $SO_2$ is extensively reviewed by Calvert et al. (1978). The most important is the reaction of $SO_2$ with the OH radical :

$$SO_2 + OH + M \rightarrow HSO_3 + M \tag{R19}$$

The $HSO_3$ radical rapidly reacts with $H_2O$ and $O_2$ to form sulfuric acid. Since (R19) is the rate determining step, the rate of formation of sulfuric acid can be expressed by

$$\frac{dc_{H_2SO_4}}{dt} = k_{19}\, c_{OH}\, c_{SO_2} \tag{1}$$

The value of $k_{19}$ recommended by the most recent CODATA evaluation (Baulch et al., 1982) is $2.5\ 10^{-12}$ cm$^3$ molecule$^{-1}$ s$^{-1}$ in the temperature range 200 –
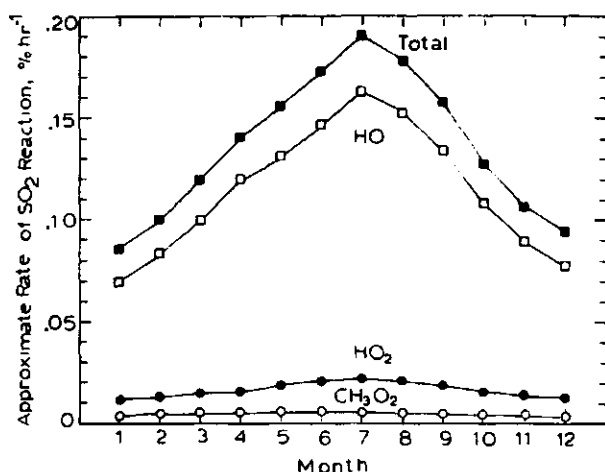


FIGURE 2.    Calculated monthly averaged conversion rate of
$SO_2$ by reaction with OH, $HO_2$ and $CH_3O_2$ respectively
(from: Calvert et al.,1978)

400 K. In the literature the term conversion rate expressed in % per hour is often used. In formula :

$$-\frac{1}{c_{SO_2}} \quad \frac{dc_{SO_2}}{dt} = k_{19} \, c_{OH} \tag{2}$$

This means that the $SO_2$ conversion rates are typical 0.1 - 1.0 %/h; an example of a computer simulation is shown in Figure 2.
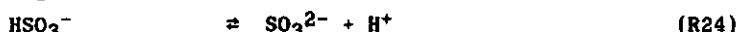
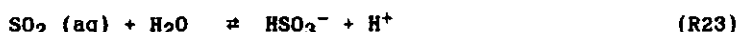Under atmospheric conditions the reactions :

$$SO_2 + HO_2 \rightarrow SO_3 + OH \tag{R20}$$
$$SO_2 + CH_3O_2 \rightarrow SO_3 + CH_3O \tag{R21}$$

and the subsequent rapid conversion of $SO_3$ to $H_2SO_4$ can be significant. However, their conversion rate is much lower than that of the $SO_2$-OH reaction, see Figure 2. Due to its low vapour pressure the gas phase sulfuric acid forms aerosol particles consisting of a concentrated sulfuric acid solution. If $NH_3$ is present, it will neutralize the acid resulting in the formation of $(NH_4)_2SO_4$ aerosol.

The aqueous phase chemistry of $SO_2$ is among others described by Cox and Penkett (1983). $SO_2$ is relatively good soluble in liquid water :

$$SO_2 \ (g) \ \rightleftharpoons \ SO_2 \ (aq) \tag{R22}$$

and then hydrolysis occurs :

$$SO_2 \ (aq) + H_2O \ \rightleftharpoons \ HSO_3^- + H^+ \tag{R23}$$
$$HSO_3^- \ \rightleftharpoons \ SO_3^{2-} + H^+ \tag{R24}$$

Clearly, the overall $SO_2$ solubility will depend on the pH. Next, the rate determining oxidation of the sulfite species lead to the formation of sulfate.

$$SO_3^{2-} \ / \ HSO_3^- \ \xrightarrow{\text{oxidant}} \ SO_4^{2-} \tag{R25}$$
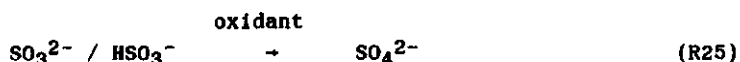
The involved oxidants are $O_2$, $O_3$ and $H_2O_2$. Figure 3 compares the rates of sulfate formation influenced by these species.
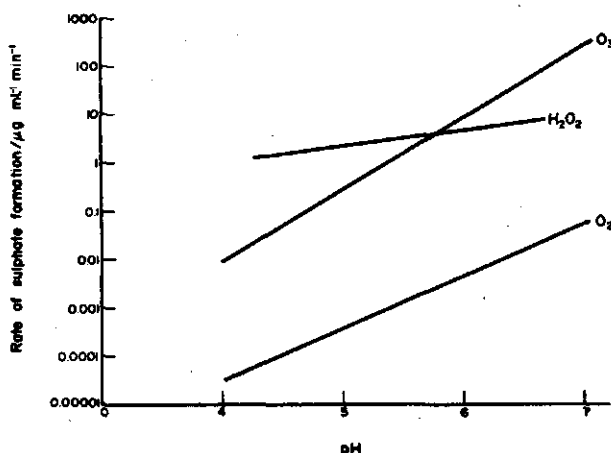
FIGURE 3.　Rate of sulfate formation resulting form aqueous phase $SO_2$ oxidation by $O_2$, $O_3$ and $H_2O_2$. Initial conditions are : $c_{SO_2}$ = 5 ppb, $c_{O_3}$ = 50 ppb, $c_{H_2O_2}$ = 1 ppb and T = 10°C (from : Penkett et al., 1979)

It is shown that the uncatalyzed oxidation by $O_2$ is relatively unimportant. However, this proces may be enhanced significantly by catalytic processes. Well known catalysts are the ionic species $Fe^{3+}$, $Mn^{2+}$ and soot particles suspended in the aqueous phase. The oxidation by $O_3$ is of importance at high pH, whereas oxidation by $H_2O_2$ is only slightly influenced by the pH. The aqueous phase $SO_2$ conversion rate in clouds is significant higher than the gas phase $SO_2$ conversion rate. Beilke (1983) reports that in Europe 40 to 80 % of the sulfate formation is due to aqueous phase processes.

The heterogeneous oxidation of $SO_2$ is not well understood. Novakov et al. (1974) have suggested that the surface of soot particles serves as a catalyst for the oxidation of $SO_2$. However, the question is whether there is sufficient active surface available in the atmosphere.

1.2.3.　Atmospheric $NO_x$ chemistry

The importance of the complex atmospheric chemistry of the nitrogen oxides has been recognized for some time, and subsequently a large number of reviews are available on this subject (e.g. Anderson, 1984; Cox, 1982). It has already been shown that $NO_x$ plays a key-role in the photochemical formation of oxidizing species, likewise the conversion of $NO_x$ into nitrate is a relevant atmospheric process.

The homogeneous gas phase oxidation of $NO_x$ is the most important formation route of nitrate. Two different mechanisms, that operate during the day and night respectively, have to be considered.

In daylight NO and $NO_2$ are part of the reaction sequence that forms the photostationary state (R7, R8, R18). Another pathway that affects the $NO_x$ chemistry is nitric acid generation according to :

$$NO_2 + OH + M \rightarrow HNO_3 + M \qquad \text{(R17).}$$

Baulch et al. (1982) recommend a value for $k_{17}$ of $3.5 \times 10^{-11}$ cm³ molecule⁻¹ s⁻¹ (200 - 300 K). The $NO_2$ conversion rate, given by :

$$- \frac{1}{c_{NO_2}} \frac{dc_{NO_2}}{dt} = k_{17} c_{OH} \qquad (3)$$

is in the order of 2 - 10 %/h. The reaction of $NO_2$ with $HO_2$ plays a minor role since its product ($HO_2NO_2$) is very unstable. This is also the case with the NO - OH reaction, its product ($HNO_2$) photodissociates to regenerate the reactants.

During the night, the $NO_x$ chemistry is totally different. The photochemistry stops and the OH radical concentration drops to zero. Now, reactions with ozone dominate the conversion of $NO_x$. Primarily, NO is rapidly converted to $NO_2$ according to

$$NO + O_3 \rightarrow NO_2 + O_2 \qquad \text{(R18)}$$

The $NO_x$ oxidation proceeds by the $NO_2$-$O_3$ reaction which leads to the formation of the $NO_3$ radical.

$$NO_2 + O_3 \rightarrow NO_3 + O_2 \qquad \text{(R26)}$$

This $NO_3$ radical can react in several ways. For example, the strong reduction of the efficiency of the $NO_2$ - $O_3$ process during daytime is caused by the rapid photolysis of $NO_3$,

$$NO_3 + h\upsilon \rightarrow NO + O_2 \qquad \text{(R27a)}$$
$$\rightarrow NO_2 + O \qquad \text{(R27b)}$$

and the rapid regeneration of $NO_2$ via :

$$NO_3 + NO \rightarrow 2NO_2 \qquad (R28)$$

At night the main removal process for $NO_3$ is the formation of dinitrogen pentoxide

$$NO_2 + NO_3 + M \rightarrow N_2O_5 + M \qquad (R29)$$

This reaction is in rapid equilibrium with the thermal dissociation of $N_2O_5$.

$$N_2O_5 + M \rightarrow NO_3 + NO_2 + M \qquad (R30)$$

The $N_2O_5$ may react with water to form nitric acid.

$$N_2O_5 + H_2O \rightarrow 2HNO_3 \qquad (R31)$$

This reaction is believed to occur quite slowly in the gas phase, but may also occur heterogeneously. The heterogeneous process is generally assumed to be an efficient removal process for $N_2O_5$. The $NO_3$ radical can also react with a number of organic species, especially with aldehydes and olefins (Atkinson et al., 1984). The aldehyde-$NO_3$ reaction probably involves H-atom abstraction and yields a $HNO_3$ molecule.

$$RCHO + NO_3 \rightarrow RCO + HNO_3 \qquad (R32)$$

Neglecting the reactions with organic species, the formation rate of nitric acid at night can be expressed by :

$$\frac{dc_{HNO_3}}{dt} = 2 \, k_{31} \, c_{N_2O_5} \, c_{H_2O} \qquad (4)$$

The $N_2O_5$ concentration can be evaluated assuming that both $NO_3$ and $N_2O_5$ have short characteristic reaction times, so the pseudo-steady-state approximation can be made for these components. In the situation that the raction mechanism is formed by the reactions (R26) and (R28) to (R31), this assumption is plausible for $NO_3$. The reactions (R28) and (R29) are fast in such a manner that the characteristic reaction time of $NO_3$ will probably be short. For $N_2O_5$ this assumption is questionable since no relevant kinetic parameters in order to quantify the atmospheric $N_2O_5$ hydrolysis are currently available. Nevertheless, applying the pseudo-steady-state approximation for both components, one finds:

$$\frac{dc_{HNO_3}}{dt} = \frac{2\ k_{26}\ k_{29}\ k_{31}\ c^2_{NO_2}\ c_{O_3}\ c_{H_2O}}{k_{28}\ c_{NO}\ (k_{31}\ c_{H_2O} + k_{30}) + k_{29}\ k_{31}\ c_{H_2O}\ c_{NO_2}} \tag{5}$$

Relation (5) shows the important role of NO. If the NO concentration is sufficiently low, that the condition :

$$k_{28}\ c_{NO}\ (k_{31}\ c_{H_2O} + k_{30}) \ll k_{29}\ k_{31}\ c_{H_2O}\ c_{NO_2} \tag{6}$$

may be applied, then (5) simplifies to :

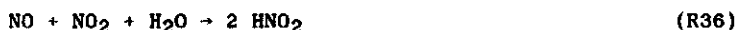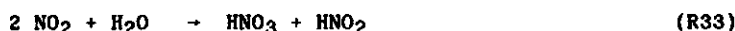$$\frac{dc_{HNO_3}}{dt} = 2\ k_{26}\ c_{NO_2}\ c_{O_3} \tag{7}$$

In this case the rate of nitric acid formation is governed by the rate determining reaction (R26). The $NO_2$ conversion rate can be evaluated as :

$$\frac{dc_{HNO_3}}{dt} = - \frac{dc_{NO_2}}{dt} \tag{8}$$

$$- \frac{1}{c_{NO_2}}\ \frac{dc_{NO_2}}{dt} = 2\ k_{26}\ c_{O_3} \tag{9}$$

Baulch et al. (1982) recommend $k_{26} = 3.2 \times 10^{-17}$ cm$^3$ molecule$^{-1}$ s$^{-1}$ at 298 K for $c_{O_3} = 10 - 40$ ppb the $NO_2$ is converted into $NO_3$ with a rate of 6 - 24 %/h. This means that , in theory, the nighttime $NO_3$-formation rate can be appreciably higher than the rate of the daytime mechanism, which has been estimated to be 2 - 10 %/h.

Some minor pathways for the $NO_x$ chemistry are the reactions :

$$2\ NO_2 + H_2O \rightarrow HNO_3 + HNO_2 \tag{R33}$$

$$HNO_3 + HNO_2 \rightarrow 2NO_2 + H_2O \tag{R34}$$

$$HNO_3 + NO \rightarrow HNO_2 + NO_2 \tag{R35}$$

$$NO + NO_2 + H_2O \rightarrow 2\ HNO_2 \tag{R36}$$

Although most of these reactions are believed to proceed heterogeneously, the current reported rate constants (England and Corcoran, 1974; Kaiser and Wu, 1977; Streit et al., 1979) are too low to indicate an important role

for these processes.

The $HNO_3$ formed can exist as a gas, but, due to its high solubility in water, it easily be incorporated in cloud and rain droplets. Moreover, in the presence of $NH_3$, the $HNO_3$ is partly neutralized by the equilibrium :

$$NH_3 + HNO_3 \rightleftharpoons NH_4NO_3 \qquad\qquad (R37)$$

Because of its low vapour pressure the $NH_4NO_3$ nucleates to form aerosol particles.

Finally, the aqueous formation of nitrate is considered. The following aqueous phase processes are possible :

$$
\begin{array}{lll}
NO \ (g) & \rightleftharpoons \ NO \ (aq) & (R38) \\
NO_2 \ (g) & \rightleftharpoons \ NO_2 \ (aq) & (R39) \\
NO(aq) + NO_2(aq) + H_2O & \rightarrow 2H^+ + 2NO_2^- & (R40) \\
2NO_2(aq) + H_2O & \rightarrow 2H^+ + NO_2^- + NO_3^- & (R41)
\end{array}
$$

The nitrite is not stable, it is oxidized to $NO_3^-$ or reduced to NO. Recently Lee and Schwarz (1981) have reported that these processes are unimportant under atmospheric conditions, because of the low physical solubility of the $NO_x$ species. Beilke (1983) reports $NO_2$ conversion rates of $10^{-4} - 10^{-5}$ %/h. However, the influence of oxidants has not been fully investigated yet and may be of considerable importance.

## 1.3. AIM AND OUTLINE OF THE PRESENT DISSERTATION

In this dissertation the results of laboratory investigations on the $NO_2$ – $O_3$ atmospheric chemistry are reported and discussed.

The importance of studying mutual interaction between $NO_2$ and $O_3$ is evident, since both components pay an essential role in the atmospheric chemistry of a number of air pollution problems. It is therefore necessary to identify and characterize the mechanisms involved in $NO_2$-$O_3$ chemistry. The recent interest in this system has been arisen from its potential as a formation route for atmospheric nitric acid, so it is relevant with respect to the acid deposition problem.

The study of the $NO_2$ – $O_3$ chemistry becomes even more relevant as a consequence of the continuous increase of $NO_x$ emissions and tropospheric $O_3$ concentration respectively. As a result the observed atmospheric nitrate

deposition exhibits a clear upward tendency on both European and North-American continents.

The main object of the present dissertation is to contribute to the fundamental knowledge of the atmospheric chemistry of $NO_2$ - $O_3$ systems. Gaps in this knowledge are generally identified as one of the most important areas of uncertainty of atmospheric chemistry.

More specific the objectives of this study contain the determination of the relevant reaction kinetic parameters at low $NO_2$ and $O_3$ concentrations, and to study the influence of $H_2O$ and aerosol particles. The term aerosol particles must be interpreted widely, it may range from submicron particles to cloud and rain droplets. Therefore both gas phase and aqueous phase processes have been studied.

In chapter 2 a selection of the current available literature with respect to the subject of this thesis is given. The experimental methods applied in this study are summarized in chapter 3.

The results are reported and discussed in the chapters 4, 5, 6, and 7. Chapter 4 describes the stoichiometry and reaction kinetics of the gas phase $NO_2$ - $O_3$ system and studies the influence of temperature and relative humidity. Chapter 5 deals with the dynamic behaviour of submicron aerosol particles in the reaction vessel. In chapter 6 the influence of submicron NaCl and $MgCl_2$ aerosol particles on the processes described in chapter 4 is determined. Chapter 7 is devoted to the aqueous phase chemistry of $NO_2$ and $NO_2/O_3$ mixtures.

A general evaluation is given in chapter 8. We will attempt to establish to what extent these investigations have contributed to the knowledge of the atmospheric chemistry of $NO_2$-$O_3$ systems.

**CURRENT LITERATURE RELATED TO THE ATMOSPHERIC CHEMISTRY OF THE $NO_2$-$O_3$ SYSTEM**

## 2.1. INTRODUCTION

In recent years, much research related to atmospheric chemistry has taken place. It has resulted in a comprehensive range of publications dealing with all aspects of atmospheric chemistry. This is surely the case in respect of the atmospheric oxidation of $NO_2$ to nitrate. In this chapter we pay attention to this part of the current literature with emphasis on the non-photochemical oxidation of $NO_2$ initiated by reaction with $O_3$.

The presentation has been subdivided in four sections. In the first three sections, laboratory, field and model studies are discussed separately. In the last section the current state of our knowledge is evaluated and some research needs are formulated.

## 2.2. LABORATORY STUDIES

**The $NO_2$-$O_3$ reaction**

The reaction sequence describing the non-photochemical oxidation of $NO_2$ is initiated by the reaction :

$$NO_2 + O_3 \rightarrow NO_3 + O_2 \tag{R26}$$

after which the equilibrium :

$$NO_2 + NO_3 + M \rightleftarrows N_2O_5 + M \qquad\qquad (R29)\ (R30)$$

is rapidly reached. The net result of this reaction sequence depends on the reactivity of $NO_3$ and $N_2O_5$.

The kinetics of reaction (R26) has been the subject of a considerable amount of laboratory investigations (Johnston and Yost, 1949; Ford et al., 1957; Wu et al., 1973; Stedman and Niki, 1973; Davis et al., 1974; Huie and Herron, 1974; Graham and Johnston, 1974; Cox and Coker, 1983). The method generally applied involves the measurement of either the decay of $NO_2$ in excess $O_3$ or the $O_3$ decay in excess $NO_2$. The rate constants reported and their temperature dependence agree reasonably well; in the CODATA evaluation (Baulch et al., 1982) the data have been summarized and have lead to a preferred value of :

$$k_{26} = (1.2 \pm 0.5) \times 10^{-13} \cdot \exp(-(2450 \pm 150)/T) \text{ cm}^3 \text{ molecule}^{-1} \text{ s}^{-1}$$

A feature of these laboratory measurements is the lower-than-two reaction stoichiometry as observed in some studies (Wu et al., 1973; Graham and Johnston, 1974; Cox and Coker, 1983). The reaction stoichiometry is defined as the ratio of the amount of $NO_2$ reacted to the amount of $O_3$ reacted. Theoretically a value of two is expected, since at ambient temperatures the forward reaction of the equilibrium (R29, R30) is favoured. Several alternative minor processes have been suggested to account for the low stoichiometry. The well-known side reactions,

$$NO_2 + NO_3 \rightarrow NO + NO_2 + O_2 \qquad\qquad (R42)$$
$$2\ NO_3 \rightarrow 2\ NO_2 + O_2 \qquad\qquad (R43)$$
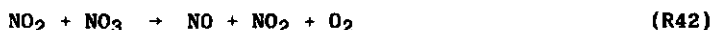
cannot be responsible for the observed stoichiometry, since the reported rate constants (Graham and Johnston, 1978) are much too low to compete with the rapid $N_2O_5$ formation (R29). Wu et al. (1973) have suggested the side reaction :

$$NO_2 + O_3 \rightarrow NO + 2O_2 \qquad\qquad (R44)$$

with extra loss of ozone as it reacts with NO. Graham and Johnston (1974) have tested the mechanisms, in which NO formation is proposed, by looking

for the chemiluminescence of the $NO-O_3$ reaction (R18). Since no chemilumi-
nescent signal has been observed, they conclude from the sensitivity of the
method that only 0.2 % of the $NO_3$ reacts to give NO, so that NO can be
ruled out as an intermediate. However, Graham and Johnston neglect the
rapid non-chemiluminescent reaction, ($k_{28}$ = 2 x $10^{-11}$ $cm^3$ $molecule^{-1}$ $s^{-1}$;
Baulch et al., 1982) :

$$NO + NO_3 \rightarrow 2 NO_2 \hspace{3cm} (R28)$$

Cox and Coker (1983) have shown that taking (R28) into account only 20 % of
the NO will react via the chemiluminescent reaction (R18). This means that
approximately 1 % of the $NO_3$ may react to form NO. This amount is still far
too small to meet the observed stoichiometries. Since the value of 1 %
must be considered as an upper limit, it seems unlikely that NO acts as an
intermediate. Cox and Coker (1983) suggest the formation of the unsym-
metrical ONOO as an intermediate, which subsequently regenerates $NO_2$ by
reaction with $O_3$ or $NO_3$. Another possibility is the $NO_3$ decay to reform
$NO_2$. Graham and Johnston (1978) and Ten Brink et al. (1982) report that
this $NO_3$ decay takes place heterogeneously at the wall of the reaction
vessel.

In conclusion, the reason for the lower-than-two stoichiometry is not
yet fully understood. Yet it is well established that $N_2O_5$ is the only
stable N-containing product in the $NO_2-O_3$ model system, which is supported
by the observation that the $N_2O_5$ yield is one-half the amount of $NO_2$ con-
verted (Wu et al., 1973; Cox and Coker, 1983). And if NO is excluded as an
intermediate, it is likely that a side reaction, in which $NO_2$ is rege-
nerated from $NO_3$ or $N_2O_5$, is operative.

## The $NO_2-NO_3-N_2O_5$ equilibrium

Several laboratory studies concerning the equilibrium formed by the
reactions (R29, R30) have been performed. The equilibrium constant and the
rate constant for the forward and backward reaction have been determined.
The laboratory investigations on the thermal decomposition of $N_2O_5$ (R30) by
Connell and Johnston (1979) and Viggiano et al. (1981) have recently
been reevaluated by a theoretical study of Malko and Troe (1982). They have
deduced the temperature dependence of the high pressure limit of $k_{30}$. The T
dependent relation for $k_{29}$ has been obtained by combining the $k_{30}$ data with

thermodynamic estimates of the equilibrium constant. These data have be[...] adopted by the most recent CODATA evaluation (Baulch et al., 1982), and a[...] listed in Table I. The accuracy is estimated to be about 25 %.

TABLE I.    The preferred values for the high pressure rate constants
            of the equilibrium $NO_2 + NO_3 \rightleftharpoons N_2O_5$

| Parameter | T dependent equation | T range (K) | Value at 298 K |
|---|---|---|---|
| $k_{29}$ (cm$^3$ molecule$^{-1}$ s$^{-1}$) | $1.6 \times 10^{-12}$ $(T/300)^{0.2}$ | 220 - 520 | $1.6 \times 10^{-11}$ |
| $k_{30}$ (s$^{-1}$) | $9.7 \times 10^{14}$ $(T/300)^{0.1}$ $\exp(-11080/T)$ | 220 - 300 | $6.9 \times 10^{-2}$ |
| | $9.7 \times 10^{14}$ $(T/300)^{-0.0}$ $\exp(-11080/T)$ | 300 - 500 | |
| $K_{eq} = k_{30}/k_{29}$ (molecule cm$^{-3}$) | $6.1 \times 10^{26}$ $(T/300)^{-0.1}$ $\exp(-11080/T)$ | 220 - 300 | $4.3 \times 10^{10}$ |

The equilibrium constant given in Table I only slightly differs from t[...] experimental derived value of Graham and Johnston (1978). Recent dire[...] determinations of $K_{eq}$ at 298 K using modern spectroscopic techniques ha[...] confirmed the value given in Table I (Perner et al., 1985) or have lead [...] a smaller value by a factor of approximately 1.5 (Tuazon et al., 1984). T[...] first direct determination of the rate constant of the forward reacti[...] (R29) has been reported by Kircher et al. (1984). They find excelle[...] agreement (within 5 %) with the value listed in Table I. Similar work [...] Burrows et al. (1984) shows analogous results. Table I seems to provide [...] reasonable data set based on both experimental and theoretic[...] considerations.

### The $N_2O_5$ hydrolysis

The hydrolysis of $N_2O_5$ is considered to be the most important sink f[...] $N_2O_5$ at average atmospheric conditions. Nitric acid is formed according to

$$N_2O_5 + H_2O \quad \rightarrow \quad 2HNO_3 \qquad\qquad (R31)$$

In this equation it is left undecided whether the hydrolysis is a homogeneous process or a heterogeneous one.

Laboratory investigations of the kinetics of this reaction show a large variability. The erroneous value of $k_{31}$ of about $10^{-10}$ $cm^3$ $molecule^{-1}$ $s^{-1}$ deduced from the experiment of Jaffe and Ford (1967) has been the earliest gas phase rate constant quoted in the literature. However, the first direct measurements of (R31) carried out by Morris and Niki (1973) have shown that this value is several orders of magnitude too high. Morris and Niki monitored the $N_2O_5$ decay rates at various relative humidities (R.H. 0 - 20 %). Pseudo-first-order decay rates, which were directly proportional to the concentration of water vapour, were observed. The rate constant was found to be independent of the nature of the wall and of the total gas pressure, suggesting a homogeneous gas phase reaction. However, in view of the possible heterogeneity of the reaction, they report the rate constant as an upper limit : $k_{31}$ < $1.3$ $10^{-20}$ $cm^3$ $molecule^{-1}$ $s^{-1}$ (298 K). Smog chamber studies (Carter et al., 1979; Atkinson et al., 1982) showed a significantly lower $k_{31}$ value and even this value was attributed to a heterogeneous reaction at the chamber walls. The recent direct determination of the rate of (R31) by Tuazon et al. (1983) has confirmed this lower value. Tuazon and co-workers measured the $N_2O_5$ decay rates as well as the gas phase $HNO_3$ formation rates as a function of the concentration of water vapour (R.H. 2 - 65 %) in two teflon reaction vessels of different volume. The results clearly indicated that the overall $N_2O_5$ decay involved both homogeneous and heterogeneous components. From the measurements of $HNO_3$ formation a value of $k_{31}$ = $1.3$ $10^{-21}$ $cm^3$ $molecule^{-1}$ $s^{-1}$ was obtained at 298 K. Even this value must be regarded as an upper limit, since the $HNO_3$ may have been revaporized from the wall, as is commonly encountered in teflon vessels (Spicer and Miller, 1976).

From smog chamber studies (Spicer and Miller, 1976; Carter et al., 1979; Atkinson et al., 1982; Grosjean, 1985) and infrared spectroscopic $N_2O_5$ measurements (Ten Brink et al., 1982; Cox and Coker, 1983; Perner et al., 1985) there is ample qualitative proof for a heterogeneous $N_2O_5$ hydrolysis. The quantitative data will be chamber dependent and are difficult to be compared or to be interpret in relation to atmospheric conditions. Under ambient circumstances $N_2O_5$ may react at the surface of 'wet' aerosols. Such $N_2O_5$-aerosol interactions have rarely been studied in the laboratory.

Cox (1974) has found positive evidence for a heterogeneous $N_2O_5$ reaction with deliquescent ammonium sulfate aerosol, but a quantitative treatment of the data is not given. Harker and Straus (1981) measured surface hydrolysis of $N_2O_5$ with sulfuric acid aerosols and found collision efficiencies of $10^{-5}$ to $10^{-4}$.

Clearly, much has to be learned about $N_2O_5$-$H_2O$ interactions in order to establish the fate of $N_2O_5$ in the atmosphere. Where the reaction with water vapour seems of minor importance, the heterogeneous reaction is likely to be a significant sink for $N_2O_5$.

**Other $NO_3$ loss processes**

Alternative loss processes for $NO_3$, other than $N_2O_5$ formation, are regularly studied in the laboratory. $NO_3$ photolysis (R27) has been studied by Magnotta and Johnston (1980) and has been shown to be an important loss mechanism during daylight hours. Another efficient $NO_3$ loss process is the rapid reaction between NO and $NO_3$ (R28), for which a rate constant of $2 \times 10^{-11}$ $cm^3$ $molecule^{-1}$ $s^{-1}$ is reported (Graham and Johnston, 1978). These reactions bring about that the $NO_2$-$O_3$ interaction does not lead to the oxidation of $NO_2$ by day, but only leads to a net loss of $O_3$.

The $NO_3$ radical may also react with organic trace constituents. In the last few years, a large number of rate constants have been determined by laboratory investigations of Atkinson and co-workers (see references in Perner et al., 1985). The effect of these reactions in the atmosphere will be largely dependent on the availability of organic species.

**Aqueous phase reactions**

Another possible non-photochemical formation pathway for nitrates is the liquid phase oxidation of $NO_x$. A large body of laboratory work pertinent to the reactive dissolution of $NO_x$ orginates from the interest of these systems in respect of the industrial manufacture of nitric acid. This work has recently been reviewed and has been tested for its applications under atmospheric conditions by Schwartz and White (1982). Let us restrict ourselves to the uptake of $NO_2$ by liquid water according to :

$$NO_2 \text{ (g)} \quad \rightleftharpoons \quad NO_2 \text{ (aq)} \quad\quad\quad \text{(R39)}$$

$$2NO_2 \text{ (aq)} + H_2O \quad \rightleftharpoons \quad NO_2^- + NO_3^- + 2H^+ \quad\quad\quad \text{(R41)}$$
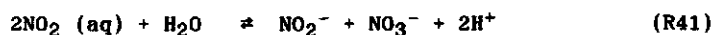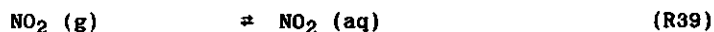
Schwartz and White (1981) have shown that for thermodynamic reasons this process is potentially important. The Henry's constant for the physical dissolution has been evaluated by Schwartz and White (1982) and a value of $(1.0 \pm 0.3) \times 10^{-2}$ M atm$^{-1}$ is recommended. In the same work a preferred value for $k_{41}$ of $(0.7 \pm 0.3) \times 10^{8}$ M$^{-1}$ s$^{-1}$ is given. These values are partly derived from laboratory studies concerning the $NO_2$ uptake at low partial pressure (Lee and Schwartz, 1981a). With the use of these values the rate of uptake of $NO_2$ by atmospheric liquid water can be shown to be too slow and does not lead to any significant nitrate formation (Lee and Schwartz, 1981b). Not much is known about the influence of several ionic species, that may react with $NO_2$(aq) or catalyse the $NO_2$ uptake. Recently, Lee and Schwartz (1983) have investigated the influence of $HSO_3^-$ and have found that reaction of $NO_2$(aq) with $HSO_3^-$ may be a potential pathway for atmospheric nitrate formation. The influence of oxidants on the aqueous phase chemistry of $NO_2$ is not well understood and has rarely been studied. Lee (1984) has shown that $H_2O_2$ reacts only slowly with $NO_2$(aq).


2.3. FIELD STUDIES

Field experiments are essential for atmospheric chemical research. The data obtained from observations in the atmosphere form the basis of atmospheric chemistry. The interpretation of atmospheric observations is difficult and can often be performed in several ways. For example, the frequently observed correlation between the $O_3$ concentration level and nitrate concentrations (e.q. Martin and Barber, 1984; Ayers and Gillet, 1984; Kelly et al., 1984) cannot be regarded as definitive experimental evidence for nitrate formation by the non-photochemical $NO_2-O_3$ reaction since the $O_3$ concentration level also directly relates to photochemical activity.

Therefore, the explanations proposed in this section have to be interpreted with care. The statements given often are hypotheses rather than conclusions. The field studies presented in this section are focussed on the following subjects : direct maesurement of the $NO_3$ radical concentration, some specific nocturnal observations, the diurnal and seasonal variation of atmospheric nitrate and the nitrate formation in clouds and fogs.

## NO$_3$ radical measurements

The measurement of the atmospheric concentrations of NO$_3$ and N$_2$O$_5$ provides direct information about the importance of the reaction sequence initiated by the NO$_2$-O$_3$ reaction. Unfortunately, observations of atmospheric N$_2$O$_5$ are currently not available. NO$_3$ measurements have been recently reported by Noxon and co-workers as well as Platt and co-workers (Noxon et al., 1978; 1980; Platt et al., 1980; 1981; 1982; 1984; 1985). The NO$_3$ concentrations were obtained with a long path UV/VIS absorption technique measuring the two strong absorption bands of NO$_3$ at 623 and 662 nm. In Figure 1 an example of a NO$_3$ night-time profile is shown.
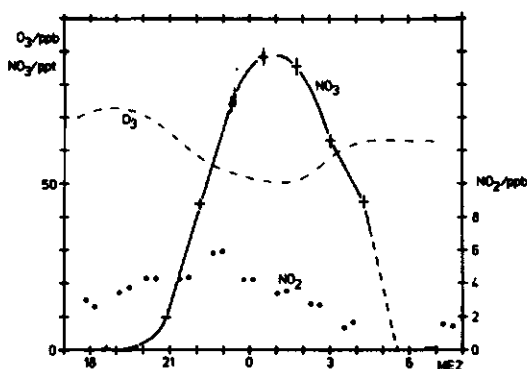


FIGURE 1.    Results of NO$_3$, NO$_2$, O$_3$ measurements in Deuselbach,
West-Germany; R.H. = 50% (from : Platt et al., 1985).

It can be seen from this particular example that NO$_3$ is formed immediately after sunset and gradually increases during the night. Platt and co-workers have measured such night-time profiles on several occasions with different atmospheric circumstances. They were able to obtain much useful information about the NO$_3$ and NO$_2$ reaction scheme. From simultaneous data sets of NO$_3$ and NO$_2$ concentrations, the equilibrium constant of (R29, R30) was found to be 3 times higher than the current recommended literature value (Baulch et al., 1982). In a more recent field study, Perner et al. (1985) deduced values in accordance with the recommended data. The higher values of Platt may have resulted from an inaccurate estimate of the temperature.

From their observations Platt et al. (1984) calculated an average life-

time of $NO_3$ applying a steady-state assumption. This calculated $NO_3$ life-
time is shown as a function of relative humidity in Figure 2.



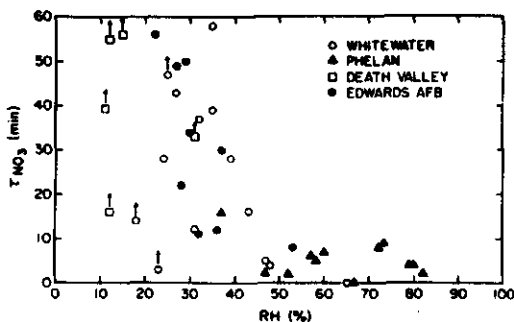FIGURE 2.    Plot of the calculated $NO_3$ lifetime ($\tau$) versus relative
humidity (from: Platt et al., 1984)

Above R.H. 50 % the $NO_3$ lifetime is only in the order of a few minutes or
less. This indicates a rapid loss of $NO_3$ or $N_2O_5$ at relative high R.H. The
loss process is not the homogeneous $N_2O_5$ hydrolysis, for which Platt et al.
(1985) report an upper limit of : $k_{31} < 2 \times 10^{-22}$ $cm^3$ $molecule^{-1}$ $s^{-1}$. The
removal process is very likely to be due to a heterogeneous reaction of
either $N_2O_5$ or $NO_3$ with liquid water. This suggestion is further confirmed
by the quick decrease of $c_{NO_3}$ observed during fog formation. At R.H. < 50 %
the $NO_3$ lifetime is limited to about 1 - 2 hours, which suggests a relati-
vely slow $NO_3$ loss process. This limit is measured in the absence of NO
emissions at moderate $O_3$ concentration, which means that the $NO-NO_3$ reac-
tion (R28) does not seem to be the loss process. The nature of the removal
mechanism is not yet recognized, but it appears that it regenerates $NO_2$.

Recently, Atkinson et al. (1986) have evaluated all the field measure-
ments of the $NO_3$ radical concentrations. The concentration profiles are
explained by assuming either a $NO_3$ loss process or $N_2O_5$ removal. If the $NO_3$
loss process is considered, its first-order rate constant roughly varies
between $\approx 3 \times 10^{-4}$ $s^{-1}$ and $10^{-1}$ $s^{-1}$ unaffected by the temperature. The $N_2O_5$
removal is assumed to occur via the $N_2O_5-H_2O$ reaction and the results are
considered as upper limits of the homogeneous reaction. The upper limits of
$k_{31}$   are found to be a function of the temperature : $k_{31} < 10^{-22}$ $cm^3$

molecule$^{-1}$ s$^{-1}$ at 284 K, increasing to < $10^{-21}$ cm$^3$ molecule$^{-1}$ s$^{-1}$ at 298 K.

Although the details are not yet fully understood, the identification and measurement of $NO_3$ in the atmosphere has confirmed the night-time $NO_x$ conversion as a relevant atmospheric chemical process.

## Nocturnal measurements

Field studies concerning the measurement of the conversion rate of $NO_x$ into nitrate are commonly performed during day-time. Of the few night-time observations the plume study of Forrest et al. (1981) is often cited. Forest et al. (1981) measured combined gas phase and particulate nitrate formation in a coal-fired power plant plume. Some experiments were performed before dawn and the nitrate formation rates ranged from 0.1 - 3 % h$^{-1}$. These rates were averages for the entire time since the plume was emitted. Therefore, the $NO_2$ oxidation rates were probably appreciably larger, since the $NO_2$ oxidation just began after the plume was dilute enough to contain ozone and the NO had been converted into $NO_2$. The slow nitrate formation of about 0.1 % was observed in a plume that was stable enough that NO was not fully converted into $NO_2$ by background ozone. This means there was little opportunity for the night-time oxidation of $NO_2$ to take place. A similar study was performed by Clark et al. (1984), who made measurements of a plume of a coal-fired power plant during its transport over the North Sea. The $NO_x$ concentrations, particulate nitrate and the nitrate content of cloud water were measured close to source on a late afternoon in January. The measurements were repeated the next day early in the morning some 550 km further from the source. An average nitrate formation rate of about 0.5 % h$^{-1}$ was registrated. NO was still present with a maximum of about 50% of the total $NO_x$ at the plume axe. Consequently the $O_3$ concentrations in the plume were very low. Hence a rather low nitrate formation rate may be expected. This observation is a good example of the important role of NO in limiting the nitrate formation during the night.

Martin (1984) determined the washout coefficient for $NO_2$ at day and night by measuring the $NO_2$ concentration before and after a rain event. The night-time coefficient was considerably higher than that of the day-time. Martin (1984) suggested that, because of the low solubility of $NO_2$, $N_2O_5$ washout was registrated. Assuming a fast scavenging of $N_2O_5$ by rain droplets, the apparent $NO_2$ washout rate was governed by the rate of the

$NO_2-O_3$ reaction. Furthermore, it was probable that $N_2O_5$ was read as $NO_2$ by the chemiluminescent analyzer. Qualitative evidence for the $NO_x-NO_3^-$ conversion was found by Ayers et al. (1984), who analyzed the nitrate formation during night-time rain events. Significant amounts of nitrate were observed. Night-time $NO_2$ oxidation was suggested since there was a strong positive correlation between nitrate concentration in rain and the ambient $c_{O_3}$ level.

**Diurnal and seasonal variation of atmospheric nitrate**

The diurnal variation of gaseous nitric acid and/or particulate nitrate has been determined by a large number of investigators (e.g. Appel et al., 1978; 1980; 1981; Van Duuren and Römer, 1982; Shaw Jr. et al., 1982; Forrest et al., 1982; Spicer et al., 1982; Grosjean, 1983; Gailey et al., 1983; Anlauf et al., 1985). Although the profiles are quite variable, there are a number of general features. Gaseous nitric acid commonly exhibits a day-time maximum occurring during the afternoon. This observation reflects the photochemical origin of gaseous $HNO_3$. At night the measured $c_{HNO_3}$ is much lower, but nearly never drops below the detection limit of the various nitric acid measurement methods. Occasionally, an increase of $c_{HNO_3}$ is registrated during the night. Quite different is the diurnal variation of particulate nitrate. In this case the maximum concentrations are observed during the night or early in the morning. An example of a typical diurnal variation is shown in Figure 3.
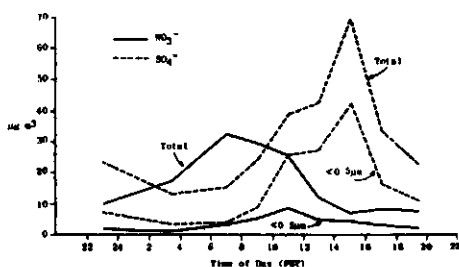


FIGURE 3.   Diurnal variation for particulate nitrate and
            sulfate (from: Appel et al., 1978)

This profile indicates a non-photochemical nitrate formation mechanism that operates during the night. Night-time particulate nitrate peak values are frequently reported under various atmospheric circumstances and at various measuring sites. The differences in the diurnal variation between gaseous and particulate nitrate can be partly explained on the basis of thermodynamic considerations for the formation of ammonium nitrate.

The seasonal variation of gaseous $HNO_3$ subscribes to the diurnal variation. The $HNO_3$ concentrations mostly peak in summer (Okita et al., 1976; Diederen, 1984; Cadle, 1985; Meixner et al., 1985), although some spring maxima are reported (Meszaros and Horvath, 1984; Ferm et al., 1984). The average summer $c_{HNO_3}$ is approximately 2 - 4 times higher than the average winter $c_{HNO_3}$. A seasonal variation of particulate nitrate is not clearly percievable. The absence of a seasonal trend is observed at several locations (Okita et al., 1976; Diederen, 1984; Meixner et al., 1985). However, some studies indicate the occurence of significant maxima which may be found in winter (Van Duuren and Römer, 1982; Meszaros and Horvath, 1984; Willison et al., 1985) as well as in summer (Cadle, 1985) or in spring (Ferm et al., 1983). The same indistinctness is observed in the seasonal variation of nitrate determination in rain water. In the U.S.A. the nitrate content of rain water peaks in winter (Galloway and Likens, 1981), whereas in Europe slight summer maxima (Freyer, 1978; Ridder and Frantzen, 1983) as well as spring maxima (Martin and Barber, 1984; Horvath and Meszaros, 1984) are observed. If we consider the sum of atmospheric nitrate, it appears that the nitrate level is fairly constant throughout the year with a possible maximum during the summer caused by gaseous nitric acid.

In order to interpret these results several season-dependent factors such as emissions, meteorological parameters, atmospheric (photo)chemistry must be considered. It appears that if it is assumed that nitrate is only formed by photochemical processes (i.e. the $NO_2$-OH reaction (R17)) a much more pronounced seasonal variation than generally observed would result. Obviously, there are other nitrate formation pathways that mainly operate during wintertime.

**Nitrate in cloud and fog water**

Nitrate is an important constituent of cloud water (e.g. Kelly et al., 1984; Römer et al., 1985). The nitrate may originate from the scavenging of

gaseous and particulate nitrate by cloud droplets. Moreover, nitrate par-
ticles act as cloud condensation nuclei. Although some studies report that
the nitrate in cloud water results entirely from these processes (Daum et
al., 1984; Marsh, 1983), some recent field measurements suggest nitrate
formation within the cloud (Kelly et al., 1984; Castillo and Jiusto, 1983;
Lazrus et al., 1983; Hegg et al., 1984). Lazrus et al. (1983) estimated the
rate of nitrate production in a precipitating cloud to be about 1 ppb $h^{-1}$
Hegg et al. (1984) report in-cloud scavenging coefficients for nitrate > 1
and suggest that nitrate may be formed by dissolution of N(V)-compounds
other than $HNO_3$ or that nitrate can be produced within cloud droplets.

Since photochemical formation of nitrate in a situation of reduced
insolation, such as within a cloud, is unlikely, the conversion of $NO_2$ into
$N_2O_5$ in the interstitial air and the subsequent absorption of $N_2O_5$ in the
cloud droplets may contribute to the in-cloud nitrate production. Likewise,
liquid water oxidation of $NO_x$ promoted by oxidants or catalysts may be a
possibility.

Similar considerations can be made concerning fog studies. In fog water
nitrate is observed as one of the dominant ionic species (Waldman et al.,
1982; 1983; Brewer et al., 1983; Jacob et al., 1985; Georgii and Schmitt,
1985). An increase of the nitrate concentration as a function of time is
regularly observed, especially during night-time fog events. Occasionally,
extreme high nitrate concentrations are found in nocturnal fog occurring in
winter in an urban area (Waldman et al., 1982). The above-mentioned results
again suggest nitrate formation by the $NO_2$-$O_3$ reaction system. However, it
must be realized that most fog events were analysed during the winter
months under stagnant meteorological conditions, with which fogs are often
formed. Because of the suppressed vertical mixing the $NO_x$ concentrations
may be extremely high in an urban area. This implies that the efficiency of
nitrate formation via the $NO_2$-$O_3$ reaction is strongly reduced, since the
$c_{O_3}$ level will be low and the $NO_3$ radical formed will be rapidly destroyed
by reaction with NO. Therefore, significant nitrate formation may origi-
nate from aqueous phase processes which are much more effective at these
high $NO_x$ concentrations.

## 2.4. MODEL STUDIES

The confrontation between laboratory results and field measurements can only be realized by model studies. In a model the emissions, meteorology, deposition processes and atmospheric chemistry are parameterized and their mutual relations are mathematically described. Although the theoretical formulations embody some degree of approximation and a variety of assumptions must be used, models can be considered as useful diagnostic tools for exploring atmospheric processes. In practice, there are models in many forms and for many purposes. Some of the model studies focus on the atmospheric chemical aspects. From these studies a selection is presented in this section, with emphasis on the $NO_2-O_3$ interactions.

### Homogeneous chemistry

Calvert and Stockwell (1983) report computer simulations of the acid generation in the troposphere by gas phase chemistry using a realistic che-
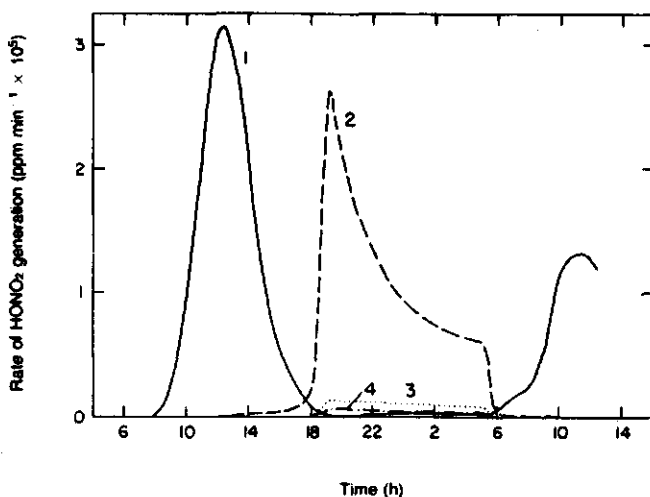


Time (h)

FIGURE 4.    Theoretical rates of $HNO_3$ generation from various reaction
            pathways for moderately polluted air masses with (1) $NO_2$-OH
            reaction, (2) $N_2O_5$-$H_2O$ reaction, (3) $CH_2O$-$NO_3$ reaction and
            (4) $CH_3CHO$-$NO_3$ reaction (from: Calvert and Stockwell, 1983)

mical reaction scheme based upon the current knowledge. The meteorology has been restricted to typical summer conditions, whereas transport and deposition have not been treated. Therefore, the results have to be seen as the maximum potential for acid generation. The results are presented as time profiles of the rate of acid generation. The degree of contamination has been considered by varying the initial conditions and the emission rates of the pollutants. An example of a result is given in Figure 4.

The $N_2O_5-H_2O$ reaction has been considered as a homogeneous gas phase reac on with a rate constant of $3 \times 10^{-21}$ cm$^3$ molecule$^{-1}$ s$^{-1}$ at R.H. 50 %. Under these conditions the rate of $HNO_3$ production during the night is comparable with the day-time rate. Similar profiles are presented as a function of contamination level. In most cases the nocturnal $NO_2$ conversions rate is calculated in the order of 10 – 30 %/h. However, in situations with extreme high $O_3$ levels the $NO_2$ conversions rate at night is as high as 80 %/h, whereas in the case of large NO emission nocturnal $NO_2$ conversion is ineffective.

Russell et al. (1985) have also studied the gas phase $HNO_3$ generation, applying a trajectory model, which includes an up-to-date detailed chemical reaction scheme. The fate of $NO_x$ emissions along a 24-h trajectory across the Los Angeles basin has been computed using the proper meteorology and including deposition processes. The total nitric acid produced by the various reactions is shown in Table II. Note that the reaction numbering deviates from the numbering in this work.

TABLE II. Percentage of total nitric acid production by each reaction along a 24-h trajectory (from: Russell et al., 1985)

| Reaction step producing HNO$_3$ | Base case (%) | $k_{46}$ decreased by 10x (%) | $k_{46}$ of Morris and Niki (%) | $k_{46} = 0$ (%) | Aerosol scavenging | | |
|---|---|---|---|---|---|---|---|
| | | | | | ($\alpha = 0.001$) (%) | ($\alpha = 0.1$) (%) | ($\alpha = 1.0$) (%) |
| NO$_2$ + OH (18) | 44 | 53 | 36 | 56 | 44 | 37 | 29 |
| N$_2$O$_5$ + H$_2$O(g) (46) | 24 | 6 | 44 | 0 | 22 | 5 | tr* |
| NO$_3$ + HCHO (53) | 4 | 7 | 2 | 7 | 4 | 1 | tr |
| NO$_3$ + RCHO (54) | 28 | 34 | 18 | 37 | 28 | 11 | 4 |
| N$_2$O$_5$ + Aerosol | | | | | | 2 | 46 | 67 |
| Percentage of base case nitric acid produced | 100% | 97 | 117 | 93 | 101 | 114 | 124 |

* tr, trace amount, less than 1%.

In the base case the rate constant of the $N_2O_5-H_2O$ reaction given by Tuazon et al. (1983) has been used. The results demonstrate a non-linear rela-

tionship between the rate constant of the $N_2O_5$ hydrolysis and the amount of
nitric acid produced by this reaction. Furthermore, it can be seen that the
total production of $HNO_3$ is not greatly affected by perturbing the rate
constant of the $N_2O_5$ hydrolysis, which appears to lead to a redistribution
of the amount of nitric acid produced by each reaction.

Another result of the model study by Russell et al. (1985) is the ver-
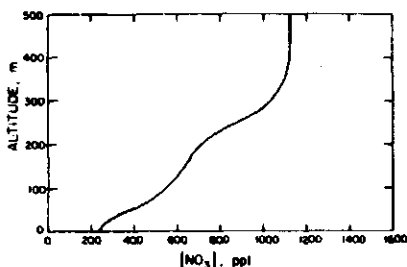tical distribution of the $NO_3$ radical as shown in Figure 5



FIGURE 5.   An example of a predicted vertical $NO_3$
            concentration profile (from: Russell et al., 1985)

The very pronounced vertical $NO_3$ concentration profile shows the important
role of NO, which is emitted at ground level. Figure 5 also indicates the
potential importance of night-time nitric acid production aloft, where $NO_3$
and $N_2O_5$ concentrations are predicted to be much greater than those
observed at ground level.

Heterogeneous chemistry

Up to now only homogeneous gas phase reactions have been considered,
whereas heterogeneous reactions are also significant in $NO_x$ atmospheric
chemistry. Unfortunately, the rates of these reactions are unknown, and
have to be estimated. This estimation can be performed by calculating the
collision rate of the gas molecules with the aerosol surface. The actual
reaction rate is determined by assuming a value for the collision effi-
ciency, which is mostly denoted by $\alpha$. Sometimes the terms 'accomodation

coefficient' or 'sticking coefficient' are used instead of collision efficiency. The reaction rate also depends on the total available aerosol surface area, which is determined by the aerosol size distribution function.

Russell et al. (1985) have used this method, applying a typical aerosol distribution as measured by Whitby et al. (1972) and assuming that the nitric acid formed is reentered in the gas phase. The results are shown in Table II. With the use of $\alpha = 10^{-3}$ the situation only slightly differs from the homogeneous base case. The heterogeneous reactions are important at high collision efficiencies ($\alpha > 0.01$), and may lead to a significant increase in the total nitric acid production.

Heikes and Thompson (1983) have computed the effect of heterogeneous processes on nitrate formation in clouds, applying an empirical cloud droplet distribution. The results show that under atmospheric day-time conditions the heterogeneous $N_2O_5$ hydrolysis can account for considerable nitrate formation within a cloud if $\alpha$ is greater than 0.01. At night nitrate formation is already significant at $\alpha = 10^{-3}$. Similar model studies have been performed by Seigneur and Saxena (1984) using the heterogeneous $N_2O_5$ hydrolysis rate of Harker and Strauss (1981) (i.e. $\alpha = 10^{-4}$) and a monosize cloud droplet distribution. They conclude that 80 % of the nitrate is formed via $N_2O_5$. The potential importance of nocturnal nitrate formation in a power plant plume by heterogeneous $N_2O_5$ hydrolysis is clearly demonstrated in a model investigation of Sverdrup and Hov (1984) with the use of typical in-plume aerosol loadings and a collision efficiency of 0.01.

Chameides and Davis (1983) have suggested that the scavenging of $NO_3$ radicals in cloud droplets followed by nitrate formation is an important heterogeneous mechanism. Because of the $NO_3$-$N_2O_5$ equilibrium, the above-mentioned considerations may also be applied for heterogeneous $NO_3$ reaction with the restriction that only half the amount of nitrate is formed and provided that the heterogeneous $N_2O_5$ hydrolysis is neglected. However, if $NO_3$ and $N_2O_5$ scavenging are considered together with an equivalent collision efficiency then the $NO_3$ reaction is relatively unimportant, since in the ambient situation $N_2O_5$ is favoured by the $NO_3$-$N_2O_5$ equilibrium. Seigneur and Saxena (1984) have shown that $NO_3$ scavenging is an effective pathway for nitrate formation, if its $\alpha$-value exceeds that of $N_2O_5$ scavenging by at least three orders of magnitude.

Several authors have tried to simulate the $NO_3$ profile measured by Platt et al. (1980) at September 12, 1979 (Heikes and Thompson, 1983; Jones and Seinfeld, 1983; Stockwell and Calvert, 1983; Russell et al., 1985). The computer simulations are in accordance with Platt's measurements provided some kind of assumption is made. These assumptions are either a constant source of NO or heterogeneous $NO_3$ and $N_2O_5$ scavenging. However, the simulations do not predict the correct $NO_2$ and $O_3$ profile as measured by Platt. It seems that additional reaction pathways yet unknown need to be incorporated in the models.

**Aqueous phase chemistry**

In some model studies aqueous phase reactions of $NO_x$ have been included, but it is found that these reactions do not significantly contribute to nitrate formation (Heikes and Thompson, 1983; Seigneur and Saxena, 1984). The kinetic parameters used are those from the measurements of Lee and Schwartz (1981a,b). For the aqueous $NO_2$ auto-oxidation of 1 ppb $NO_2$ in a cloud with a liquid water content of 1 $g/m^3$, the $NO_2$ conversion rate can be calculated to be as low as $4 \times 10^{-6}$ %/h. However, it must be realized that the kinetic parameters were obtained in pure liquid water. The possibility that alternative reaction pathways in atmospheric water may enhance the $NO_2$ uptake, is not yet inquired.

At high $NO_x$ levels the rate of aqueous $NO_x$ uptake becomes appreciable, because of its quadratic dependence on $NO_x$ partial pressures. In a recent model study Kasting and Ackerman (1985) point out that above 100 ppb $NO_x$ direct dissolution of $NO_x$ is an important $NO_x$ removal process, especially since $HNO_3$ formation by gas phase processes is inhibited. Such a situation may occur in urban fog.

## 2.5. EVALUATION

A fragmentary literature survey of the non-photochemical nitrate formation has been presented in this section. The different methods, that may be employed to investigate atmospheric chemistry, notably : laboratory, field and model studies, have been considered. Each of these approaches has its individual strengths and weaknesses. Together they form the foundation of our understanding of atmospheric chemistry.

With respect to the atmospheric $NO_2-O_3$ chemistry there is ample evidence that it plays a dominant role in atmospheric $NO_x$ chemistry and is one of the major pathways for nitrate formation. In order to quantify this process more detailed information needs to be obtained from further research. Laboratory studies, that establish the fate of the $NO_3$ radical and $N_2O_5$ molecule, need to be performed. Of special concern is the role of water vapour and aqueous aerosols. More field studies, that investigate the night-time $NO_x$ chemistry, are necessary, especially data of the ambient concentrations of $N_2O_5$ are needed.

Quite different is the situation with respect to the aqueous phase reactions of $NO_x$, which is poorly understood and is sporadically investigated. More research is therefore necessary to determine the atmospheric significance of aqueous phase processes. Such studies must pay attention to the influence of oxidants, ionic species, potential catalysts and temperature.

Similar recommendations for further research are given in a number of review studies (Anderson, 1982; Asman, 1982; Cox, 1982; Cox and Penkett, 1983).

In this work the above formulated research needs are partly considered. With that it is one of the many efforts to learn more about this system. The present interest is perhaps best illustrated by the fact that the majority of the work cited in this section has been published during the course of the present investigation.

**EXPERIMENTAL TECHNIQUES**

## 3.1. INTRODUCTION

All experiments described in this thesis have been performed using flow systems, which are the most suitable as measurements can be made under steady-state conditions. The general features of such a flow system are schematically represented in Figure 1.
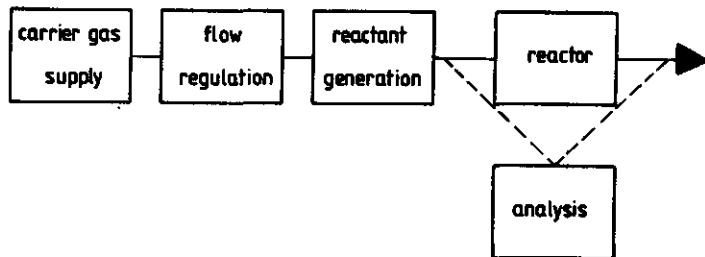


FIGURE 1. Schematic outline of the experimental equipment.

A more detailed description of the experimental aspects denoted in each of the blocks of Figure 1 is given in the next sections. The parts of the equipment, which are in contact with the gases, are constructed of stainless steel, brass, Pyrex glass or Teflon. The gas tubing materials are flexible polypropylene (Imperial Eastman 'Impolene') or Teflon (PTFE) with inner diameters of 1/4" or 3/8". In particular, $O_3$ is only exposed to glass and Teflon surfaces. Connections between the tubing are made by means of

quick-connect fittings of brass, stainless steel, nylon or Teflon (Swagelok) or by means of Pyrex glass Tee connections. All chemicals that have been used, are 'analytical grade'.

## 3.2. CARRIER GAS SUPPLY AND FLOW REGULATION

Either compressed air (Laboratory provision) or nitrogen (taken from cylinders) are used as a carrier gas, after it has been purified within the apparatus. The purification is performed by means of columns with active coal (Merck), molecular sieves (Union Carbide type 3A) and oxidation catalyst (Hopcalite). Organic vapours are removed by active coal. Water vapour and larger molecules such as $NO_2$, $CO_2$ are filtered by the molecular sieves. Small molecules such as NO, CO are first catalytically oxidised to $NO_2$, $CO_2$ and subsequently removed by molecular sieves. The purification is performed at room temperature. The purification columns can be activated by a high temperature treatment.

After purification the carrier gas is separated into several lines in which the reactants are generated or which are used for dilution. The flow in each line is regulated and controlled by mechanical means. For low volumetric flow rates (0 - 20 l/h) a flow controller (Brooks model 8844) in series with a rotameter (Brooks R-2-15-AAA or R 2-15-A) is used. For higher flow rates a constant flow unit based on critical orifices (as depicted in Figure 2) is applied (NEN 2042, 1982).
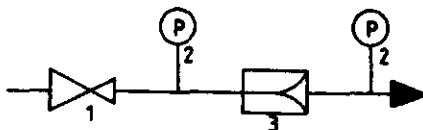


FIGURE 2.    Schematic outline of a constant flow unit based on critical orifices.    (1) pressure regulator, (2) manometer, (3) critical orifice.

The volumetric flow rate (Q) is directly proportional to the pressure before the critical orifice ($p_b$), provided that the ratio of the pressure before and after the critical orifice exceeds a value of two. The pressure

before the critical orifice can be varied with a pressure regulator (Conoflow) and is measured with a high precision manometer (Econosto type 347). An example of the linear $Q$-$p_b$ relations of some control flow units used in this study is shown in Figure 3.
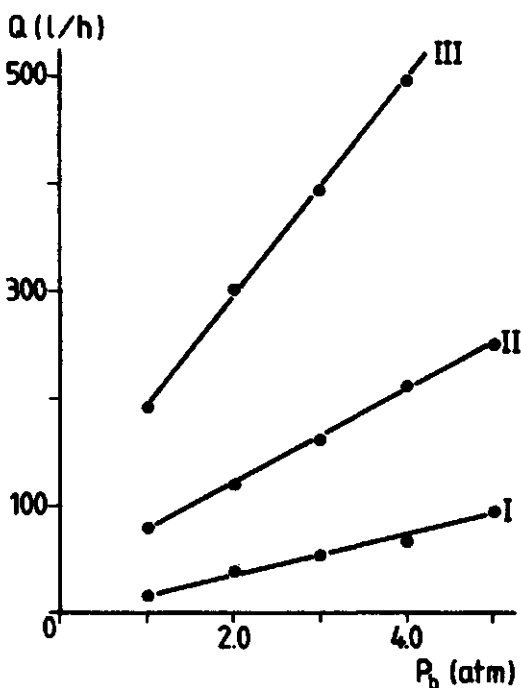


FIGURE 3.  $Q$-$p_b$ relations for critical orifices of (I) 0.15 mm; (II) 0.30 mm; (III) 0.45 mm.

## 3.3.  REACTANT GENERATION

The generation of nitrogen dioxide, ozone, water vapour and aerosol particles are described consecutively. The methods used are those commonly applied for the production of calibration mixtures.

### 3.3.1.  Nitrogen dioxide

Low, constant concentrations of nitrogen dioxide are prepared with the use of permeation tubes (Lindqvist and Lanting, 1972; Hughes et al., 1977; NEN 2042, 1982). The construction of a permeation tube is shown in Figure 4.

FIGURE 4. Design of a permeation tube. (1) Glass vessel filled with $N_2O_4$; (2) Teflon stopper; (3) Permeation surface.

The glass container is partly filled with pure, liquid $N_2O_4$ by the condensation of a pure, dry $NO_2/N_2O_4$ gas mixture. Above the liquid there is equilibrium according to:

$$N_2O_4 \text{ (l)} \rightleftarrows \quad N_2O_4 \text{ (g)} \quad \rightleftarrows 2 \ NO_2 \text{ (g)} \tag{R45}$$

The glass container is closed with a teflon stopper, through which the $NO_2(g)$ can permeate. Provided the temperature does not change, constant $NO_2$ delivery in time is obtained. Therefore, the permeation tube is placed in a temperature controlled chamber, in which it is flushed with temperature regulated carrier gas with a volumetric flow rate of 3 l/h. The rate of permeation is registrated by a biweekly weighing of the permeation tube using an analytical balance (Sartorius type 1712).

Figure 5 represents the mass loss as a function of time of two of the permeation tubes used in this study.

The gas stream leaving the permeation chamber is diluted with carrier gas in a mixing chamber. The ultimate $NO_2$ concentration is determined by the permeation rate and the total flow rate. Different concentration levels can be obtained by variation of the temperature, the permeation surface of the teflon stopper and the total flow rate.
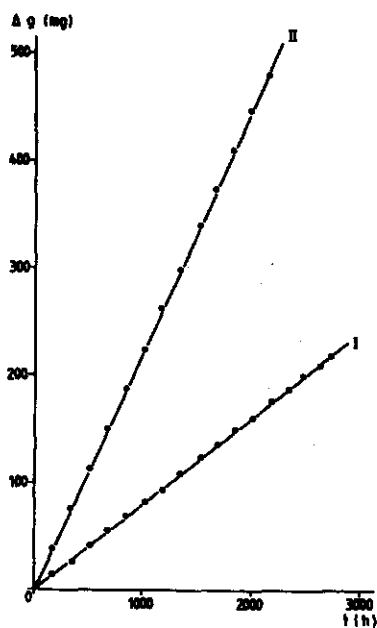
FIGURE 5.  The mass loss of a permeation tube ($\Delta g$) as a function of time.
Permeation rate: (I) 0.08 mg/h;  (II) 0.22 mg/h.


In the present investigation $NO_2$ concentrations between 0 and 10 ppm have been applied by means of permeation devices. The accuracy can be estimated to be about 2%.

In a few experiments, $NO_2$ concentrations above 10 ppm have been used; this has been achieved with standard $NO_2/N_2$ mixtures and further dilution.

### 3.3.2.  Ozone

Low constant ozone concentrations are prepared by photolysis of dry air with UV-light ($\lambda < 245$ nm) (NPR 2047, 1982). $O_3$ is produced according to:

$$O_2 \ + \ h\nu \qquad \rightarrow \ 2 \ O \ (^3P) \tag{R46}$$

$$O_2 \ + \ O \ (^3P) \ + \ M \rightarrow \ O_3 + M \tag{R8}$$

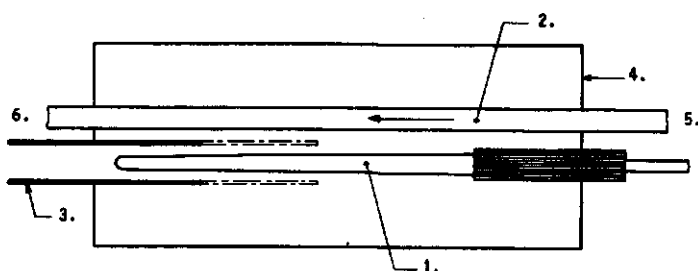The radiation device used in this study is shown in Figure 6.

FIGURE 6.   Apparatus for the production of low $O_3$ concentrations.
(1) UV-Lamp;   (2) photolysis cell (quartz tube);
(3) movable diaphragm;   (4) housing;   (5) air inlet;
(6) ozonised air outlet.

The UV-lamp consists of a Pen-Ray mercury discharge Lamp (Ultra violet Products SOG 1) producing stable 185 nm UV-radiation. The $O_3$ concentrations can be varied by covering part of the Pen-Ray Lamp with the diaphragm. $O_3$ concentrations between 20 and 200 ppb have been used applying this radiation device. The fluctuations of $c_{O_3}$ are typical within 1%.

Ozone concentrations of several ppm have been applied in the aqueous phase studies. In this case the $O_3$ has been produced with a commercial ozonizer (Fischer type 0500). The principle of the apparatus rests on the atomization of molecular oxygen (R46) by an electric discharge, and subsequent formation (R8). It must be noted that fluctuations as high as 10% may be expected.

3.3.3.   Water vapour

Two methods have been used to introduce water vapour into the flow system. One method is the saturation of part of the carrier gas with water vapour using a bubbler. The other method is the in-line evaporation of liquid water which is supplied with a constant rate using a peristaltic pump (Gibson Minipuls 2). The desired relative humidity can be adjusted by setting the proper flows and by varying the amount of dry and humid air used.

### 3.3.4  Aerosol particles

Aerosol particles were generated with a 'constant output atomizer' (TSI model 3076). The apparatus is extensively described by Liu and Lee (1975). The heart of the apparatus is depicted in Figure 7.
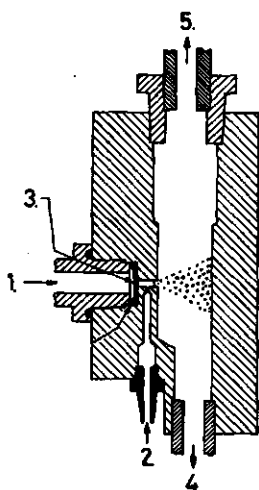


FIGURE 7.  Design of the atomizer device.
(1) compressed air (3 atm); (2) liquid feed;
(3) critical orifice (0.34 mm); (4) excess liquid;
(5) aerosol outlet.

Dry filtered compressed air expands through the critical orifice to form a high velocity jet. The liquid to be atomized is supplied to the jet by the Pitot-effect and becomes atomized by the high velocity jet. Coarse droplets in the spray are removed by impaction on the opposite wall and the excess liquid collected in this manner is allowed to drain off to a closed reservoir. The small droplets leave the atomizer at the top suspended in a constant air flow.

This method is particularly suitable for the generation of aerosol particles of substances that are soluble in water. In this study experiments with NaCl and $MgCl_2$ aerosol have been performed. The atomizer produces a polydispers aerosol, which can be described by a lognormal distribution. The mean particle size can be varied between 0.01 and 0.3 μm by the use of solutions with different concentration. The number concentration of the particles can be changed by circulating a well-known part of the aerosol

stream over an absolute filter (HEPA, Gelman).

The generated aerosol is highly charged and needs to be neutralized in order to avoid electrostatic deposition. The principle of the aerosol charge neutralizer used (TSI model 3054) is based on the ionization of air molecules by a radioactive source (Kr-85 $\beta$ radiation). The air ions subsequently collide with opposite charged aerosol particles and neutralization occurs. The aerosol particle charge is thus reduced to the minimum level as described by Boltzmann's Law (Liu and Pui, 1974a; 1974 b).

If aerosol is needed in dry air a diffusion dryer can be used. The aerosol stream is passed through a porous tube, which is surrounded by silica gel. The aerosol will pass through the tube, but water vapour will diffuse to the porous wall and will be absorbed by the silica gel.

### 3.4. REACTOR

For the gas phase and aerosol experiments, a continuous stirred tank reactor (CSTR) has been used. The CSTR is a Pyrex glass vessel, roughly spherical in shape, fitted with inlets and outlets. Two different reaction vessels have been used, both provided with a Pyrex glass/Teflon stirrer. In both vessels, the temperature is maintained at a constant value, which can be varied. Both vessels are protected against light.

The vessel volumes are determined by registrating the decay in NO concentration, when it is purged with clean air. Provided the flow rate is constant, the decay is described by:

$$c_{NO,t} = c_{NO,o} \ \exp\left(- \frac{Q}{V} t\right) \tag{1}$$

or

$$\ln \frac{c_{NO,o}}{c_{NO,t}} = \frac{Q}{V} \cdot t \tag{2}$$

The results are plotted in Figure 8. From the slopes of the plots, the vessel volumes can be calculated to be 67 l and 236 l respectively.

The volume of the smaller vessel is to be compared with a value of 69 l, which is obtained by filling the vessel with liquid water. The mixing in the vessel appears to be good. This is supported by the perfect exponential
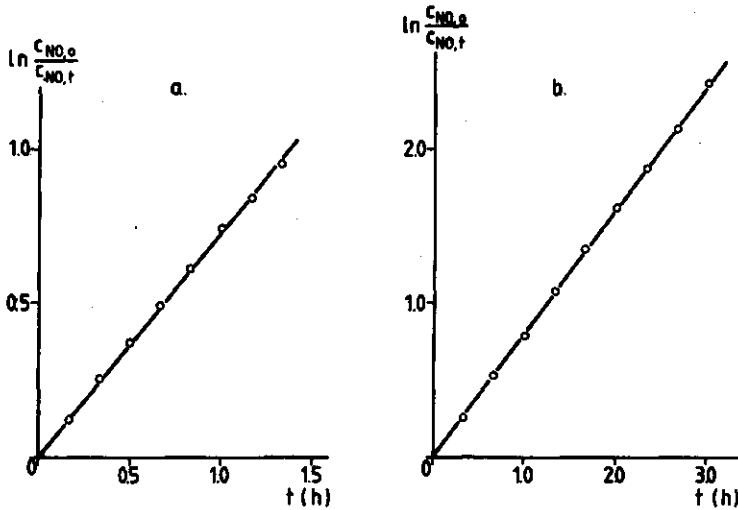
FIGURE 8.   Determination of the vessel volume according to equation (1).
(a) small vessel, Q = 48 l/h; (b) large vessel, Q = 190 l/h.

decay obtained in $c_{NO,t}$. Good mixing may be expected since it has been theoretically asserted that turbulent convection already occurs in the case of local temperature differences of $10^{-8}$ to $10^{-4}$ K (Van de Vate, 1980; Holländer et al., 1984).

Before use, the vessels have been cleaned, dried and treated with an ozone concentration of several vol.%. The latter procedure has been performed in order to minimize the $O_3$ decomposition at the reactor wall.

The liquid phase experiments have been performed with the use of an all-Pyrex glass bubbler as reactor. The gas is supplied to the liquid as finely dispersed bubbles by flowing through a glass frit. The bubbler is equipped with a water jacket for temperature control.


3.5.   ANALYSIS

Several analytical techniques have been employed to measure the $NO_2$ and $O_3$ concentration, relative humidity and aerosol characteristics. In the

aqueous phase studies the determination of the $NO_2^-$ and $NO_3^-$ concentration has been performed. In this section the back-grounds of these techniques are described.

### 3.5.1.   Nitrogen dioxide

Most measurements of the $NO_2$ concentration have been made with a Bendix model 8101 C $NO_x$ analyzer, an often employed commercial $NO_x$ analyzer. The technique involves the measurement of the chemiluminescence of the $NO-O_3$ reaction which has been amply described in the literature (cf. Fontijn et al., 1970; Helas et al., 1981; Drummond et al., 1985). The chemiluminescence is due to the reactions:

$$NO \; + \; O_3 \; \rightarrow \; NO_2^* \; + \; O_2 \tag{R47}$$

$$NO_2^* \quad \rightarrow \; NO_2 \; + \; h\nu \tag{R48}$$

where $NO_2^*$ denotes an activated $NO_2$ molecule. Besides by light production, $NO_2^*$ can also be deactivated by quenching,

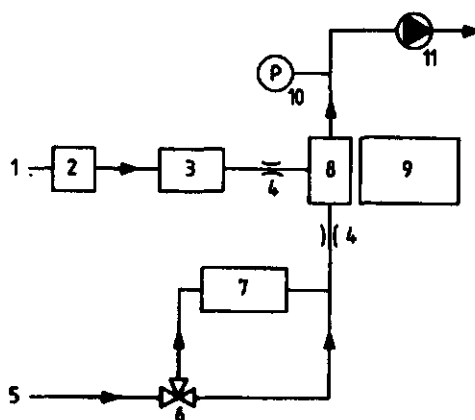$$NO_2^* \; + \; M \rightarrow \; NO_2 \; + \; M \tag{R49}$$



FIGURE 9.   Schematic design of the $NO_x$ analyzer.
(1) air inlet;  (2) dryer;  (3) ozonizer;  (4) capillary;
(5) sample air inlet; (6)  three way valve; (7) $NO_2$ converter;
(8) reaction chamber; (9)  photomultiplier; (10) manometer;
(11)  pump.

A schematic design of the $NO_x$ analyzer is shown in Figure 9. The apparatus consists of a reaction chamber, which is viewed by a cooled photomultiplier through a red filter, and which is connected in series with a gas flow system.

The reaction chamber is fed by ozonized air and sample air. The actual light production is registrated by the photomultiplier. For NO measurement the sample air is directly supplied to the reaction chamber, for $NO_x$ (= NO + $NO_2$) measurement the sample air is first passed through a converter for $NO_2$ to NO. In the apparatus an automatic three way valve alternately supplies the sample air to the reaction chamber either directly or via the converter. Therefore, the analyzer continuously outputs the NO, $NO_x$ and $NO_2$ (by difference) concentration.

Of special interest is the operation of the $NO_2$ converter. Several types such as catalytic (molybdenum), chemical (heated carbon or $FeSO_4$) and photolytic converters are commonly used. Some of these converters may convert nitrogeneous species other than $NO_2$. For example, nitric acid may be converted into NO by a catalytic molybdenum converter (Winer et al., 1974). The Bendix analyzer is provided with a chemical 'heated carbon' converter, for which no detailed information is available. Therefore, the $NO_2$ measurements have been performed using three different methods of analysis notably: $NO_x$ analyzer with build-in converter, $NO_x$ analyzer with a $FeSO_4$ converter and the wet-chemical Salzman method. The $FeSO_4$ converter is known to be specific for $NO_2$ (Helas et al., 1981). The Salzman method also is specific for $NO_2$. Good agreement between the results obtained with the different methods of $NO_2$ analysis has been observed. Furthermore, 0,5 ppm gas phase nitric acid, prepared by bubbling through a solution of 45% $HNO_3$ and dilution, has been supplied to the $NO_x$ analyzer and no $NO_2$ response has been observed.

In order to avoid a large quenching effect, the pressure in the reaction chamber is kept low (< 0.2 atm) and constant. Moreover, the quenching efficiency is a function of the chemical nature of the third body (M) (Myers et al., 1966; Matthews et al., 1977; Zabielski et al., 1984). Water vapour in particular has a high quenching efficiency, which means that the sensitivity of the method is a function of the relative humidity. Deviations as high as 10% may occur if the R.H. of the sample gas is 70% and the instrument is calibrated with dried carrier gas.

The method requires calibration, which can be performed with the permeation device described earlier. The calibration has to be performed with the same carrier gas and the same relative humidity as that of the sample, in order to avoid errors due to quenching. The accuracy of the chemiluminescent method is reported by the manufacturer to be about 5 ppb (Full scale 500 ppb). This is in accordance with the accuracy obtained during this study.

In some experiments the wet-chemical Saltzman method has been employed for $NO_2$ analysis. The details of this method are described elsewhere (Saltzman, 1954; Huygen and Lanting, 1975; Adema, 1979; NEN 2040, 1982). The method is based on the red colouring of an acid solution of sulfanilamide and N-(1-naftyl)-ethyleen diammonium dichloride after interaction with $NO_2$. The extinction of the coloured solution at 540 nm is a measure of the $NO_2$ concentration. $O_3$ interference is avoided with the use of a special designed sample bottle (Adema, 1979). The accuracy is about 10%.

3.5.2.  <u>Ozone</u>

The $O_3$ concentration has been measured with a Bendix 8002 $O_3$ analyzer. The method is based on the chemiluminescent reaction of ozone and ethylene (Pitts Jr. et al., 1972). In practise, the sample air is mixed with ethylene in a reaction chamber and the amount of light produced is measured by a photomultiplier. Quenching is much less effective than compared with the $NO$-$O_3$ reaction. The apparatus is provided with an internal calibration system based on $O_3$ production by UV light. The performance of this calibration system is tested with a NO gas phase titration according to NEN 2045 (1981). The accuracy of the method is about 1 ppb (full scale 200 ppb).

In some experiments, the $O_3$ concentration has been determined using the wet-chemical indigotin disulphonate method (Adema, 1979; NEN 2789, 1983). A blue solution of 5,5'-disodium indigotin disulphonate is discoloured by $O_3$. The discolouration is measured at 610 nm with the use of a Vitratron colorimeter. The decrease in extinction is a measure for the $O_3$ concentration. The results must be corrected for a slight $NO_2$ interference. The accuracy of the method is about 5%.

### 3.5.3. Relative humidity

Several types of hygrometers have been used to determine the relative humidity. With a Becker type 4010 hygrometer low values (< 10%) of R.H. can be measured. For higher values of R.H., a Lambrecht hygrometer has been used, with which a rough estimate of R.H. is obtained. More accurate measurements have been performed applying the method of the 'dry' and 'wet' temperature. From the difference of these temperatures, the R.H. can be deduced.

### 3.5.4. Aerosol particles

The properties of the aerosol particles have been determined by two methods, which are both available as commercial instruments manufactured by Thermo-Systems Incorporated (TSI): a model 3020 Condensation Nucleus Counter (CNC) and a model 3030 Electrical Aerosol Analyzer (EAA).

With the CNC the particle number concentration of the aerosol particles in the size range 0.01 - 1.0 $\mu$m can be measured. The principle of the apparatus is expounded referring to Figure 10.
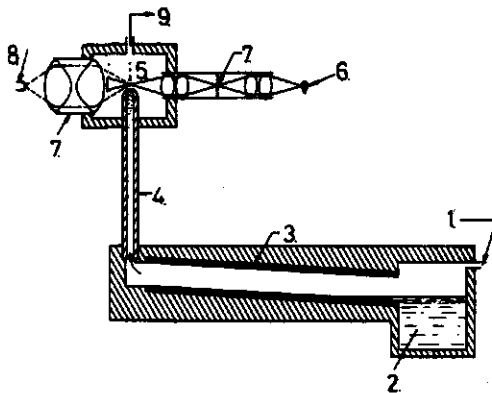


FIGURE 10.    Schematic design of the CNC.
            (1) aerosol stream inlet; (2) butanol bath; (3) saturator
            (35 °C); (4) condensor (10 °C); (5) detection cell; (6) lamp;
            (7) optical system; (8) photo-detector; (9) pump.

First, the aerosol stream is led through the saturator, which consists of a tube kept at 35 °C and in open connection with a butanol bath. In this way the aerosol stream becomes saturated with butanol vapour. Next, this stream is supplied to a tube held at 10 °C (the condensor). Because of the decrease in temperature, the butanol vapour becomes supersaturated and preferentially condenses on the aerosol particles. The particles grow and form droplets with a diameter of a few micrometers, large enough that appreciable light scatter is caused. The forward scattered light is detected as a measure for the particle number concentration.

The instrument has only been used in its 'continuous mode', for which the instrument has been calibrated by the manufacturer in the particle number concentration range $10^3$ to $2 \times 10^6$ $cm^{-3}$. The count efficiency is reported to be 100% for particle diameters $> 0.02$ $\mu m$ (Agarwal and Sem, 1980). The accuracy of the method is about 5%; the reproducibility is good.

The size distribution of the aerosol particles has been obtained with the use of the EAA. The many aspects of this instrument are described by Liu et al. (1974); (1976) and Liu and Pui (1975). The performance of the apparatus employed in the present investigation is given by Buringh (1980). The principle of measurement is the size dependence of the electrical mobility of aerosol particles. In the instrument, this is realized as shown in Figure 11.

The aerosol is first passes through a diffusion charger in which it becomes positively charged. The charged aerosol is brought in a grounded stainless steel cylinder provided with a stainless steel rod (collector rod) in its centre. An electrical field is created by applying a high, negative voltage to the collector rod. Due to this electrical field, the positively charged particles are deflected towards the collector rod. A part of the particles is precipitated on the rod, the other are collected on an absolute filter, which is placed downstream the cylinder. The collected particles decharge and cause a small current, which is measured with a sensitive electrometer. This current is a measure for the particle number concentration.

The amount of particles collected on the rod is a function of the electrical mobility of the particles, which itself is a function of the particle diameter. By varying the voltage on the collector rod, the mobility distribution (and subsequently the size distribution) can be ob-
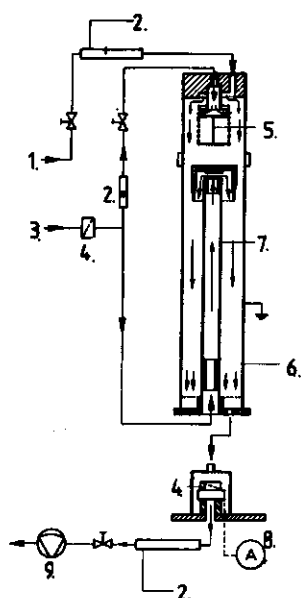
FIGURE 11.   Schematic design of the EAA.
(1) aerosol inlet; (2) flow meter; (3) sheet air inlet;
(4) absolute filter; (5) diffusion charger; (6) stainless
steel cylinder; (7) collector rod; (8) electrometer;
(9) pump.


tained. In the apparatus the classification is organized by the increase of
the negative voltage on the rod in eleven consecutive steps. In this man-
ner eleven size classes are created with midpoint particle diameters ($d_p$)
between 0.0032 $\mu$m and 1.0 $\mu$m (with $\Delta$log $d_p$ = 0.25). At each voltage, the
current produced on the absolute filter is determined. By taking the dif-
ference of the consecutive values of the current and applying the calibra-
tion data of Liu et al. (1976), the number particle concentration in each
size class is obtained. In this way, a profile of the size distribution of
the aerosol particles can be deduced.

Since the particle size distribution of the aerosol offered to the EAA
is likely to be a lognormal distribution, the data have been reduced with
the computer program developed by Liu and Kapadia (1977). This method
corrects the data for cross-sensitivity and fits the measured size distri-
bution with a lognormal distribution by minimization of the chi-square. The

output of the computer program contains the parameters that determine the lognormal distribution, i.e. the geometrical mean diameter ($d_{p,g}$), the geometrical standard deviation ($\sigma_g$) and the total number concentration of the aerosol particles (N). Thus, the aerosol number distribution is found; the aerosol surface and aerosol volume distribution can be obtained by assuming monodispersity in each size class.

In order to increase the accuracy, the measurement has been started with the fourth size class (lower limit 0.024 μm) and the total number concentration has been kept in the range $10^3$ - $5 \times 10^4$ cm$^{-3}$. The latter means that often the aerosol stream has to be diluted. This is performed by the method given by Whitby et al. (1972). Taking into account the above-mentioned precautions, the accuracy of the parameters determined with the computer model is approximately 5 to 10%. The comparison between the total number concentration measurements of the CNC and the EAA shows good agreement as depicted in Figure 12.
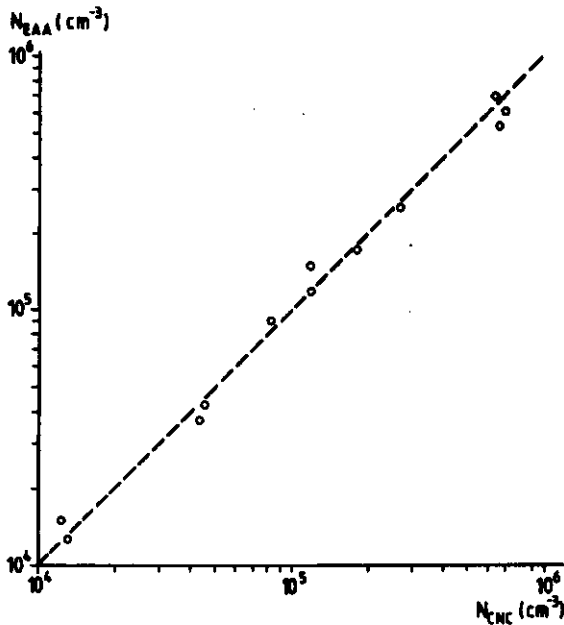


FIGURE 12.    Comparison of total number concentration measured by the CNC and the EAA.

The major disadvantage of the EAA is its low size-resolution. Recently, a high-resolution electrical mobility aerosol spectrometer (MAS) has been

developed by Ten Brink et al. (1983). Unfortunately, this instrument was not available for the present study. When both instruments are compared, considerable discrepancies can occur but, however, the best agreement is found when the EAA data are corrected for cross-sensitivity by the procedure described by Liu and Kapadia (1977). Moreover, the aerosol volume and surface concentration as measured with MAS and EAA appears to agree fairly well.

### 3.5.5. Nitrite and nitrate

The nitrite and nitrate concentrations have been determined simultaneously by means of ion chromatography. A convential isocratic HPLC equipment has been used with separation on an anion exchanger and detection with UV-spectroscopy at 210 nm (Gerritse, 1979; Leuenberger et al., 1980). The instruments used are: a high pressure pump (Kipp model LC 414) and an UV-detector (Kratos Spectroflow 757). A IonoSpher column (Chrompack) has been used. The calibration is performed with standard $NO_2^-$ and $NO_3^-$ solutions. The accuracy is 3%.

### 3.5.6. Data registration

Recorders (Kipp model BD 41) have been used in most cases. The EAA data have been registrated with a micro computer (Hewlett-Packard model HP 85) connected with the EAA via a data acquisition/control unit (Hewlett Packard model HP 3421). The registration of the ion chromatograms has been performed with an automatic integrator (Spectra Physics model SP 4270).
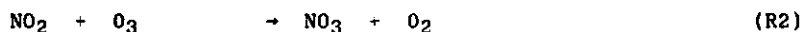
# THE $NO_2$-$O_3$ SYSTEM AT SUB-PPM CONCENTRATIONS: INFLUENCE OF TEMPERATURE AND RELATIVE HUMIDITY

## 4.1. INTRODUCTION

It is now generally accepted that there are two important mechanisms for the formation of atmospheric nitric acid (Richards, 1983; Cox and Penkett, 1983). The first one involves atmospheric nitric acid being formed by the reaction of $NO_2$ with the OH radical:

$$NO_2 + OH + M \rightarrow HNO_3 + M \qquad (R1)$$

which dominates during day-time. In the second mechanism a reaction pattern which is initiated with the $NO_2$ oxidation by $O_3$:

$$NO_2 + O_3 \rightarrow NO_3 + O_2 \qquad (R2)$$

$$NO_2 + NO_3 + M \rightarrow N_2O_5 + M \qquad (R3)$$

$$N_2O_5 + M \rightarrow NO_2 + NO_3 + M \qquad (R4)$$

$$N_2O_5 + H_2O \rightarrow 2\ HNO_3 \qquad (R5)$$

The second process occurs mainly at night, because by day the $NO_3$ radical is rapidly photolized. Likewise, $NO_3$ reacts rapidly with NO:

$$NO_3 + NO \rightarrow 2\ NO_2 \qquad (R6)$$

The importance of the night-time $NO_2$ oxidation is confirmed by recent field measurements (Platt et al, 1981; Platt et al., 1984) and model stu-

dies (Calvert and Stockwell, 1983; Jones and Seinfield, 1983; Heikes and Thompson, 1983). The $NO_2$ conversion rate to $HNO_3$ associated with this process might even exceed the $NO_2$ conversion rate of the daylight reaction (R1).

The influence of relative humidity (R.H.) seems to be of crucial importance. Platt et al. (1984) report that the lifetime of $NO_3$ calculated from their observations of atmospheric $NO_3$ decreases with increasing R.H. The involvement of water in the loss process for $NO_3$ or $N_2O_5$ is suggested. For example, the $N_2O_5$ scavenging in clouds or on aerosol surfaces where $H_2O$ is present in its aqueous state, is considered as a potential loss process.

The influence of R.H. on the kinetics and stoichiometry of the $NO_2$-$O_3$ system has rarely been studied in laboratory experiments. Table I lists the results of some laboratory studies of the past decades. In none of these studies attention was paid to the influence of R.H.. Table I shows reasonable agreement for the rate constant $k_2$ and its temperature dependence. In some studies the stoichiometry ($\Delta NO_2/\Delta O_3$) was determined; most values were lower than 2, the value expected on the basis of (R2), (R3) and (R4). The reason for this low stoichiometry is not yet understood, although there are as many suggestions as there are determinations of the reaction stoichiometry.

TABLE 1  Laboratory studies concerning the $NO_2$-$O_3$ system (from: Verhees and Adema, 1985)

| Study | Concentration | | $k_2 \times 10^{17}$ at 298 K ($cm^3$ molecule$^{-1}$ s$^{-1}$) | Arrhenius-expression | Stoichi-ometry |
|---|---|---|---|---|---|
| | $NO_2$ (ppm)[a] | $O_3$ (ppm)[a] | | | |
| Ford et al. (1957) | 0.2–1.0 | 0.25–0.63 | 3.3 ± 1.5 | | 0.88–4.75 |
| Wu et al. (1973) | 6–24 | 4–21 | 4.3 ± 0.7 | | 1.53–2.03 |
| Stedman and Niki (1973) | 0.01–0.1 | 1–8 | 6.5 ± 0.8 | | |
| Davis et al. (1974) | 100–400 | 5–40 | 2.8 ± 0.3 | $9.8 \times 10^{-14}$ exp($-2427/T$) | |
| Huie and Herron (1974) | 25–250 | 2.5–6.3 | 3.8 ± 0.1 | $1.6 \times 10^{-13}$ exp($-2509/T$) | |
| Graham and Johnston (1974) | 9–60 | 5–50 | 3.5 ± 0.2 | $1.3 \times 10^{-13}$ exp($-2466/T$) | 1.89 ± 0.08 |
| Becker et al. (1974) | | | 4.2 | | |
| Cox and Coker (1983) | 8–80 | 8–80 | 3.5 ± 0.1 | | 1.85 ± 0.09 |

[a] 1 ppm = 1000 ppb = $2.5 \times 10^{13}$ molecule cm$^{-3}$ (1 atm; 298 K).

In most of the studies summarized in Table I, the reactant concentration were at ppm level or higher. Only the dated and inaccurate study of

Ford et al. (1957) used sub-ppm concentrations for both reactants. One of the objectives of the present study is to check the validity of the kinetic parameters (as listed in Table I) at sub-ppm concentrations of $NO_2$ and $O_3$. At the same time, this chapter deals with the influence of the temperature and relative humidity on the kinetics and stoichiometry of the $NO_2$-$O_3$ reaction system.

## 4.2. EXPERIMENTAL

The equipment in which the experiments were performed is schematically shown in Figure 1. The system operates as a continuous stirred tank reactor (CSTR) flow system.
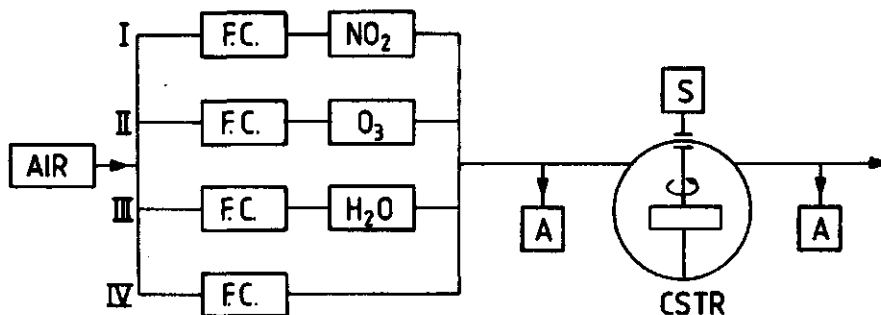


FIGURE 1: Schematic outline of the experimental set-up.
AIR: clean, dry compressed air (6 atm); F.C.: flow controlling device; $NO_2$, $O_3$, $H_2O$: generation of $NO_2$, $O_3$, $H_2O(g)$ respectively; S: stirrer; CSTR: continuous stirred tank reactor; A: sampling

The tank reactor consists of a roughly spherical all-Pyrex glass vessel with a Pyrex glass/Teflon stirrer operating at a frequency of about 1 Hz. Two vessels of different size (volume 67 and 236 l, respectively) were used. The vessels were wrapped with rubber tubing and were insulated with glass wool. The rubber tubing was fed with water from a PMT-Tamson TC 9 thermostat. Thus, the temperature in the vessels is kept constant and can be varied between 277 and 340 K to within an accuracy of 0.02 K. To screen light exposure, the insulated reaction vessel was covered with aluminium foil.

Clean, dry air was used as a carrier gas which was split into four lines. Three lines were used for the generation of the reactants and the fourth line was used for dilution. In each line the flow could be controlled. In line I by means of a Brooks flow controller model 8844 and a Brooks R-2-15-AAA flow meter and in the other lines by a constant flow unit based on critical orifices (NEN 2042, 1982).

In line I, $NO_2$ was generated using a permeation tube system. A permeation tube filled with pure, liquid $N_2O_4$ was kept at a constant temperature in a permeation chamber and flushed with a flow of 3 l/h air. The $NO_2$ concentration could be changed by using several permeation tubes.

In line II, $O_3$ was produced by radiating the air with 185 nm UV-light using a Pen-Ray tube (Ultraviolet Products SOG-1). The $O_3$ concentration could be varied by covering part of the Pen-Ray tube. Both $NO_2$ and $O_3$ were generated in accordance with Dutch standards (NEN 2042, 1982; NPR 2047, 1982) for the production of calibration gases. Water vapour was introduced by saturating the flow through line III, the desired relative humidity and/or total flow could be adjusted by setting the proper flows through lines III and IV.

The $NO_2$ and $O_3$ concentrations were determined before and after the reaction vessel. The analysis of $NO_2$ was performed with a Bendix 8101C $NO_x$ analyzer based on the chemiluminescent reaction of NO with ozone. In most experiments $NO_2$ was converted to NO using the built-in converter, and in a few experiments a $FeSO_4$ converter operating at room temperature was used. The analyzer had been calibrated with the permeation system described above. The $O_3$ concentrations were measured by the chemiluminescent reaction with ethylene using a Bendix 8002 $O_3$ analyzer. A gas phase titration with NO was used to calibrate the $O_3$ monitor (NEN 2045, 1981). In some of the experiments wet chemical methods such as the Saltzman method for $NO_2$ and the indigotinedisulphonate method for $O_3$ were applied as described by Adema (1979).

In this experimental set-up several kinetic experiments were performed with a number of variables illustrated in Table II.

Generally the experiments can be divided into two parts: those under 'dry conditions' and those under 'wet conditions'. 'Dry conditions' are defined as being when no water vapour is introduced into the reaction

TABLE II.  Summary of the reaction conditions and its variations

| Variable | Symbol | Range |
|----------|--------|-------|
| Input $NO_2$ concentration | $c_{o,NO_2}$ | 40 - 330 ppb |
| Input $O_3$ concentration | $c_{o,O_3}$ | 20 - 200 ppb |
| reaction vessel volume | $V$ | 67  ; 236 l. |
| space velocity[a] | $\theta$ | 1.1 ; 1.5 ; 2.2 $h^{-1}$ |
| temperature | T | 277 - 325 K |
| relative humidity | R.H. | <0.1% - 80% |

a)  Space velocity defined as: $\theta = Q/V$ with Q: volumetric flow rate

vessel. The water vapour content of the dried carrier gas was measured using a Becker type 4010 Hygrometer and a value of about 8 ppm $H_2O$ (g) was obtained. This corresponded to a relative humidity of less than 0.1%.

The experimental data are reduced using the mass balance for every component i in the CSTR. The mass balance is expressed by:

$$Q.c_{o,i} = Q.c_{t,i} - V. \sum_j r_{ij} + V.dc_{t,i}/dt \tag{1}$$

with  Q  = volumetric flow rate ($cm^3$ $s^{-1}$)
$c_{o,i}$  = input concentration of component i (molecule $cm^{-3}$)
$c_{t,i}$  = concentration of component i in the reaction vessel at time t (molecule $cm^{-3}$)
$r_{ij}$  = rate of formation of component i by reaction j (molecule $cm^{-3}$ $s^{-1}$)
V  = reaction vessel volume  ($cm^3$)
$dc_{t,i}/dt$ = accumulation of component i (molecule $cm^{-3}$ $s^{-1}$)

In course of time a stationary state is achieved, then :

$$dc_{t,i}/dt = 0 \; ; \; c_{t,i} = c_{ss,i} \tag{2}$$

$c_{ss,i}$  = steady state concentration of component i

Hence

$$Q.c_{o,i} = Q.c_{ss,i} - V.\sum_j r_{ij} \tag{3}$$

or $\quad \theta \cdot c_{0,i} = \theta \cdot c_{ss,i} - \sum_j r_{ij}$ $\hspace{4cm}$ (4)

$\quad \theta \qquad = $ space velocity defined as Q/V $(s^{-1})$

Note that the reciprocal value of $\theta$ is the mean residence time of a component in the reaction vessel.


## 4.3. RESULTS

### 4.3.1. $O_3$-decay

To determine the stability of the reactants with respect to the vessel wall, the CSTR was flushed with a carrier gas containing either $NO_2$ or $O_3$. $NO_2$ was found to be stable under all experimental conditions but $O_3$ appeared to decay. If we consider the $O_3$ wall loss to be a first-order reaction, its rate can be characterized with the rate constant $k_{O_3}$. In the steady state, $k_{O_3}$ can be derived from (4):

$$k_{O_3} = \frac{(c_{0,O_3} - c_{ss,O_3}) \cdot \theta}{c_{ss,O_3}}$$ $\hspace{2cm}$ (5)

In the 67 l reaction vessel, a $k_{O_3}$ value of $(1.2 \pm 0.3) \times 10^{-5}$ s$^{-1}$ was obtained and in the 236 l vessel $k_{O_3} = (2.8 \pm 0.8) \times 10^{-5}$ s$^{-1}$ was found. The $O_3$ decay was measured several times during the experiments; $k_{O_3}$ was always within the limits given above.

As a function of temperature, $k_{O_3}$ tends to decrease slightly with increasing temperature but, however, in the temperature range under examination (277-325 K) the value for $k_{O_3}$ remains in the range given above. $k_{O_3}$ increases with R.H., a value of about $2.5 \times 10^{-5}$ s$^{-1}$ is found in the 67 l vessel at R.H. 50%.

### 4.3.2. The $NO_2$-$O_3$-system under 'dry-conditions'

Stoichiometry

The measurements were performed using the following standard procedure. The reaction vessel was continuously flushed with carrier gas with a $NO_2$ concentration of $c_{0,NO_2}$. An experiment was started with the initiation of

the $O_3$ production so that during the experiment the gas flow through the reaction vessel remained constant. Both $NO_2$ and $O_3$ concentrations in the reaction vessel were recorded as a function of time, using the chemilumi-nescent analyzers. Figures 2a and 2b illustrate the course of $c_{t,NO_2}$ and $c_{t,O_3}$ during an experiment. As can be seen from the figures, a steady-state is reached after some time. In steady-state conditions input and output concentrations were measured by applying the same analyzers (see Figures 2a, 2b) and wet chemical methods.
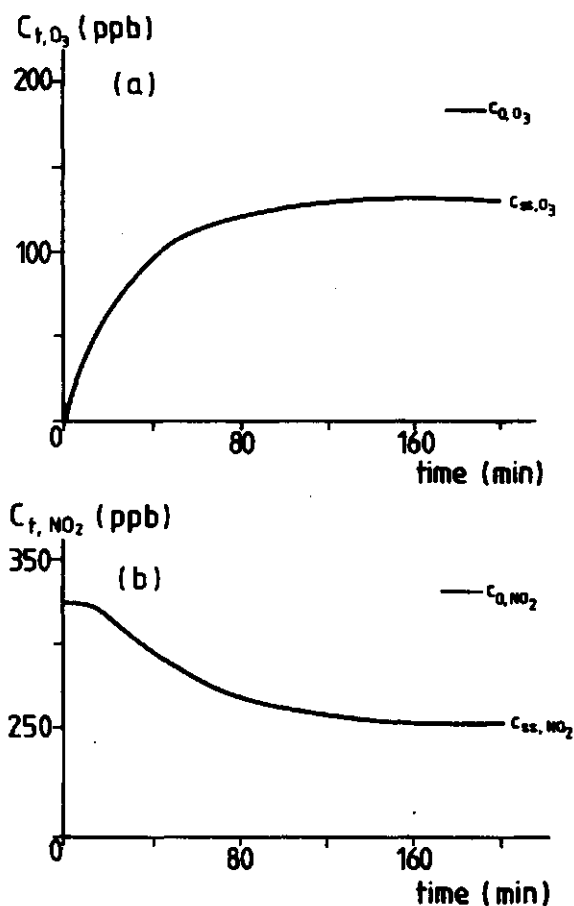


FIGURE 2:   (a) Ozone concentration as a function of time.
            (b) Nitrogen dioxide concentration as a function of time

We define the stoichiometric factor (S) of the reaction system as:

$$S = \frac{c_{o,NO_2} - c_{ss,NO_2}}{c_{o,O_3} - c_{ss,O_3}} (1 + k_{O_3} / \theta) \tag{6}$$

In this formula the term $(1+k_{O_3}/\theta)$ is used to correct the $O_3$ decomposition on the wall.

Table III lists the stoichiometric factors determined in the 67 l vessel with the use of different methods of $NO_2$ analysis. Here $c_{o,O_3}$ has been varied between 40 and 200 ppb. It appears, however, that S does not depend on $c_{o,O_3}$. As follows from Table III there is a good agreement between the different methods of analysis. Further description concerns results obtained with the chemiluminescent analyzers only.

TABLE III.  The stoichiometric factor at 293 K; 67 l vessel,
Reaction conditions $\theta$ = 1.5 $h^{-1}$, $c_{o,NO_2}$ = 325 ppb,
$c_{o,O_3}$ = 40 - 200 ppb.

| Method of analysis | S | $\sigma_s$[a] | n[a] |
|---|---|---|---|
| chemiluminescent analyzers | 1.12 | 0.09 | 18 |
| ibid, with $FeSO_4$ converter for $NO_2$ analysis | 1.09 | 0.07 | 4 |
| wet chemical | 1.1 | 0.2 | 18 |

a)  Standard deviation based on n measurements

The influence of the temperature on S is illustrated in Table IV. At higher temperatures, a clear decrease in the stoichiometric factor results.

Table V shows the results obtained in the 236 l vessel at a constant temperature of 298 K. Here $c_{o,O_3}$ has been varied between 20 - 80 ppb, but again S is found to be independent of $c_{o,O_3}$. In this set of experiments $c_{o,NO_2}$ has also been changed, as shown in Table V. Reducing $c_{o,NO_2}$ results in a lower stoichiometric factor.

TABLE IV. The stoichiometric factor as a function of temperature; 67 l vessel, $\theta = 1.5$ h$^{-1}$, $c_{o,NO_2} = 325$ ppb, $c_{o,O_3}$ = 40 - 200 ppb.

| T (K) | S | $\sigma_S$ | n |
|-------|------|------|----|
| 277 | 1.37 | 0.09 | 4 |
| 287 | 1.29 | 0.08 | 5 |
| 293 | 1.12 | 0.09 | 18 |
| 298 | 0.94 | 0.07 | 4 |
| 301 | 0.85 | 0.08 | 5 |
| 313 | 0.70 | 0.10 | 8 |
| 325 | 0.44 | 0.14 | 5 |

TABLE V. The stoichiometric factor at different $c_{o,NO_2}$; 236 l vessel, T = 298 K, $\theta = 1.7$ h$^{-1}$, $c_{o,O_3} = 20 - 80$ ppb.

| $c_{o,NO_2}$ (ppb) | S | $\sigma_S$ | n |
|-------|------|------|----|
| 328 | 1.3 | 0.2 | 6 |
| 110 | 0.81 | 0.16 | 6 |
| 44 | 0.41 | 0.04 | 7 |

Comparing the results of the two different reaction vessels, it can be seen that under corresponding reaction circumstances, a higher value for S is found in the 236 l vessel.

Finally, the influence of space velocity is described. This has been varied by a change in the total flow, but since the same permeation tube has been used, $c_{o,NO_2}$ changes inversely proportional to the space velocity. Under these conditions, it was found that S remained constant. This behaviour was observed in both vessels at 293 K and 313 K. Thus, a constant stoichiometric factor results, when the product $\theta \cdot c_{o,NO_2}$ remains constant. If the space velocity only is varied, the dependence of S on $\theta$ will be opposite to the dependence of S on $c_{o,NO_2}$.

**Kinetics and Mechanism**

The kinetic analysis has been performed based on expression (4). The relevant kinetic parameters are described in the term $\sum_j r_{ij}$. The exact composition of this term depends on the reaction mechanism in the CSTR. Because this mechanism is not known, we have examined several combinations of reactions given in Table VI. The reactions (R2), (R3) and (R4) are always included but, however, when only these three reactions are considered a stoichiometric factor of 2 is found to contrast with the results.

TABLE VI.  Summary of the reactions used for kinetic analysis.

| Reaction | Expression | Rate constant as $f(T)$[a] | T-range |
|---|---|---|---|
| R2 | $NO_2 + O_3 \rightarrow NO_3 + O_2$ | $1.2 \times 10^{-13} \exp(-2450/T)$ | 230-360 |
| R3 | $NO_2 + NO_3 + M \rightarrow N_2O_5 + M$ | $1.6 \times 10^{-12}(T/300)^{0.2}$ | 220-520 |
| R4 | $N_2O_5 + M \rightarrow NO_2 + NO_3 + M$ | $9.7 \times 10^{14} \exp(-11080/T)$ | 220-500 |
| R7 | $NO_2 + NO_3 \rightarrow NO + NO_2 + O_2$ | $2.5 \times 10^{-14} \exp(-1127/T)$ | 338-396 |
| R8 | $2\ NO_3 \rightarrow 2\ NO_2 + O_2$ | $8.5 \times 10^{-13} \exp(-2450/T)$ | 298-329 |
| R9 | $NO_2 + O_3 \rightarrow NO + 2\ O_2$ | | |
| R10 | $NO_3 + W \rightarrow NO_2 + \frac{1}{2} O_2 + W$ | | |
| R11 | $NO_3 + W \rightarrow NO + O_2 + W$ | | |
| R12 | $N_2O_5 + W \rightarrow 2\ NO_2 + \frac{1}{2} O_2 + W$ | | |
| R13 | $N_2O_5 + W \rightarrow NO + NO_2 + O_2 + W$ | | |
| R14 | $NO + O_3 \rightarrow NO_2 + O_2$ | $2.3 \times 10^{-12} \exp(-1450/T)$ | 200-360 |
| R6 | $NO + NO_3 \rightarrow 2\ NO_2$ | $2 \times 10^{-11}$ | |
| R5 | $N_2O_5 + H_2O \rightarrow 2\ HNO_3$ | | |
| | M : third molecule ; W : wall | | |

a)  Rate constant units are $s^{-1}$ (first-order reaction) and $cm^3$ molecule$^{-1}s^{-1}$ (second-order reaction).
Rate constants are the recommended values for the given T-range from Baulch et al. (1982), except for (R7) and (R8) which are taken from Graham and Johnston (1978).

Therefore, it is necessary to consider additional reactions. A combination with (R7), (R6) and (R14) or with (R8) might be possible. Both (R7) and R(8) have been reported in literature (Graham and Johnston, 1978) but, however, the reported rate constants are too low to match the stoichiometric factors found.

The results of such an analysis agree with the present data only when one of the reactions (R9) to (R13) is included. The possibility of (R9) has been indicated by Wu et al. (1973). Reactions (R10) to (R13) are the wall decomposition of $NO_3$ or $N_2O_5$ with the formation of $NO_2$ or NO. In case there is NO formation, the reactions (R6) and (R14) are also inserted into the reaction combination.

For any combination of reactions the term $\sum_j r_{ij}$ can be composed. All reactions are considered elementary, so they are first-order in the reactants. From (4) we get i equations where $\theta$, $c_{o,i}$ and $c_{t,i}$ for $NO_2$ and $O_3$ are known variables, while the other (i-2) values for $c_{t,i}$ are unknown. This means that two rate constants can be determined in the term $\sum_j r_{ij}$. In our analysis we have determined the rate constant for reaction (R2), $(k_2)$, and the rate constant for the reaction selected from the set (R9) to (R13), $(k_j)$. For the other rate constants we have used the literature values given in Table VI.

TABLE VII.  Results of the kinetic analysis at R.H. < 0.1%; T = 298 K.

| Reaction combination | 67 l vessel | | 236 l vessel | |
|---|---|---|---|---|
| | $k_2$ [a] | $k_j$ [a] | $k_2$ | $k_j$ |
| R2, R9 | $2.2 \times 10^{-17}$ | $9.8 \times 10^{-16}$ | $2.9 \times 10^{-17}$ | $5.9 \times 10^{-16}$ |
| R2, R10 | $3.4 \times 10^{-17}$ | $8.2 \times 10^{-2}$ | $3.7 \times 10^{-17}$ | $3.7 \times 10^{-2}$ |
| R2, R11 | $3.2 \times 10^{-17}$ | $4.1 \times 10^{-2}$ | $3.5 \times 10^{-17}$ | $1.9 \times 10^{-2}$ |
| R2, R12 | $3.4 \times 10^{-17}$ | $4.8 \times 10^{-4}$ | $3.7 \times 10^{-17}$ | $2.0 \times 10^{-4}$ |
| R2, R13 | $3.2 \times 10^{-17}$ | $2.4 \times 10^{-4}$ | $3.5 \times 10^{-17}$ | $1.0 \times 10^{-4}$ |

a)  Rate constant units are $s^{-1}$ (first-order reaction) and $cm^3 molecule^{-1} sec^{-1}$ (second-order reaction).

The system of i equations with i variables obtained in this manner, can be solved. In Table VII, the rate constants as found with the different reaction combinations are given for the experiments at 298 K in the 67 and 236 l vessels. We note that in all cases the $k_2$ values are nearly equal and that the same reaction combination yields a corresponding $k_2$ value in both reaction vessels. Likewise, we see a clear difference in the $k_j$ values obtained with the same reaction combination but with different reaction vessels.

## 4.3.3. The $NO_2-O_3$-system under 'wet conditions'

**Stoichiometry**

Table VIII shows the stoichiometric factor as a function of relative humidity. The results are corrected for the influence of R.H. on the chemiluminescent detection techniques.

TABLE VIII. The stoichiometric factor as a function of R.H.; 67 l vessel, T = 293 K, $\theta$ = 1.5 h$^{-1}$, $c_{o,NO_2}$ = 325 ppb, $c_{o,O_3}$ = 180 ppb.

| R.H. (%) | S | $\sigma_s$ | n |
|---|---|---|---|
| <0.1 | 1.12 | 0.09 | 18 |
| 30 | 1.20 | 0.11 | 8 |
| 48 | 1.26 | 0.07 | 5 |
| 68 | 1.34 | 0.08 | 6 |
| 78 | 1.40 | 0.10 | 7 |
| 78[a] | 1.96 | 0.04 | 3 |

a) after exposure to R.H. 78 % for ca. 100 h.

From Table VIII we observe a significant increase of S with R.H. It is of importance to mention that $H_2O(g)$ was only suppplied during the experiment. The $H_2O(g)$ supply was started simultaneously with the beginning of the $O_3$ generation. It was stopped after $c_{O,NO_2}$ and $c_{O,O_3}$ were measured. This means that during night-time and at the weekends no $H_2O(g)$ was supplied.

When an experiment is performed after the reaction vessel has been exposed to a R.H. of 78% for a longer period (ca. 100 h), there is a significant change in S, which increases drastically to a value of 1.96 ± 0.04.

## Kinetics and Mechanism

Most likely the influence of $H_2O(g)$ can be attributed to the conversion of $N_2O_5$ according to reaction (R5) (Table VI). This $N_2O_5$ conversion causes a shift to the right of the equilibrium formed by the reactions (R3) and (R4) which results in an increase of S.

The reaction rate constants of the reactions (R2) and (R5) have been calculated. That of (R5) is considered as a pseudo-first-order reaction rate constant ($k_5'$) because of excess $H_2O$. The k values are given in Table IX. The results refer to the reaction combination (R2), (R3), (R4), (R5), (R10). For $k_{10}$, the value obtained under 'dry conditions' has been used and $k_3$ and $k_4$ have been taken from literature (Baulch et al., 1982).

TABLE IX.   Results of the kinetic analysis at different R.H.;
T = 293 K; 67 l vessel.

| R.H. (%) | $k_2$ (cm$^3$molecule$^{-1}$ s$^{-1}$) | $k_5'$ (s$^{-1}$) |
|---|---|---|
| <0.1 | $2.7 \times 10^{-17}$ | 0 |
| 30 | $2.6 \times 10^{-17}$ | $8.4 \times 10^{-5}$ |
| 48 | $2.7 \times 10^{-17}$ | $1.5 \times 10^{-4}$ |
| 68 | $2.7 \times 10^{-17}$ | $2.6 \times 10^{-4}$ |
| 78 | $2.8 \times 10^{-17}$ | $3.6 \times 10^{-4}$ |

## 4.4. DISCUSSION

4.4.1.
### The $NO_2$-$O_3$ system under 'dry conditions'

One of the major points of discussion is the question of which reaction combination best explains the observed phenomena. To answer this question we first consider the stoichiometric factor obtained in the two reaction vessels used. Comparing the results at 298 K and $c_{o,NO_2}$ = 325 - 328 ppb, a significant higher stoichiometric factor is found in the 236 l vessel; S = 0.94 in the 67 l (Table IV) and S = 1.3 in the 236 l vessel (Table V). The different behaviour in different reaction vessels can also be illustrated by the disparity in the $k_j$ value (see Table VII). If only homogeneous processes occur, the result in both vessels would be similar. Since this is not the case, an influence of the reactor wall is obvious. Most likely, the decomposition of $NO_3$ or $N_2O_5$ (R10) to (R13) is involved. Next, we consider the results as a function of $c_{o,NO_2}$ (Table V). If we compute the stoichiometric factor as a function of $c_{o,NO_2}$ using the rate constants found in the experiment with $c_{o,NO_2}$ = 328 ppb, we obtain for the combination (R2), (R3), (R4) and (R10) the dashed line given in Figure 3.



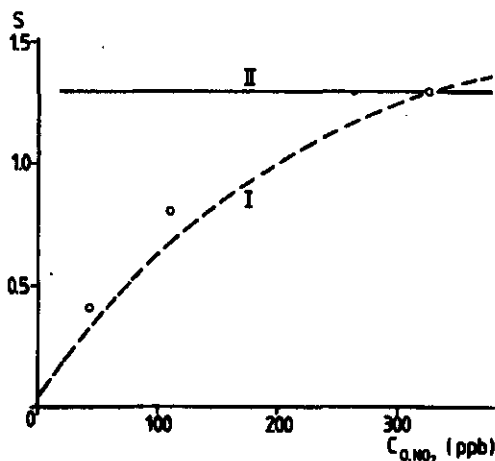FIGURE 3. The stoichiometric factor as a function of $c_{o,NO_2}$.
     (o)      experimental data points
     (----)   calculated line using reaction combination with (R10) or (R11).
     (——)   calculated line using reaction combination with (R12) or (R13)

If we use the combination (R2), (R3), (R4), (R6), (R11) and (R14) nearly the same line is found but, however, calculations with the reaction combinations including (R12) or (R13) show a stoichiometric factor that is independent of $c_{0,NO_2}$ in the range 5-500 ppb (solid line in Figure 3). More information is provided by the measurements with different space velocity. Simulation of S using the rate constants found with $\theta = 1.5$ h$^{-1}$ show marked differences between the various reaction combinations, as illustrated in Figure 4.
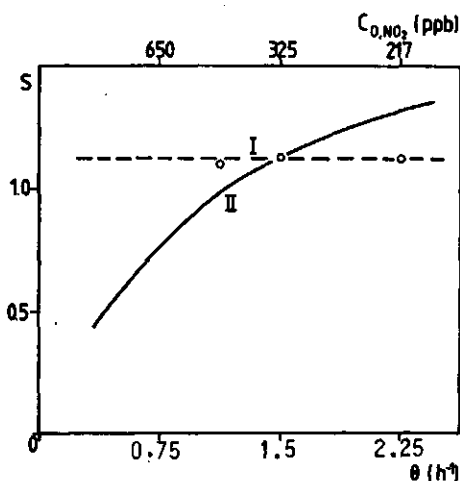


FIGURE 4. The stoichiometric factor as a function of space velocity.
       (o)      experimental data points
      (----)   calculated line using reaction combination with (R10) or (R11).
      (——)   calculated line using reaction combination with (R12) or (R13).

We see that when (R12) or (R13) is used, a dependence of S on the space velocity (and a corresponding change in $c_{0,NO_2}$) results, whereas reaction combinations with (R10) or (R11) lead to a constant value for S. The experimental results are also indicated in the Figure 3 and 4. From a comparison between the computed lines and the experimental data points, which have not been used in the calculations, it appears that only reaction combinations with (R10) or (R11) are in accordance with the observations. We may conclude, that the low stoichiometric factor is caused by a wall reaction involving $NO_3$ with subsequent formation of $NO_2$ or NO.

On the basis of the present results, we cannot discriminate between (R10) and (R11). According to Graham and Johnston (1974), it is unlikely that NO acts as an intermediate, since they failed to detect the chemiluminescence from (R14) in the $NO_2$-$O_3$ system. Combining this with the present results, the combination (R2), (R3), (R4) and (R10) is preferable to any other reaction combination. Graham and Johnston (1978) insert reaction (R10) in their reaction mechanism, and they report that this mechanism is capable of explaining the laboratory reactions of the $NO_x$-$O_3$ system in the dark. The possibility of (R10) is also reported by Ten Brink et al. (1982). In the further discussion we restrict ourselves to the reaction combination with (R10).

Let us now consider the numerical value of $k_{10}$. A wall reaction, such as (R10), can be considered as a two step process, that involves diffusion of $NO_3$ to the wall followed by reaction at the surface. Either diffusion or surface reaction can limit the reaction rate.

In the surface-reaction-limited situation, the first-order rate constant of a wall reaction, $k_{10}$, can be expressed by (Grosjean, 1985):

$$k_{10} = \frac{A}{V} \cdot \frac{\alpha \, v_g}{4} \tag{7}$$

where    $A/V$ = surface area to volume ratio of the reaction vessel ($cm^{-1}$)
         $\alpha$ = accommodation coefficient
         $v_g$ = mean thermal velocity of the gas molecule ($cm \, s^{-1}$)

The accomodation coefficient (or sticking coefficient or collision yield) is the fraction of collisions on the surface that actually lead to reaction. The mean thermal velocity of the gas molecules can be derived from the kinetic theory of gases:

$$v_g = \sqrt{\frac{8 \, R \, T}{\pi \, M}} \tag{8}$$

where M denotes the molecular weight, and R is the gas constant. In the case of $NO_3$, $v_g = 3.2 \times 10^4$ cm/s. From the $k_{10}$ values given in Table VII and A/V values of 0.12 $cm^{-1}$ (67 l vessel) and 0.08 $cm^{-1}$ (236 l vessel), we find $\alpha$ values of $8.5 \times 10^{-5}$ and $5.8 \times 10^{-5}$ respectively. These values are rather low compared to the accommodation coefficients for OH radical scavenging as reported by Chameides and Davis (1982). However, they are clearly higher

than the $\alpha$ values for the $O_3$ wall decomposition given by Grosjean (1985) or deduced from the values of $k_{O_3}$ given in section 4.3.1. ($\alpha$ values in the order of $10^{-6}$).

In the case of diffusion limitation, the results can be discussed in terms of the following model (Van de Vate, 1980; Ten Brink et al., 1982). In this model it is assumed that in a well-stirred reaction mixture the rate of a wall reaction is controlled by the molecular diffusion through a thin boundary layer near the wall. From Fick's laws, the rate constant of a wall reaction can be derived:

$$k_{10} = \frac{D}{\delta} \frac{A}{V} \qquad (9)$$

where   $D$ = diffusion constant      $(cm^2 \ s^{-1})$
        $\delta$ = boundary layer thickness $(cm)$

From $k_{10}$ (Table VII) and A/V = 0.12 $cm^{-1}$ (67 l vessel) and $D_{NO_3}$ = 0.12 $cm^2 s^{-1}$ (calculated following the method outlined by Perry and Chilton (1973)) one finds: $\delta$ = 0.18 cm. For the 236 l vessel, we obtain $\delta$ = 0.26 cm. In order of magnitude, these results agree well with the considerations of Ten Brink et al. (1982), who state that in flow reactors the thickness of the boundary layer is of the order of millimeters.

From the present results, it cannot be determined whether the wall reaction (R10) is surface-reaction-limited or diffusion-limited or that it is controlled by both diffusion and surface reaction. The problem is that neither $\alpha$ nor $\delta$ can be obtained independently of the value of $k_{10}$. Therefore, we may only conclude that the $\alpha$ values are lower limits, whereas the values of $\delta$ are upper limits.

Temperature behaviour is considered as the last point of discussion in this section. A clear reduction of S was found with increasing temperature (Table IV). This reduction is mainly caused by the strong temperature dependence of the equilibrium formed by the reactions (R3) and (R4). From the rate constants for (R3) and (R4) given in Table VI, it can be seen that the equilibrium shifts to the left at higher temperatures which results in a lower stoichiometric factor. From the kinetic analysis at several temperatures, the Arrhenius expression for reaction (R2) can be deduced (the Arrhenius plot is given in Figure 5). From a least-squares fit of the data points, the Arrhenius expression can be expressed as:

$$k_2 = (2.3 \pm 0.2) \times 10^{-13} \exp ((-2620 \pm 90)/T) \; cm^3 \; molecule^{-1} \; s^{-1} \qquad (10)$$
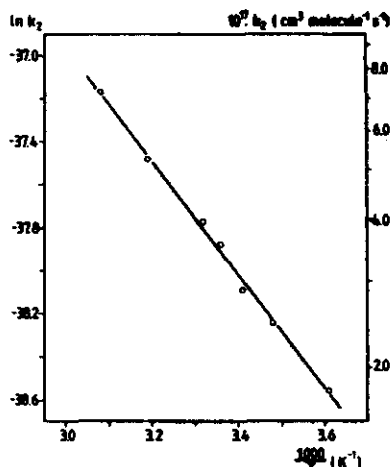


FIGURE 5.   Arrhenius-plot for reaction (R2).

This result is compared with the preferred value recommended by Baulch et al. (1982) given in Table VI. This value has been derived from the data of the three temperature depended studies mentioned in Table I. The activation energy agrees reasonably well, but there is a difference in the pre-exponential factor. The reason for this discrepancy is not obvious, but might be due to the different experimental systems and different analytical techniques. The pre-exponential factor appears to agree well with the theoretical value based on the transition state theory as calculated by Herschbach et al. (1956).

## 4.2.   The $NO_2$-$O_3$ system under 'wet conditions'

The increase in S at higher R.H. was related to reaction (R5). The results of the kinetic analysis are summarized in Table IX. From this table it can be seen that the $k_2$ values obtained both under 'dry' and 'wet conditions' show no differences. The observed values for $k_5'$ are shown in Figure 6 as a function of R.H. It appears that $k_5'$ is not directly proportional to R.H.
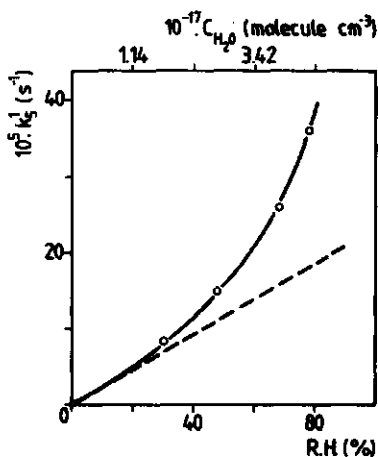
FIGURE 6. $k_5'$ as a function of R.H.; T = 293 K.

This means that most probably (R5) is a heterogeneous reaction of which the rate strongly depends on the amount of $H_2O$ deposited on the vessel wall. This result contrasts with the observations of Morris and Niki (1973) who state that (R5) might be a homogeneous gas phase reaction. Also quantitative agreement is lacking; Morris and Niki (1973) report a rate constant of $1.3 \times 10^{-20}$ $cm^3$ $molecule^{-1}$ $s^{-1}$ at 298 K, this corresponds with a pseudo-first-order rate constant of $4.5 \times 10^{-3}$ $s^{-1}$ at R.H. 50%. With the use of this rate constant the stoichiometric factor can be calculated to be 1.85, much higher than the value found in the present study. Our results agree much better with Atkinson et al. (1982), who report a rate constant of $3.0 \times 10^{-21}$ $cm^3$ $molecule^{-1}$ $s^{-1}$ ($k_5'$ is $1.0 \times 10^{-3}$ $s^{-1}$ at R.H. 50 %) and note that the reaction is heterogeneous.

In a recent paper, Tuazon et al. (1983) report on the $N_2O_5$ decay rates as a function of water vapour concentration, an upper limit to $k_5$ of $2.4 \times 10^{-21}$ $cm^3$ $molecule^{-1}$ $s^{-1}$ is found. It appears that the $N_2O_5$ decay involves both homogeneous and heterogeneous processes. From the measured concentrations of gas phase nitric acid an upper limit estimate of the gas phase homogeneous rate constant for (R5) of $1.3 \times 10^{-21}$ $cm^3$ $molecule^{-1}$ $s^{-1}$ (298 K) is obtained.

An upper limit estimate of the homogeneous rate constant can also be

determined from the present results. To that end, we take the tangent of the R.H.-$k_5'$ curve, as shown in Figure 6. The slope of this line can be considered as the upper limit estimate: $4 \times 10^{-22}$ cm$^3$ molecule$^{-1}$ s$^{-1}$ at 293 K.

This value is lower than that of Tuazon et al. (1983) but, however, this might be due to the different temperature. In fact, a rough estimate of the activation energy can be obtained: 170 kJ/mol. This rather high value might reflect the complexity of the atom shuffling that presumably occurs in the passage from reactants to products. Such a strong temperature dependence has also been deduced from atmospheric $NO_3$ concentration measurements (Atkinson et al., 1986).

The heterogeneous contribution of (R5) can be discussed using equations (7) to (9). It is unlikely that diffusion limitation occurs, since equation (9) leads to unrealistic high values of $\delta$. With the equations (7) and (8) accommodation coefficients of $10^{-9}$ to $10^{-6}$ can be obtained from the values of $k_5'$ given in Table IX.

The heterogeneity of (R5) is further confirmed by the behaviour of the reaction system after exposure of the reaction vessel to a R.H. of 78% for some time. We see a sharp increase in S (Table VIII). This is also the case with $k_5'$, which can be calculated to be $1.5 \times 10^{-2}$ s$^{-1}$. This means that in this situation the rate of $N_2O_5$ hydrolisis is comparable to the rate of $NO_3$ wall conversion. This is an indication that these rates are controlled by molecular diffusion through a thin boundary layer near the wall. We believe that the rapid scavenging of $N_2O_5$ is due to the presence of sufficient $H_2O$ in its condensed state. Possibly during the exposure with $H_2O(g)$ a water layer is formed at the reactor wall or $H_2O(l)$ is deposited in the pores of the reactor wall (capillary condensation). Under such conditions the system is dominated by the $N_2O_5$ scavenging as follows from the stoichiometric factor which approximates a value of 2. Ten Brink et al. (1982) also concluded that the $N_2O_5$ scavenging is enhanced by a water layer formed at the wall of a reaction vessel.

In the above considerations, the influence of R.H. on the $NO_2$-$O_3$ system is treated using the rate constant of the $NO_3$ wall reaction ($k_{10}$) obtained at R.H. <0.1%. It must be realized that this rate constant may undergo changes, since the wall properties are believed to change in the presence of $H_2O$. However, we believe that there are no significant changes in $k_{10}$ to

be expected (see also Chapter 6). Another aspect, which has not yet been discussed, is the possibility of $NO_3$ wall scavenging leading to formation of nitrate as reported by Chameides and Davis (1983). This process alone cannot be responsible for the observed phenomena, since model calculations show that the stoichiometric factor decreases when R.H. increases, in contrast with the present results. The $NO_3$ scavenging may still occur simultaneously with $N_2O_5$ scavenging. However, the rate of $NO_3$ scavenging will be very small compared to that of $N_2O_5$ scavenging as follows from the stoichiometric factor of about 2.

**THE DYNAMIC BEHAVIOUR OF AEROSOL PARTICLES IN A CONTINUOUS STIRRED
TANK REACTOR**

5.1. INTRODUCTION

In the previous chapter we have ascertained that heterogeneous processes
occurring at the reactor wall seem to be essential in the description of
the chemistry of the $NO_2-O_3$ system. In the ambient environment these
heterogeneous processes may occur through interactions with aerosol
particles. Before we discuss the $NO_2-O_3$-aerosol chemistry, we must pay
attention to the dynamic behaviour of aerosol particles when they are
flushed through a spherical continuous stirred tank reactor.

The aerosol behaviour in a reaction vessel is determined by the process
of coagulation and by deposition processes. The theory of these processes has
been extensively described by Van de Vate (1980). A brief summary is given
below.

Aerosol particles move in arbitrary direction with different velocities.
Mutual inelastic collisions leading to the formation of new particles cause
the so-called Brownian coagulation. Besides particle growth, Brownian coagu-
lation leads to a decay of the particle number concentration (N), which for a
polydispers aerosol is expressed by:

$$- \frac{d\ N_{t,n}}{dt} = \sum_{m=1}^{n} K_{nm}\ N_{t,n}\ N_{t,m} \qquad (1)$$

where $K_{nm}$ is the coagulation constant. The subscripts n and m denote a given
size range. The coagulation constant is a function of several parameters such
as particle diameter, diffusion coefficient of the particle and the average
velocity of the particles. Several theories that describe $K_{nm}$ as a function
of these parameters are available in the literature (e.g. Fuchs. 1964;

Walter, 1973; Davies, 1979). The coagulation process is especially effec-
tive for relatively high particle number concentrations, because it is a
second-order process.

Another important aerosol loss process is that of deposition of the aerosol
particles on the walls of the reaction vessel. Several mechanisms can act
as driving force for deposition: gravitational sedimentation, Brownian and
turbulent diffusion, thermophoresis, diffusiophoresis, electrophoresis and
photophoresis. In general, the deposition loss rate is defined by the
equation:

$$- \frac{d \ N_{t,n}}{dt} = \beta_n \ N_{t,n} \tag{2}$$

where $\beta_n$ denotes the wall loss coefficient. Equation (2) holds provided the
aerosol in the vessel is well mixed, except in a small boundary layer near
the wall. The wall loss coefficient can be considered as the product of the
deposition velocity ($v_{d,n}$) and the surface/volume-ratio (A/V) of the reaction
vessel.

$$\beta_n = v_{d,n} \ \frac{A}{V} \tag{3}$$

Theoretical relations of the deposition velocity for the different deposi-
tion mechanisms are given by Van de Vate (1980). It appears that irrespec-
tive of the deposition mechanism, $v_{d,n}$ is a function of the particle diameter.

This chapter deals with the determination of the properties of an arti-
ficially generated aerosol, which is supplied to a continuous stirred tank
reactor. The difference between the characteristics of the input aerosol
and the aerosol characteristics in the CSTR under steady-state conditions
is discussed.

## 5.2. EXPERIMENTAL

A design of the flow system with which the experiments were performed is
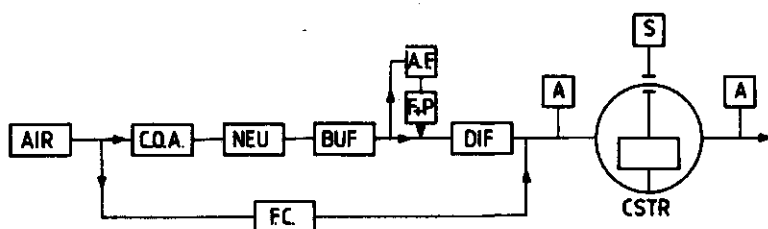is schematically shown in Figure 1.

FIGURE 1. Schematic outline for the experimental set-up.
AIR : clean, dry compressed air (3 atm.); F.C. :flow
controlling divice; C.O.A. : constant output atomizer;
NEU : neutralizer; BUF : 10 l buffer vessel; A.F. :
absolute filter; F + P : pump in connection with flow
controller and flowmeter; DIF : diffusion dryer; A :
sampling point; CSTR : continuous stirred tank reactor;
S: stirrer.

A large part of the experimental set-up consisted of an air flow system
in which aerosol particles were generated and treated for proper use. This
stream was diluted with air to a total flow rate of 400 l/h and sub-
sequently fed to the CSTR. The 236 l reaction vessel used was described in
the chapters 3 and 4. The temperature in the reaction vessel was kept at
298 K and light was excluded in all experiments.

The aerosol was produced by atomization of NaCl or $MgCl_2$ solutions by means
of a Constant Output Atomizer (TSI model 3076), followed by passage through
a Kr-85 charge neutralizer (TSI model 3054). Next, the aerosol was passed
through a 10 l buffer vessel in order to avoid fluctuations in the particle
number concentration. Dilution of the aerosol was realized by circulating
a well-known part of the aerosol stream over an absolute filter (HEPA,
Gelman). In this way the particle number concentration could be easily
varied.

Two types of aerosols were distinguished : 'dry' aerosol (only NaCl) and
'wet' aerosol (NaCl and $MgCl_2$). The 'dry' aerosol was obtained by passing
the aerosol particles through the diffusion dryer, which reduced the rela-
tive humidity to 25%. Through dilution with dried air, the R.H. in the
vessel was about 15%. Under these conditions the aerosol consisted of small
NaCl crystals. In the case of 'wet' aerosol, the diffusion dryer was

bypassed and the dilution air was partly humidified, which led to a R.H. of about 78% in the vessel. At this R.H., NaCl as well as $MgCl_2$ is deliquescent: the 'wet' aerosol can be considered as small droplets of concentrated NaCl or $MgCl_2$ solutions.

The system was allowed to reach steady state, after which measurements were made of both the CSTR output and the feed. The particle number concentrations were measured with a Condensation Nucleus Counter (TSI model 3020). Size distributions were obtained with an Electrical Aerosol Analyzer (TSI model 3030). The currents measured with EAA were converted to particle number concentrations using the monodisperse sensitivities of Liu et al. (1976) as well as the method of Liu and Kapadia (1977). With the latter method the EAA data were corrected for cross-sensitivity and the size distribution was lognormally described.


5.3. RESULTS

With the applied aerosol generation method, a constant supply of aerosol particles could be maintained for several hours. Figure 2 shows an electron micrograph of feed NaCl 'dry' aerosol particles. The aerosol has
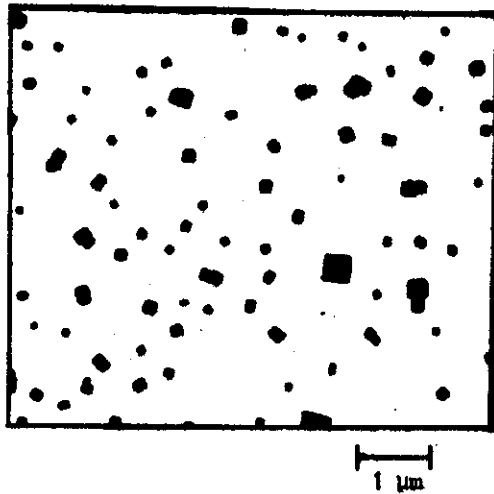


1 μm

FIGURE 2.    Transmission electron micrograph of the 'dry' NaCl aerosol

been sampled on the electron microscope grid by electrostatic precipitation with an electrostatic precipitator as described by Van de Vate et al. (1978). The polydisperity of the aerosol generated is clearly indicated by the electron micrograph. Likewise, the cubic structure of the NaCl aerosol can be seen, which is an indication for the crystalline properties of the 'dry' aerosol.
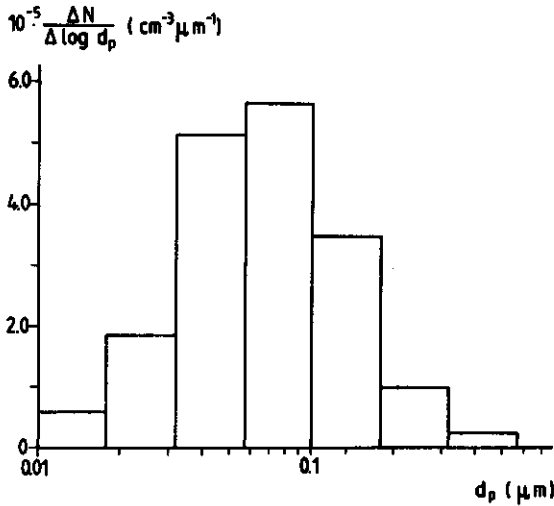


FIGURE 3.    Histogram of the size distribution of the feed aerosol.
Experiment 1, Table I

A size distribution of feed aerosol is shown in Figure 3. The histogram depicts the direct output of the EAA converted to particle number concentrations. The lognormal distribution, described by :

$$\frac{dN}{d \log d_p} = \frac{1}{\sqrt{2\pi} \log \sigma_g} \exp \left( - \frac{(\log d_p - \log d_{p,g})^2}{2 (\log \sigma_g)^2} \right) \qquad (4)$$

is obtained by applying the method of Liu and Kapadia (1977) and is shown in Figure 4 by the solid line. The dashed line gives the corresponding CSTR output lognormal size distribution.

TABLE I. The results of a number of experiments[a]

| Exp. | $N_o$ $(cm^{-3})$ | $d_{p,g,o}$ $(\mu m)$ | $\sigma_{g,o}$ | $V_o$ $(\mu m^3 cm^{-3})$ | aerosol type | R.H. (%) | $N_{ss}$ $(cm^{-3})$ | $d_{p,g,ss}$ $(\mu m)$ | $\sigma_{g,ss}$ | $V_{ss}$ $(\mu m^3 cm^{-3})$ | $\beta_a$ $(s^{-1})$ | $v_{d,a}$ $(cm\ s^{-1})$ | $K_a$ $(cm^3\ s^{-1})$ |
|---|---|---|---|---|---|---|---|---|---|---|---|---|---|
| 1. | $4.3 \times 10^5$ | 0.06 | 1.87 | $2.8 \times 10^2$ | NaCl | 15 | $1.7 \times 10^5$ | 0.09 | 1.7 | $2.3 \times 10^2$ | $1.0 \times 10^{-4}$ | $1.3 \times 10^{-3}$ | $3.6 \times 10^{-9}$ |
| 2. | $4.5 \times 10^5$ | 0.065 | 1.9 | $4.1 \times 10^2$ | NaCl | 15 | $2.0 \times 10^5$ | 0.085 | 1.75 | $2.6 \times 10^2$ | $2.7 \times 10^{-4}$ | $3.4 \times 10^{-3}$ | $1.6 \times 10^{-9}$ |
| 3. | $1.2 \times 10^5$ | 0.06 | 1.8 | 64 | NaCl | 15 | $6.3 \times 10^4$ | 0.08 | 1.6 | 47 | $1.7 \times 10^{-4}$ | $2.1 \times 10^{-3}$ | $4.1 \times 10^{-9}$ |
| 4. | $2.7 \times 10^6$ | 0.07 | 1.9 | $3.1 \times 10^3$ | NaCl | 15 | $7.8 \times 10^5$ | 0.13 | 1.6 | $2.3 \times 10^3$ | $1.6 \times 10^{-4}$ | $2.0 \times 10^{-3}$ | $1.3 \times 10^{-9}$ |
| 5. | $1.3 \times 10^5$ | 0.09 | 2.0 | $4.3 \times 10^2$ | NaCl | 15 | $8.4 \times 10^4$ | 0.13 | 1.7 | $3.4 \times 10^2$ | $1.2 \times 10^{-4}$ | $1.5 \times 10^{-3}$ | $1.6 \times 10^{-9}$ |
| 6. | $1.2 \times 10^6$ | 0.10 | 1.95 | $4.7 \times 10^3$ | NaCl | 15 | $5.1 \times 10^5$ | 0.15 | 1.7 | $3.2 \times 10^3$ | $2.2 \times 10^{-4}$ | $2.75 \times 10^{-3}$ | $0.8 \times 10^{-9}$ |
| 7. | $1.2 \times 10^4$ | 0.11 | 1.9 | $5.3 \times 10^3$ | NaCl | 15 | $5.4 \times 10^5$ | 0.16 | 1.7 | $3.9 \times 10^3$ | $1.7 \times 10^{-4}$ | $2.1 \times 10^{-3}$ | $0.8 \times 10^{-9}$ |
| 8. | $7.0 \times 10^6$ | 0.11 | 1.95 | $3.6 \times 10^4$ | NaCl | 15 | $1.7 \times 10^6$ | 0.17 | 1.8 | $2.1 \times 10^4$ | $3.4 \times 10^{-4}$ | $4.3 \times 10^{-3}$ | $0.7 \times 10^{-9}$ |
| 9. | $6.5 \times 10^4$ | 0.13 | 1.9 | $4.8 \times 10^4$ | MgCl$_2$ | 78 | $1.7 \times 10^6$ | 0.21 | 1.7 | $2.9 \times 10^4$ | $3.1 \times 10^{-4}$ | $3.9 \times 10^{-3}$ | $0.6 \times 10^{-9}$ |
| 10. | $6.7 \times 10^6$ | 0.17 | 1.95 | $1.3 \times 10^5$ | MgCl$_2$ | 78 | $1.6 \times 10^6$ | 0.29 | 1.7 | $7.3 \times 10^4$ | $3.7 \times 10^{-4}$ | $4.6 \times 10^{-3}$ | $0.7 \times 10^{-9}$ |
| 11. | $1.8 \times 10^6$ | 0.17 | 1.9 | $3.0 \times 10^4$ | MgCl$_2$ | 78 | $5.3 \times 10^5$ | 0.27 | 1.7 | $1.9 \times 10^4$ | $2.7 \times 10^{-4}$ | $3.4 \times 10^{-3}$ | $1.6 \times 10^{-9}$ |
| 12. | $8.4 \times 10^5$ | 0.16 | 2.0 | $1.6 \times 10^4$ | MgCl$_2$ | 78 | $2.8 \times 10^5$ | 0.25 | 1.8 | $1.1 \times 10^4$ | $2.1 \times 10^{-4}$ | $2.6 \times 10^{-3}$ | $1.6 \times 10^{-9}$ |

a) Symbols: $d_{p,g}$ = geometrical mean diameter; $\sigma_g$ = geometrical standard deviation; $N$ = particle number concentration; $V$ = particle volume concentration; $\beta_a, v_{d,a}, K_a$ : see text (5.4 Discussion)

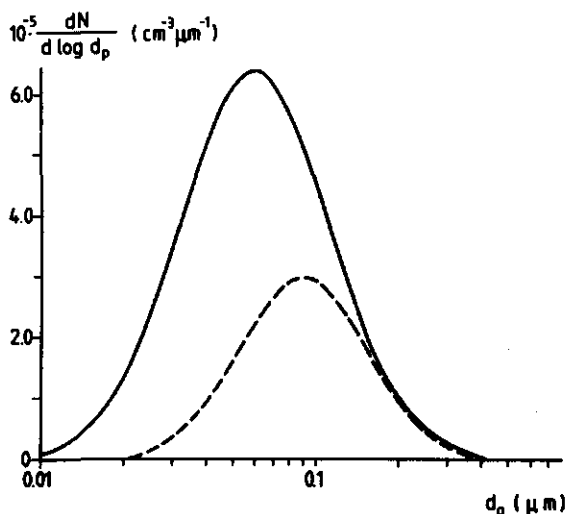Subscripts: o = feed; ss = steady state.

FIGURE 4.    Lognormal distribution of the feed (————) and output (·····)
aerosol. Experiment 1; Table I.

Several experiments were performed where the lognormal distribution of
the feed and of the steady-state output aerosol was determined. Table I
gives the results. The particle number concentration, the geometrical mean
diameter, the geometrical standard deviation and the particle volume con-
centration of both feed and steady-state output aerosol are given for
several types of aerosol. The size distribution parameters given are the
average of five EAA measurements. A general feature of the results is the
clear decrease in the particle number concentration, when the aerosol is
passed through the CSTR, whereas the particle volume concentration only
slightly decreases. Also the size distribution changes, notably : an
increase of the geometrical mean diameter and a decrease of the geometrical
standard deviation.


5.4.   DISCUSSION

It can be expected that Brownian coagulation is an important process in
the CSTR, because of the relatively high feed particle number concentration.
Table I clearly indicates that this is the case. Brownian coagulation leads
to a decrease in N and to a change of the size distribution. Recently, some
theoretical work on the Brownian coagulation of a lognormally distributed

aerosol has been reported (Lee, 1983; Lee et al., 1984). Assuming that the lognormal distribution is preserved during the coagulation process, it can be shown that the size distribution shifts to a larger $d_{p,g}$ and a smaller $\sigma_g$. These considerations are in accordance with the observations in this study.

Apart from Brownian coagulation, deposition of aerosol particles on the wall takes place in the reaction vessel. This is illustrated by the difference between the feed and steady-state particle volume concentration. This difference is due to wall deposition, since the aerosol volume is conserved in the coagulation process. The wall loss coefficient can be calculated with the steady state balance of the particle volume concentration :

$$V_0 \cdot \theta = V_{ss} \cdot \theta + \beta_a \, V_{ss} \qquad (5)$$

The wall loss coefficient is denoted $\beta_a$, since it is an average value for the polydisperse aerosol during its residence time in the CSTR. The values of $\beta_a$ obtained with this method are given in Table I, together with the corresponding values for $v_{d,a}$ taking $A/V = 0.08$ cm$^{-1}$.

These results can be discussed referring to the various deposition mechanisms as mentioned in the introduction. The mechanisms of photophoresis, thermophoresis and diffusiophoresis are ineffective in the dark, temperature controlled reaction vessel and in the absence of strong condensation or evaporation. Deposition due to gravitation settling can also be considered as an unimportant factor. The gravitational sedimentation velocity can be calculated from Stokes law (see Van de Vate, 1980) : for particles of 0.3 $\mu$m with a particle density of 1.2 g/cm$^3$, the sedimentation velocity is about $10^{-4}$ cm/s.

The mechanisms of electrophoresis as well as Brownian and turbulent diffusion have to be considered, since both are likely to be relevant in the present study.

The deposition velocity of diffusion is given by :

$$v_d = \frac{D}{\delta} \qquad (6)$$

Van de Vate (1980) reports on diffusion processes in an enclosed reaction vessel without mechanical stirring. He finds that the boundary layer

thickness ($\delta$) is a function of the diffusion constant (D). The following empirical relation was given :

$$\delta = 4.6 \ D^{\ 0.265} \tag{7}$$

where D is the Brownian diffusion constant, which can be expressed as :

$$D = \frac{kT}{3\pi \ \eta \ d_p} \cdot C \tag{8}$$

where      k = Boltzmann constant
                   $\eta$ = viscosity of air
                   C = slip correction factor

Using this method, we find for particles with $d_p = 0.1$ $\mu$m at 298 K : D = $2.3 \times 10^{-6}$ cm² s⁻¹ and subsequently $v_d = 7.2 \ 10^{-5}$ cm s⁻¹. This value is much lower than those given in Table I. The reason for this discrepancy is the fact that turbulent diffusion is not included in Van de Vate's model. Recently, it has been shown theoretically as well as experimentally (Crump and Seinfeld, 1981; Crump et al., 1983; Holländer et al., 1984; McMurry and Grosjean, 1985) that in the case of considerable dissipation of turbulent energy (such as in flow systems) the effective boundary layer thickness is much smaller as predicted by equation (7). Hence, the rate of aerosol wall deposition is significantly enhanced due to turbulent diffusion.

The present results can be best compared to the study of Crump et al. (1983), who have determined the particle wall loss rate in a spherical flow reactor of 118 l. Figure 5 shows their results at various particle diameters.
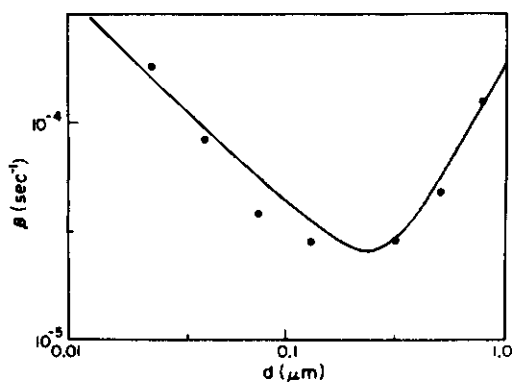


FIGURE 5.   $\beta$ as a function of $d_p$ according to Crump et al. (1983)

The shape of the curve is caused by diffusive deposition, which is effective at low $d_p$, and by gravitational settling, which is effective at high $d_p$. There are two clear differences between the results of Crump et al. (1983) and the results of Table I. Firstly, the numerical values do not agree and secondly, the results of Crump et al. (1983) show a clear decrease of $\beta$ going from $d_p = 0.06$ $\mu$m to 0.3 $\mu$m, whereas the present results appear to show no dependence on $d_p$. There is however considerable scatter in the data. The former is probably due to a difference in the experimental set-up. The reaction vessel of Crump et al. (1983) is not provided with a mechanical stirring apparatus in contra-distinction with the present investigation. Mechanical stirring leads to an increase in the dissipation of turbulent energy and, consequently, to a higher wall loss rate (Okuyama et al., 1984). The latter is possibly caused by charge effects. The particles leaving the neutralizer, attain a Boltzmann charge distribution and, since the glass wall is likely to be electrically charged, electrophoresis may occur. The effect of this electrostatic deposition on the wall loss rate is theoretically and experimentally studied by McMurry and Grosjean (1985) and is shown in Figure 6.
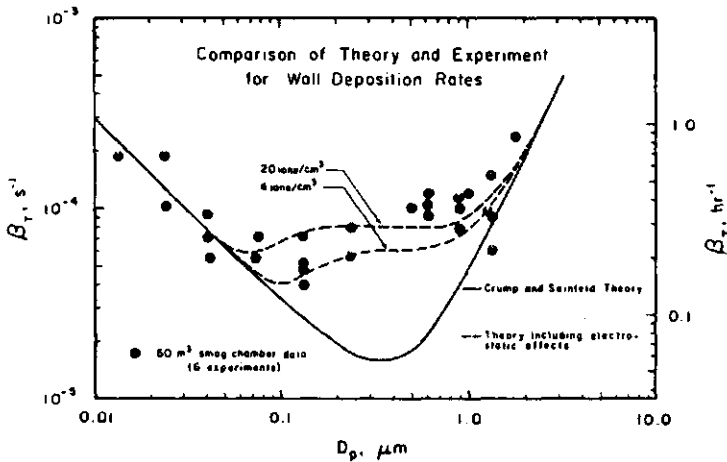


FIGURE 6.   The effect of electrostatic deposition on wall deposition rates (from: McMurry and Grosjean (1985))

It can be seen that electrostatic deposition significantly affects deposition rate for particles in the 0.05 - 1.0 $\mu$m diameter range. The wall loss

coefficient is predicted to be nearly independent of $d_p$, in accordance with the present results. It is likely that these charge effects are an highly variable uncontrolled factor and may account for the scatter in the data.

We may conclude that probably the wall deposition of the aerosol particles can be explained by turbulent diffusion and electrostatic transport.

Finally, we return to the discussion of the Brownian coagulation. Using the values of $\beta_a$, we can calculate the coagulation constant from the steady-state balance of the particle number concentration :

$$\Theta \cdot N_o = \Theta \cdot N_{ss} + \beta_a N_{ss} + K_a N_{ss}^2 \tag{9}$$

Again, the value of $K_a$ is an average for the polydisperse aerosol during the residence time in the CSTR. The values of $K_a$ are listed in Table I. There is considerable scatter in the $K_a$ data and it appears that the calculated $K_a$ value depends on $N_o$. A summary of literature data is given by Van de Vate (1980), the values commonly reported for polydisperse aerosol vary between $0.5 \times 10^{-9}$ and $2.0 \times 10^{-9}$ cm³ s⁻¹. Some of the present data agree reasonably well with the literature. A plausible explanation for the scatter in the data may be the influence charge effects.

TABLE II.    Sensitivity calculation for experiment 7 of Table I

| $N_o$ (cm⁻³) | $d_{p,g,o}$ (μm) | $\sigma_{g,o}$ | $\beta_a$ (s⁻¹) | $K_a$ (cm³s⁻¹) |
|---|---|---|---|---|
| $1.2 \times 10^6$ | 0.11 | 1.9 | $1.7 \times 10^{-4}$ | $0.8 \times 10^{-9}$ |
| $1.0 \times 10^6$ | 0.11 | 1.9 | $6.7 \times 10^{-5}$ | $0.9 \times 10^{-9}$ |
| $1.4 \times 10^6$ | 0.11 | 1.9 | $2.8 \times 10^{-4}$ | $0.5 \times 10^{-9}$ |
| $1.2 \times 10^6$ | 0.10 | 1.9 | $1.2 \times 10^{-5}$ | $1.0 \times 10^{-9}$ |
| $1.2 \times 10^6$ | 0.12 | 1.9 | $3.6 \times 10^{-4}$ | $0.4 \times 10^{-9}$ |
| $1.2 \times 10^6$ | 0.11 | 2.0 | $4.1 \times 10^{-4}$ | $0.3 \times 10^{-9}$ |
| $1.2 \times 10^6$ | 0.11 | 1.8 | $7.2 \times 10^{-6}$ | $1.1 \times 10^{-9}$ |

The scatter in the data may also be expected regarding the accuracy of the experiments. The accuracy of the parameters listed in Table I can be estimated to be 5 to 10 %. It appears that changes of this magnitude lead to drastic changes in the values of $\beta_a$ and $K_a$. See for example Table II, where the sensitivity of the calculated $\beta_a$ and $K_a$ values is shown for experiment 7 of Table I.

**THE NO$_2$-O$_3$ SYSTEM AT SUB-PPM CONCENTRATIONS: INFLUENCE OF SUB-MICRON NaCl AND MgCl$_2$ AEROSOL**

## 6.1.  INTRODUCTION

In chapter 4, we have focussed attention on the oxidation of NO$_2$ by O$_3$ as a formation mechanism of atmospheric nitric acid. It is shown that the results give rise to consider heterogeneous reactions. The NO$_3$ wall conversion to NO$_2$ and the N$_2$O$_5$ wall scavenging in the presence of H$_2$O are suggested to account for the observed results.

In the atmosphere, heterogeneous reactions mainly manifest themselves as interactions between gaseous species and aerosol particles. With respect to the atmospheric NO$_2$-O$_3$ chemistry the potential significance of such hetero-geneous interactions has been recognized for some time. Especially, the nitrate formation by heterogeneous N$_2$O$_5$ hydrolysis is believed to play a role in nocturnal NO$_x$ chemistry. It has been proposed as an explanation for a number of field observations (Richards, 1983; Heikes and Thomson, 1983; Atkinson et al., 1986). Furthermore, a number of model studies (Heikes and Thomson, 1983; Russell et al., 1985; Seigneur and Saxena, 1984) have shown the potential importance of nitrate formation by N$_2$O$_5$ scavenging on wet particles. However, the model results are limited to sensitivity studies alone because the necessary information to quantify the N$_2$O$_5$ sca-venging is unavailable. For example, a realistic value of the accommodation coefficient for in-cloud N$_2$O$_5$ scavenging is not available.

The heterogeneous N$_2$O$_5$ hydrolysis has been investigated in a few laboratory studies. Cox (1974) has studied the influence of artificially generated ammonium sulfate aerosol on the NO$_2$-O$_3$ chemistry. It was shown that at high R.H.. when the ammonium sulfate aerosol consisted of droplets,

the incorporation of the $NO_2$ oxidation products was particularly efficient. Unfortunately, a value of the accommodation coefficient was not given. Harker and Strauss (1981) investigated the interaction of $N_2O_5$ with sulfuric acid aerosol and reported accommodation coefficients of about $10^{-3}$ to $10^{-4}$ depending on the temperature.

Heterogeneous loss processes of the $NO_3$ radical have received considerably less attention. Chameides and Davis (1983) have suggested that the scavenging of $NO_3$ radicals by droplets may lead to significant nitrate formation. Model sensitivity calculations have shown that $NO_3$ radical scavenging is only effective if its scavenging efficiency is significantly higher than that of $N_2O_5$ (Heikes and Thompson, 1983; Seigneur and Saxena, 1984). An $NO_3$ loss process with subsequent formation of $NO_2$ such as the wall reaction proposed in chapter 4 has not yet been reported in the literature.

In this chapter, we report on the influence of sub-micron aerosol particles on the $NO_2$-$O_3$ chemistry as encountered in chapter 4. The aerosol particles used consisted of NaCl and $MgCl_2$. Particles of this type were used because of their abundant presence in the atmosphere and because of their hygroscopic nature, so they form droplets at high R.H.. Moreover, they could easily be artificially generated as described in chapter 5. The dynamic behaviour of this type of aerosol was also described in the previous chapter.

## 6.2. EXPERIMENTAL

The experimental equipments described in the chapters 4 and 5 were connected. Only the 236 l vessel was used. In all experiments, the temperature was kept constant at 298 K, whereas the flow rate was maintained constant at 400 l/h. The input concentrations were hold at 395 ppb for $NO_2$ and 190 ppb for $O_3$. The particle number concentration and the size distribution of the aerosol were varied. The methods of analysis for both gaseous species and aerosol particles were also described in the previous chapters.

Again 'dry' and 'wet' aerosol particles were distinguished. With the use of a diffusion dryer and dilution with dry air, a 'dry' aerosol (NaCl) was obtained at a R.H. of 15% in the reaction vessel. 'Wet' aerosol (NaCl,

$MgCl_2$) was obtained by bypassing the diffusion dryer and dilution with humid air to a R.H. of 78% in the reaction vessel.

The following procedure was applied in all experiments. The $NO_2$ and $O_3$ were supplied to the reaction vessel and the desired relative humidity was realized by feeding the atomizer with pure, liquid water and proper dilution. This means that an experiment was started without a supply of aerosol particles. This system was allowed to reach steady-state, after which measurements of the $NO_2$ and $O_3$ concentration were made. Next, the pure, liquid water was replaced by the salt solution to be atomized, so that the aerosol particles were supplied to the reaction vessel. Again, the system was allowed to reach steady state, after which the change in $NO_2$ or $O_3$ concentration was detected and the aerosol properties were measured. After that the aerosol feed was characterized. During the night and at the weekends, the system was fed with dry air only, in order to avoid the formation of a water layer on the vessel wall.

In a number of experiments the aerosol particles were sampled for nitrate analysis. The particles were collected on a Teflon filter using a Teflon filter holder and a pump connected in series with a gasmeter. The sample time was two minutes, the flow through the filter was approximately 200 l/h. Next, the particles were released from the filter and dissolved in 2 ml of pure, liquid water applying an ultrasonic water bath. The nitrate analyses were performed by ion chromatography using a conventional isocratic HPLC system (described in detail in Chapter 7).

## 6.3. RESULTS

### 6.3.1. Experiments with 'dry' aerosol

In all experiments, no change in the steady-state $O_3$ concentration could be detected when the aerosol particles were supplied to the reaction vessel. This means that the kinetics of ozone removal are not significantly affected by the presence of aerosol particles. Consequently, $O_3$ is not significantly destroyed at the particle surface. Therefore, we can give the results in terms of the stoichiometric factors corrected for $O_3$ wall decomposition such as described in chapter 4. Table I summarizes the stoichiometric factors obtained.

TABLE I.  The stoichiometric factor in the presence of 'dry' NaCl aerosol.
236 l vessel; T = 298 K; $c_{o,NO_2}$ = 395 ppb; $c_{o,O_3}$= 190 ppb; $\theta$ = 1.7 $h^{-1}$; R.H. = 15%

| case | $d_{p,g,ss}$ ($\mu m$) | $\sigma_{g,ss}$ | $N_{ss}$ ($cm^{-3}$) | S | $\sigma_S$ | n |
|------|------|------|------|------|------|------|
| A | - | - | - | 1.42 | 0.05 | 10 |
| B | 0.09 | 1.7 | $1.1x10^6$ | 1.4 | 0.1 | 3 |
| C | 0.15 | 1.8 | $2.1x10^5$ | 1.4 | 0.1 | 3 |
| D | 0.17 | 1.8 | $1.7x10^6$ | 1.24 | 0.09 | 4 |

It can be seen that the $NO_2$-$O_3$ system is rather insensitive to the presence of sub-micron NaCl aerosol at R.H. 15%. Only in case D a significant decrease in S is apparent. Case D contains the most extreme aerosol conditions that can be realized with the present aerosol generation equipment. The decrease in S of case D is caused by an increase in the steady-state $NO_2$ concentration of approximately 10 ppb.

The kinetics can be described by the mass balance equations given in chapter 4 and applying the reaction combination (R2), (R3), (R4), (R5) and (R10). The relevant reaction expressions and literature data are summarized in Table VI of chapter 4. The reaction rate constants for (R2) and (R10) are determined. It is already mentioned that the kinetics of ozone removal are unaffected. This is reflected by the mean value of $k_2$, which is 3.6x $10^{-17}$ $cm^3molecule^{-1}s^{-1}$ in accordance with previous results. The mean value of $k_{10}$ for the cases A, B and C is calculated to be $3.6x10^{-2}$ $s^{-1}$, which corresponds with the rate constant for $NO_3$ loss at the wall of the reaction vessel. In case D a clear increase in $k_{10}$ is observed: $k_{10}$ = $5.5x10^{-2}$ $s^{-1}$.

### 6.3.2.  Experiments with 'wet' aerosol

Once more, the steady-state $O_3$ concentration did not change when 'wet' aerosol particles were present. The results are presented as stoichiometric factors corrected for $O_3$ wall decomposition, as shown in Table II.

TABLE II. The stoichiometric factor in the presence of 'wet' aerosol.
236 l vessel; T = 298 K; $c_{0,NO_2}$ = 395 ppb; $c_{0,O_3}$ = 190 ppb;
$\theta$ = 1.7 $h^{-1}$; R.H. = 78%

| Case | Aerosol | $d_{p,g,ss}$ (μm) | $\sigma_{g,ss}$ | $N_{ss}$ ($cm^{-3}$) | S | $\sigma_S$ | n |
|------|---------|------------|---------|--------|------|------|----|
| E | – | – | – | – | 1.54 | 0.06 | 14 |
| F | NaCl | 0.21 | 1.7 | $1.7 \times 10^6$ | 1.50 | 0.1 | 3 |
| G | $MgCl_2$ | 0.29 | 1.7 | $1.6 \times 10^6$ | 1.6 | 0.1 | 4 |
| H | $MgCl_2$ | 0.27 | 1.7 | $5.3 \times 10^5$ | 1.6 | 0.1 | 3 |
| I | $MgCl_2$ | 0.25 | 1.8 | $2.8 \times 10^5$ | 1.6 | 0.1 | 2 |
| J | $MgCl_2$ | 0.25 | 1.8 | $1.3 \times 10^5$ | 1.6 | 0.1 | 2 |

The results show that in the case of 'wet' aerosol, the stoichiometric factor is practically unchanged. The 'wet' NaCl aerosol shows a very small decrease in S, whereas with 'wet' $MgCl_2$ aerosol the stoichiometric factor is slightly increased. However, the changes in S are smaller than the standard deviation of the experiments and are in the order of magnitude of the accuracy of the $NO_x$ analyzer. It appears that the value of S is independent of the particle number concentration.

During the experiments with $MgCl_2$ aerosol, the particles were collected for nitrate analysis. Both feed and steady-state output aerosol were sampled. The feed did not contain any measurable nitrate. This is an indication that there is no artifact nitrate formation caused by $NO_2$ or the combination $NO_2-O_3$. In order to establish the possible interference of $N_2O_5$, a filter previously loaded with $MgCl_2$ aerosol was exposed to the steady-state $NO_2-O_3$ matrix at R.H. 78%. Only traces of nitrate were observed, typically in the order of magnitude of the detection limit of the ion chromatographic $NO_3^-$ analysis, i.e. 0.1 μM. This corresponds with a particle nitrate concentration of about $2 \times 10^{10}$ molecule $cm^{-3}$.

Table III gives the steady-state particle nitrate concentration obtained in the experiments with $MgCl_2$ aerosol at R.H. 78 %.

TABLE III.  Steady-state particulate nitrate concentration. Reaction
conditions: see Table II.

| Case | $c_{NO_3^-,ss}$ (molecule cm$^{-3}$) | $\sigma_c$ (molecule cm$^{-3}$) | n |
|------|------|------|---|
| G | $8.5 \times 10^{11}$ | $6 \times 10^{10}$ | 8 |
| H | $3.7 \times 10^{11}$ | $3 \times 10^{10}$ | 2 |
| I | $1.8 \times 10^{11}$ | $2 \times 10^{10}$ | 2 |
| J | $1.1 \times 10^{11}$ | $2 \times 10^{10}$ | 2 |

It can be seen that the particle nitrate concentration is clearly dependent
on the particle number concentration.

The interpretation of the kinetics is performed using the reaction com-
bination (R2), (R3), (R4), (R5) and (R10), where the rate constants for (R2)
and (R5) are calculated. For all experiments, the mean value of $k_2$ is found
consistent with previous results: $k_2 = 3.7 \times 10^{-17}$ cm$^3$molecule$^{-1}$s$^{-1}$. The
value of $k_5'$ has been calculated as a function of S, where S varies between
the limits given by the accuracy of the experiments. It is assumed that the
$NO_3$ loss reaction R(10) only takes place at the reactor wall. The results
are given in Table IV.

TABLE IV. The pseudo-first-order rate constant of (R5), $k_5'$ and its sen-
sitivity with respect to small changes in S

| S | $c_{ss,NO_2}$ (ppb) | $k_5'$ (s$^{-1}$) | $c_{ss,NO_3^-}$ (molecule cm$^{-3}$) |
|------|------|------|------|
| 1.54 | 287 | $2.9 \times 10^{-4}$ | 0 |
| 1.61 | 282 | $4.9 \times 10^{-4}$ | $5.9 \times 10^{11}$ |
| 1.69 | 277 | $7.8 \times 10^{-4}$ | $1.2 \times 10^{12}$ |

Also indicated in Table IV are the $c_{ss,NO_3}$- values that can be calculated, if it is assumed that in the lower limit of S (S=1.54) no particulate nitrate is formed. Furthermore, it is assumed that at the higher values of S the pseudo-first-order rate constant for particulate nitrate formation is given by the difference with this lower limit.

The results of Table IV have reference to all the experiments of the cases G to J. If compared with the results given in Table III, it is clear that only in case G the measured $c_{ss,NO_3}$ meets the calculated values. Obviously, the dependence on particle number concentration of $c_{ss,NO_3}$ is conflicting with the calculation based on measurements of S. Another flaw may be the assumption that the kinetics of $NO_3$ removal by (R10) are not influenced by the presence of aerosol particles.

Therefore, we have also made calculations using the results of Table III. The particulate nitrate formation can be expressed by reaction (R15):

$$N_2O_5 + \text{'wet' particle} \rightarrow 2(NO_3^- - \text{'wet' particle}) \tag{R15}$$
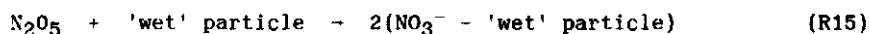
TABLE V. The calculated values of $k_{15}'$ and $k_{10}$ and their sensitivity to S. Details of the reaction conditions are given in Table II and III.

| | S = 1.54 | | S = 1.61 | | S = 1.69 | |
|------|----------|------|----------|------|----------|------|
| Case | $k_{15}'$ $(s^{-1})$ | $k_{10}$ $(s^{-1})$ | $k_{15}'$ $(s^{-1})$ | $k_{10}$ $(s^{-1})$ | $k_{15}'$ $(s^{-1})$ | $k_{10}$ $(s^{-1})$ |
| G | $3.5 \times 10^{-4}$ | $5.4 \times 10^{-2}$ | $3.3 \times 10^{-4}$ | $4.2 \times 10^{-2}$ | $3.1 \times 10^{-4}$ | $3.1 \times 10^{-2}$ |
| H | $1.2 \times 10^{-4}$ | $4.3 \times 10^{-2}$ | $1.1 \times 10^{-4}$ | $3.3 \times 10^{-2}$ | $1.1 \times 10^{-4}$ | $2.5 \times 10^{-2}$ |
| I | $5.5 \times 10^{-5}$ | $3.9 \times 10^{-2}$ | $5.2 \times 10^{-5}$ | $3.1 \times 10^{-2}$ | $5.0 \times 10^{-5}$ | $2.4 \times 10^{-2}$ |
| J | $3.2 \times 10^{-5}$ | $3.8 \times 10^{-2}$ | $3.1 \times 10^{-5}$ | $3.0 \times 10^{-2}$ | $2.9 \times 10^{-5}$ | $2.3 \times 10^{-2}$ |

Since $c_{ss,NO_3^-}$ is introduced as a new variable, an extra k value may be calculated. We have calculated the pseudo-first-order rate constant of (R15), $k_{15}'$, and the value of $k_{10}$, using the reaction combination (R2), (R3), (R4), (R5), (R10) and (R15). For $k_5'$ a value of $2.9 \times 10^{-4}$ $s^{-1}$ is used. This value represents $k_5'$ in absence of $MgCl_2$ aerosol particles.

The results are given in Table V (previous page). Again, the results are given for various values of S referring to its variability encountered in Table II. Moreover, the cases G to J are considered individually.

The dependence on particle number concentration of $k_{15}'$ as well as $k_{10}$ is obvious. Furthermore, $k_{15}'$ is rather insensitive to variations in S, whereas the change in $k_{10}$ is much more pronounced.


6.4.  DISCUSSION

6.4.1.  Experiments with 'dry' aerosol

The influence of 'dry' sub-micron particles is found to be limited. Since the extra surface area introduced by the particles is small compared to the surface area of the reactor wall, any effect can only be expected if caused by a sufficiently fast interaction with the aerosol particle. Apparently, such fast interactions do not occur. Only in case D (Table I), an appreciable decrease in S is detected.

We suggest to explain this behaviour by a $NO_3$ loss process at the surface of the 'dry' particle. The steady-state $O_3$ concentration remains constant when the particles are supplied to the reaction vessel. This implies that it is unlikely that NO acts as an intermediate since NO would have reacted with $O_3$. Therefore, the $NO_3$ loss at the particle surface can probably  be best described by reaction (R10). The consequences for the kinetics are already given: an increase of $k_{10}$ from $3.6 \times 10^{-2}$ $s^{-1}$ (without 'dry' aerosol) to $5.5 \times 10^{-2}$ $s^{-1}$ (in case D). The latter $k_{10}$ value can be written as:

$$k_{10} = k_{w,10} + k_{p,10} \tag{1}$$

where the subscripts w and p denote 'wall' and 'aerosol particle' respectively. Thus, for case D we obtain: $k_{p,10} = 1.6 \times 10^{-2}$ $s^{-1}$.

This result can be discussed with the theoretical considerations of Fuchs and Sutugin (1970) as described by Peterson and Seinfeld (1980), Chameides and Davis (1982) or Heikes and Thompson (1983). The interaction of a gaseous species with an aerosol particle can be considered as a two-body chemical reaction. The description of the rate of this reaction requires a detailed treatment of the rate of diffusion of the gaseous species to the particle, knowledge of the particle size distribution, and an examination of the accommodation coefficient.

The interaction of the gaseous species with all particles can be considered as a pseudo-first-order process and the pseudo-first-order rate constant $(k_p)$ can be expressed as:

$$k_p = \int_0^\infty \Phi(d_p) \, n(d_p) \, d(d_p) \tag{2}$$

where $n(d_p)$ denotes the number particle concentration with diameters between $d_p$ and $d_p + d(d_p)$, which can be deduced from the particle size distribution. The term $\phi(d_p)$ is the gas-to-particle diffusion rate constant for a particle of diameter $d_p$. Besides on $d_p$, $\phi(d_p)$ depends on the nature of the diffusing gaseous species and on state variables.

The term $\phi(d_p)$ is generally described referring to the characteristic parameter: the Knudsen number (Kn). Kn is defined as the ratio of the mean free path of a gas molecule in air (1) to the particle radius:

$$Kn = \frac{2 \, l}{d_p} \tag{3}$$

The theory of transport phenomena is simple in two extreme cases; at very small and very large Knudsen numbers. For Kn <<1, the so-called continuous diffusion regime, $\phi(d_p)$ can be described by the classical continuum diffusion theory (Fick's laws). For the free molecular diffusion regime (Kn >>1), the particle can be considered dynamically as if it were another molecule and $\phi(d_p)$ can be predicted by collision theory.

The case of intermediate Kn values is called the transition regime. For a spherical particle, $\phi(d_p)$ is given by

$$\phi(d_p) = 2 \, \pi \, d_p \, D \quad F \tag{4}$$

where D is the diffusion constant of the gaseous species in air. The factor F is developed by Fuchs and Sutugin (1970) to span the transition region between the free molecular diffusion regime and the continuous diffusion regime. F is expressed by:

$$F = \left[ 1 \; + \; Kn \; \left\{ \; \lambda \; + \; \frac{4 \; (1 \; - \; \alpha)}{3 \; \alpha} \; \right\} \; \right]^{-1} \tag{5}$$

where $\lambda$ is a dimensionless parameter equal to

$$\lambda \; = \; \frac{4/3 \; Kn \; + \; 0.71}{Kn \; + \; 1} \tag{6}$$

and $\alpha$ denotes the accommodation coefficient.

When the particle size distribution is known, $k_p$ can be calculated as a function of $\alpha$. Referring to the present results, we may calculate the $k_p$ values for reaction (R10). In Figure 1, some plots of $k_{p,10}$ versus $\alpha$ are shown, with $D_{NO_3} = 0.12 \; cm^2 \; s^{-1}$ and $l_{NO_3} = 0.113 \; \mu m$.

The $k_{p,10}$ values are obtained by numerical integration of equation (2) and applying the equations (3) to (6). We have used the lognormal size distributions characterized by the parameters given in Table I (cases B to D).

For case D, we have obtained a $k_{p,10}$ value of $1.6 \times 10^{-2} \; s^{-1}$, which corresponds with $\alpha = 6.5 \times 10^{-4}$. Using this $\alpha$ value, we find $k_{p,10}$ values of $2.6 \times 10^{-3} \; s^{-1}$ and $1.5 \times 10^{-3} \; s^{-1}$ for case B and C respectively. It may be clear that, compared to $k_{w,10}$, these $k_{p,10}$ values are too small to observe a measureable decrease in S.

### 6.4.2. Experiments with 'wet' aerosol

The stoichiometric factor is hardly affected by the presence of sub-micron 'wet' aerosol. The change in S appears to be that small that any dependence of S on the particle number concentration is not noticed, at least within the accuracy of the $NO_x$ analyzer. Furthermore, we observed discrepancies between the kinetic results based on the measurements of the stoichiometric factorand those based on the measurements of the particle nitrate content of the 'wet' particles.
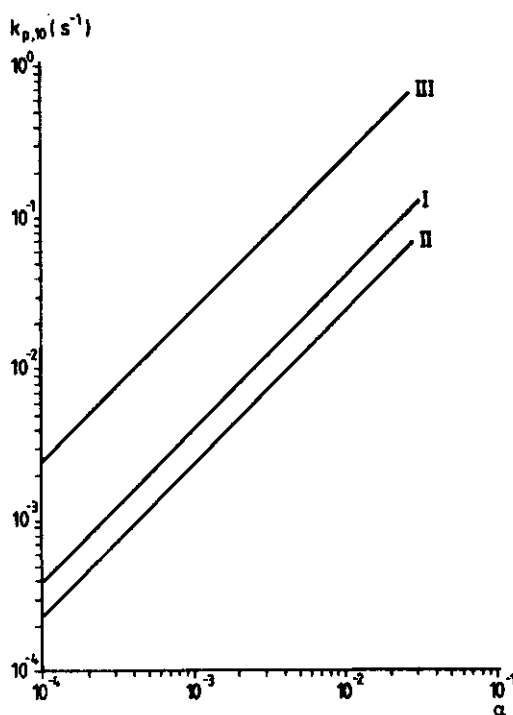
FIGURE 1. $k_{a,10}$ as a function of $\alpha$. Lognormal size distribution as in: (I) case B; (II) case C; (III) case D.

Probably, there are two competitive processes operative. Firstly, $NO_3$ scavenging with subsequent $NO_2$ formation which leads to a decrease in S. Secondly, heterogeneous $N_2O_5$ hydrolysis which leads to an increase in S. In the calculation of the kinetic results given in Table IV, we made the assumption that the $NO_3$ loss reaction R(10) only takes place at the wall of the reaction vessel. In view of the explanation given above this assumption is incorrect. Therefore, we believe that the kinetic results based on the measurements of the particle nitrate content provide a more confident data set.

The kinetic results based on the nitrate measurements are summarized in Tabel V. It can be seen that irrespective of the value of S, a rather consistent value of $k_{15}'$ is calculated.

These values of $k_{15}'$ can be compared with those calculated using the

method outlined in the previous paragraph. In Figure 2, the plots of $k_{15}'$ versus $\alpha$ for the lognormal size distributions of cases G to J are shown.
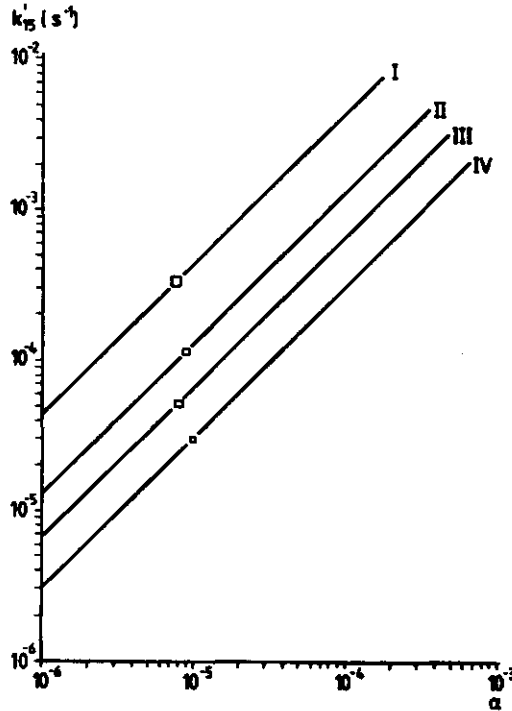


FIGURE 2.   $k_{15}'$ versus $\alpha$. Lognormal size distribution as in: (I) case G; (II) case H; (III) case I; (IV) case J. The squares depict the values given in Table V.

The $k_{15}'$ values of Table V are also depicted in Figure 2. The accommodation coefficient for $N_2O_5$ scavenging according to reaction (R15) is about $(0.8\pm0.2)\times10^{-\text{s}}$. In order of magnitude, this value agrees well with the values of Harker and Strauss (1981).

Another way to interpret the results is to search for a correlation between the $k_{15}'$ value and the steady-state particle surface concentration $(S_{ss})$. Figure 3 shows $k_{15}'$ as a function of $S_{ss}$.
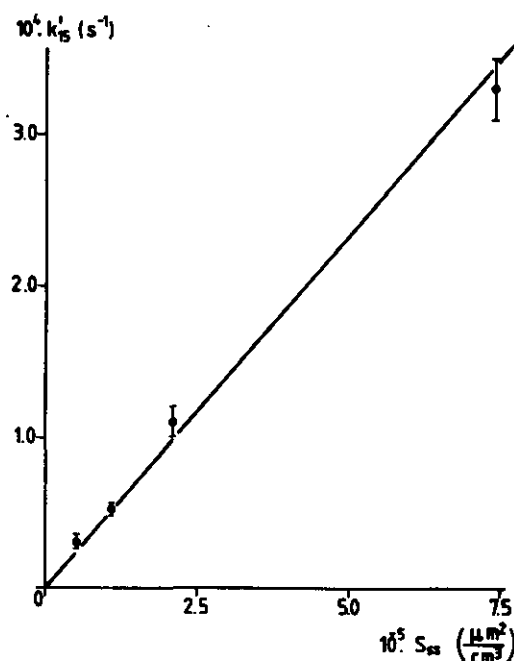
FIGURE 3.  $k_{15}'$ versus $S_{ss}$

Apparently, we obtain a lineair relationship according to:

$$k_{15}' = 2.1 \times 10^{-9} \; S_{ss} \tag{7}$$

A third way to interpret the results is to assume that the $N_2O_5$–$H_2O$ interaction takes place in the bulk of the liquid phase. The $N_2O_5$ reaction can be described as the physical dissolution of $N_2O_5$ followed by an aqueous phase reaction of $N_2O_5(aq)$ according to:

$$N_2O_5 \; (g) \quad \rightleftarrows \quad N_2O_5 \; (aq) \tag{R16}$$

$$N_2O_5 \; (aq) + H_2O \; (l) \quad \rightarrow \quad 2 \; NO_3^- + 2 \; H^+ \tag{R17}$$
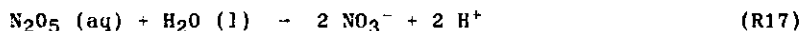
The rate of this process is governed by the Henry's law constant of $N_2O_5$ and the aqueous phase rate constant for reaction (R17). Provided the aqueous phase is saturated in $N_2O_5$, a rate constant for the overall process may be evaluated as (Lee and Schwarz, 1981).

$$k = L \ RT \ H_{N_2O_5} \ k_{17} \tag{8}$$

where L stands for the liquid water content, which is defined as the volume of liquid water ($m^3$) per $m^3$ air.

The values of $k_{15}'$ can be discussed referring to equation (8). The liquid water content can be deduced from the particle volume concentration and the Kohler curve (Pruppacher and Klett, 1978) for $MgCl_2$ aerosol. Figure 4 gives $k_{15}'$ as a function of L.
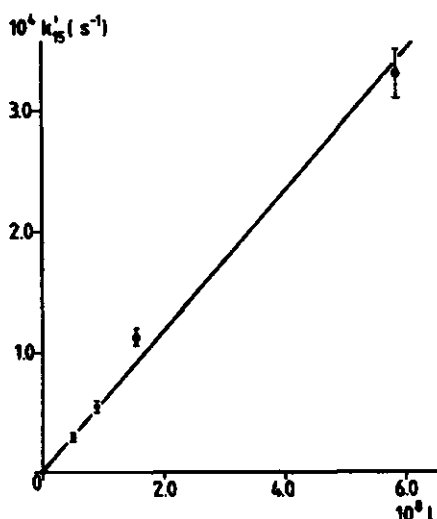


FIGURE 4.  $k_{15}'$ versus L

The value of $H_{N_2O_5} \cdot k_{17}$ can be determined from the slope of the line given in Figure 4, we obtain: $H_{N_2O_5} \cdot k_{17} = 2.4 \times 10^2$ M $atm^{-1}$ $s^{-1}$. This number must be regarded as an upper limit since mass transport processes are not considered. Mass transport processes will become rate limitting for large drops and very high chemical rates (Schwartz and Freiberg, 1981).

To the best of our knowledge, neither $H_{N_2O_5}$ nor $k_{17}$ has been reported in the literature. When compared to the reactive solubility of $HNO_3$, it appears that $N_2O_5$ is much less soluble than $HNO_3$, for which the product of Henry's law constant and the first-order aqueous phase rate constant equals $4.6 \times 10^{14}$ M $atm^{-1}$ $s^{-1}$ (Durham et al., 1981). The reactive solubility of $N_2O_5$ can be best compared with that of $N_2O_3$ and $N_2O_4$. From the recommended values given by Schwartz and White (1982), the product of Henry's law

constant and first-order aqueous phase reaction rate for both $N_2O_3$ and $N_2O_4$ can be evaluated as $1 \times 10^3$ M atm$^{-1}$ s$^{-1}$.

Finally, we consider the behaviour of the $NO_3$ radical. The kinetics of reaction (R10) are given in Table V. It can be seen that the rate constant $k_{10}$ is rather sensitive to small changes in S. In order to determine the effect of the aerosol particles on $k_{10}$, equation (1) may be used. Since $k_{w,10} = 3.6 \times 10^{-2}$ s$^{-1}$, it appears that only the $k_{10}$ values obtained for the lower values of S are realistic. Obviously, S should have a value between 1.54 and 1.6. An upper limit for the accommodation coefficient can be calculated from the $k_{p,10}$ values obtained at S = 1.54 and using the formalism outlined in paragraph 6.4.1.. This upper limit appears to be: $\alpha = (3.6 \pm 0.5) \times 10^{-4}$.

Another $NO_3$ loss process to be considered is the interaction of the $NO_3$ radical with the 'wet' particle leading to nitrate formation. This process alone cannot be responsible for the nitrate formation. Model calculations show that the formation of nitrate concentrations (such as given in Table III) would lead to a significant decrease in S, when heterogeneous $NO_3$ loss is considered to be the only nitrate forming process. Such a decrease in S is not observed. The formation of $NO_3^-$ by a combination of both $NO_3$ and $N_2O_5$ scavenging may be possible, but in that case we cannot quantify these processes with the present results. However, note that the $NO_3$ scavenging must be many times faster than $N_2O_5$ scavenging since the $N_2O_5$ concentration is several orders of magnitude higher than that of $NO_3$. Recently, Lee (1985) (has studied the hydrogen peroxide formation caused by an aqueous phase $NO_3$ reaction. From his results, Lee derived an upper limit for $H_{NO_3} \cdot k$ of $4 \times 10^{-3}$ M atm$^{-1}$ s$^{-1}$. Although Lee did not actually study the nitrate formation, this extreme low value of $H_{NO_3} \cdot k$ may be an indication that $NO_3$ scavenging is relatively unimportant.

# THE AQUEOUS PHASE CHEMISTRY OF $NO_2$ AND $NO_2$-$O_3$ MIXTURES

## 7.1. INTRODUCTION

The atmospheric chemistry of $NO_2$-$O_3$ systems is of importance since it provides one of the formation routes of atmospheric nitric acid. The gas phase chemistry has been extensively studied by laboratory, field and model studies (Verhees and Adema, 1985, and references therein). The possible chemical interactions between $NO_2$ and $O_3$ in the aqueous phase have received considerably less attention.
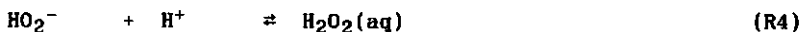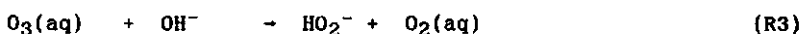
Individually, the interaction of $NO_2$ with liquid water as well as the interaction of $O_3$ with liquid water has recently been studied. Lee and Schwartz (1981a) report on a laboratory study of the reaction kinetics of the $NO_2$ reaction with liquid water at low $NO_2$ partial pressure. The $NO_2$ uptake in liquid water can be described by the physical dissolution of $NO_2$ (R1) followed by the aqueous phase disproportionation of $NO_2(aq)$ (R2) :

$$NO_2(g) \quad\rightleftarrows\quad NO_2(aq) \tag{R1}$$

$$2NO_2(aq) + H_2O(l) \quad\rightarrow\quad 2H^+ + NO_2^- + NO_3^- \tag{R2}$$
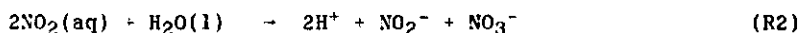
The kinetics are found to be consistent with a second-order aqueous phase reaction coupled to mass-transport processes. The rate of (R2) is established as being insensitive to the presence of $O_2$ (Lee and Schwartz, 1981b). In an extensive review on the kinetics of the reactive dissolution of the nitrogen oxides, Schwartz and White (1982) derive a value of Henry's law constant of $NO_2$ (the equilibrium constant of (R1)) as $(1.0 \pm 0.3) \times 10^{-2}$ $M.atm^{-1}$ (293-298 K) and a value of the rate constant for the aqueous phase

reaction (R2) as $(0.7 \pm 0.3) \times 10^8$ $M^{-1}.s^{-1}$ (293-298 K). With the use of these parameters the removal of $NO_2$ with pure, liquid water is found to be inefficient under most atmospheric conditions. For example, in a cloud with a liquid water content of 1 $g/m^3$ the $NO_2$ conversion rate is in the order of $10^{-4}$ % $h^{-1}$ (Beilke, 1983). However, during a fog event in an urban area associated with high $NO_x$ concentrations, the $NO_2$ aqueous phase chemistry may lead to significant nitrate formation (Kasting and Ackerman, 1985).

Some studies on the interaction of $O_3$ with liquid water have been recently reported. The physical dissolution of $O_3$ is characterized by its Henry's law constant, a value of $1.3 \times 10^{-2}$ $M.atm^{-1}$ (293 K) is recently given by Kosak-Channing and Helz (1983). Several chemical interactions between aqueous $O_3$ and pure, liquid water are known, a summary is given by Heikes (1984). A possible process is the $O_3$ decomposition to form $H_2O_2$, initiated by reaction with $OH^-$,

$$O_3(aq) \quad + \quad OH^- \quad \rightarrow \quad HO_2^- + \ O_2(aq) \tag{R3}$$

$$HO_2^- \quad + \quad H^+ \quad \rightleftharpoons \quad H_2O_2(aq) \tag{R4}$$

Reaction (R3) is the rate limiting step, the rate constants are given by Staehelin and Hoigné (1982). Likewise, it appears that heterogeneous processes and reactions with trace impurities in the aqueous phase are involved.

To the best of our knowledge, the influence of $O_3$ on the rate of $NO_2$ uptake by liquid water has never been studied. Only the oxidation of nitrite to nitrate by aqueous $O_3$ has been studied (Penkett, 1972; Damschen and Martin, 1983), and is found to be a significant sink for $NO_2^-$ under atmospheric conditions. The influence of dissolved ozone on the reactive dissolution of $SO_2$ is well-established. The aqueous phase $SO_4^{2-}$ formation is known to be enhanced by $O_3$ for several orders of magnitude (Beilke, 1983).

From chemical thermodynamics, the dissolution of $NO_2$ by reaction with $O_3$ is characterized by a large equilibrium constant (Schwartz and White, 1981) but, however, kinetic information is not available. Enhancement of the aqueous $NO_2$ uptake might occur analogously to the $NO_2$-$O_3$ gas phase chemistry, i.e. formation of an aqueous $NO_3$ species, which easily reacts with aqueous $NO_2$ to form nitrates. Another possibility is the involvement of species formed by the interaction of $O_3$ with liquid water.

This chapter deals with a laboratory study of the kinetics of the $NO_2$ uptake in liquid water as well as the influence of $O_3$ on these kinetics. The experimental method is almost identical with the method used by Lee and Schwartz (1981a), i.e. applying a gas-liquid contact reactor. Only the analysis of the ionic species is performed with ion chromatographic methods instead of conductivity measurements.

## 7.2. THEORY

### 7.2.1. The slow reaction model

The formalism to be used to describe the rates of gas-liquid reactions is given by Schwartz and White (1982); an extensive treatment is given by Danckwerts (1970). Briefly, a situation of mixed phase reaction involves a competition between (1) the rate of reaction of the physically dissolved gas and (2) the replenishment of the concentration of the dissolved gas by mass transport in each of the two phases and (3) dissolution of the reagent gas at the gas-liquid interface. In the case of the $NO_2(g)-H_2O(l)$ system gas phase mass transport can be considered sufficiently rapid, so it is not a limiting factor in the overall kinetics of $NO_2$ uptake in liquid water. Therefore, the rate is controlled by aqueous phase processes such as diffusion in the aqueous phase, convective mass transport or the aqueous phase reaction itself. For the $NO_2(g)-H_2O(l)$ system with a second-order aqueous phase reaction and $NO_2$ as the diffusing species, Lee and Schwartz (1981a) distinguish three regimes, where the overall reaction rate is controlled by one of these aqueous phase processes. They derive criteria for the partial pressure of $NO_2$ that are applicable to gas-liquid reactors as employed in their investigation. At a rough estimate, these criteria may be applied in the present study since the gas-liquid reactor used is nearly similar to the one used by Lee and Schwartz (1981a). Considering the $NO_2$ partial pressure applied, only the phase mixed and convective mass transport regimes (described below) are relevant.

In the phase mixed regime, the rate of the aqueous phase reaction is sufficiently slow, compared to the rate at which the phase equilibrium (R1) is restored, so that the aqueous phase concentration of the reagent is uniform throughout the aqueous phase. Thus, Henry's law is satified :

$$[NO_2(aq)] = H_{NO_2} \cdot p_{NO_2} \tag{1}$$

The rate determining step is the aqueous phase reaction :

$$2NO_2(aq) + H_2O(l) \rightarrow 2H^+ + NO_3^- + NO_2^- \tag{R2}$$
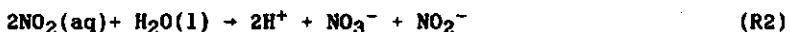
The rate of nitrate formation $R(NO_3^-) = d[NO_3^-]/dt$ as well as the rate of nitrite formation $R(NO_2^-) = d[NO_2^-]/dt$ can be expressed as :

$$R(NO_3^-) = R(NO_2^-) = k_2[NO_2(aq)]^2 = k_2(H_{NO_2} \, p_{NO_2})^2 \tag{2}$$

In the limiting situation of convective mass transport control, the rate of the aqueous phase reaction is rapid compared to convective mass transport. The rate of uptake of the gas is controlled by the rate of convection of the material present at the gas-liquid interface into the bulk aqueous phase or in term of a chemical reaction :

$$NO_2(in) \quad \rightarrow \quad NO_2(aq) \tag{Rm}$$

where (in) denotes the species at the gas-liquid interface.

When the interfacial $NO_2$ concentration is described by Henry's law, the rate of reaction (Rm) equals :

$$k_m[NO_2(in)] = k_m \, H_{NO_2} \, p_{NO_2} \tag{3}$$

Here, $k_m$ denotes a first order 'rate constant' which is the frequency of the convection of $NO_2$ from the interface to bulk solution. The rate of nitrate or nitrite formation can be given as :

$$R(NO_3^-) = R(NO_2^-) = 0.5 \, k_m \, H_{NO_2} \, p_{NO_2} \tag{4}$$

The factor 0.5 results from the reaction stoichiometry.

Situations intermediate between the phase mixed and convective mass transport controlled regimes can be described by the so-called slow reaction model. The rate of gas uptake is controlled by competition between convective mass transport and chemical reaction. Convective mass transport is considered to be a reversible process and the reaction is considered to occur in the bulk aqueous phase. In terms of chemical reactions :

$$NO_2(in) \quad \rightarrow \quad NO_2(aq) \tag{Rm}$$

$$NO_2(aq) \rightarrow NO_2(in) \qquad\qquad (R-m)$$

$$2NO_2(aq) + H_2O(l) \rightarrow 2H^+ + NO_3^- + NO_2^- \qquad\qquad (R2)$$

Applying the steady state approximation for $NO_2(aq)$, one obtains :

$$2 k_2 [NO_2(aq)]^2 + k_{-m}[NO_2(aq)] - k_m[NO_2(in)] = 0 \qquad\qquad (5)$$

Again, assuming phase equilibrium at the interface and since $k_m = k_{-m}$:

$$2 k_2 [NO_2(aq)]^2 + k_m[NO_2(aq)] - k_m H_{NO_2} p_{NO_2} = 0 \qquad\qquad (6)$$

The formation rate of the ionic species can be described as (with $R(NO_3^-) = R(NO_2^-) = R$) :

$$R = k_2 [NO_2(aq)]^2 \qquad\qquad (7)$$

Combining the equations (6) and (7), the parameter of interest, $k_2$, can be written as:

$$k_2 = \frac{R}{4 \, \tau_m^2 \, R^2 - 4 \, \tau_m \, R \, H_{NO_2} \, p_{NO_2} + H^2_{NO_2} \, p^2_{NO_2}} \qquad\qquad (8)$$

Here, the characteristic time for convective mass transport ($\tau_m$) is introduced, $\tau_m$ is the reciprocal value of $k_m$.

## 7.2.2. Influence of $O_3$

Primarily, ozone influences the $NO_2(g) - H_2O(l)$ chemistry by oxidizing nitrite (Damschen and Martin, 1983):

$$NO_2^- + O_3(aq) \rightarrow NO_3^- + O_2(aq) \qquad\qquad (R5)$$
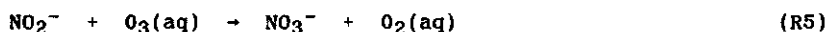
When the influence of $O_3$ is limited by reaction (R5), the rate of formation of the ionic species can be modified to:

$$R'(NO_2^-) = k_2[NO_2(aq)]^2 - k_5[O_3(aq)] [NO_2^-] \qquad\qquad (9)$$

and

$$R'(NO_3^-) = k_2[NO_2(aq)]^2 + k_5[O_3(aq)] [NO_2^-] \qquad\qquad (10)$$

The $[O_3(aq)]$ needs to be quantified. In theory, it may range between zero and saturation according to Henry's law, i.e. $H_{O_3} p_{O_3}$. Let us assume that $[O_3(aq)]$ is determined by competition between convective mass transport and chemical reaction. This means that $[O_3(aq)]$ can be obtained by a steady-state approximation analogous to equation (6):

$$k_5[O_3(aq)] [NO_2^-] + k_m[O_3(aq)] - k_m H_{O_3} p_{O_3} = 0 \tag{11}$$

or

$$[O_3(aq)] = \frac{H_{O_3} p_{O_3} k_m}{k_m + k_5[NO_2^-]} \tag{12}$$

It can be seen that $[O_3(aq)]$ is a function of $[NO_2^-]$, which itself is dependent on $p_{NO_2}$. Using the equations (9), (10) and (12), the difference between the rates of nitrate and nitrite formation can be expressed as:

$$R'(NO_3^-) - R'(NO_2^-) = 2 k_5 \frac{H_{O_3} p_{O_3} k_m}{k_m + k_5[NO_2^-]} [NO_2^-] \tag{13}$$

Ozone can also be of influence on the $NO_2$ uptake according to the overall-reaction:

$$2NO_2(aq) + O_3(aq) + H_2O(l) \rightarrow 2NO_3^- + 2H^+ + O_2(aq) \tag{R6}$$

If so, the steady-state approximations for $NO_2(aq)$ and $O_3(aq)$ as well as the nitrate formation rate may be modified as:

$$2 k_2[NO_2(aq)]^2 + 2 k_6[NO_2(aq)]^n [O_3(aq)] + k_m[NO_2(aq)] - k_m H_{NO_2} p_{NO_2} = 0 \tag{14}$$

$$k_5[O_3(aq)] [NO_2^-] + k_6[NO_2(aq)]^n [O_3(aq)] + k_m[O_3(aq)] - k_m H_{O_3} p_{O_3} = 0 \tag{15}$$

$$R''(NO_3^-) = k_2[NO_2(aq)]^2 + k_5[O_3(aq)] [NO_2^-] + 2 k_6[NO_2(aq)]^n [O_3(aq)] \tag{16}$$

The problem is that the exact mechanism of reaction (R6) is not known. For the equations (14) to (16), it is assumed that the rate of reaction (R6) is first-order in $O_3(aq)$, whereas the order in $NO_2(aq)$ is left variable and is

denoted n. The calculations are made taking either first-order or second-order kinetics, i.e. n=1 or n=2.


7.2. EXPERIMENTAL

The experiments were performed in a reaction system as schematically shown in Figure 1. The apparatus was composed of two parts: a flow system, in which the reactants could be generated, and a pump system, with which air from the flow system could be drawn through the gas-liquid reactor. The flow system consisted of a manifold of three gas streams. Clean, dry air or pure, dry nitrogen was used as a carrier gas. The gas flow was controlled by means of a Brooks flow controller model 8844 and a Brooks
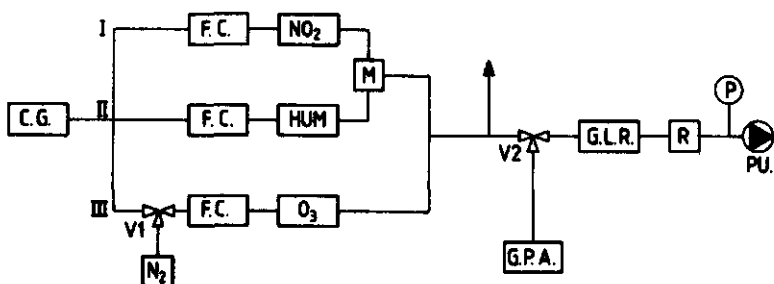
FIGURE 1. Schematic of the experimental set-up.
C.G.: carrier gas supply; F.C.: flow controlling device;
V1 and V2: three way valve; $NO_2$: $NO_2$ supply; HUM: humidifier;
$O_3$: $O_3$ generator; M: mixing vessel; G.P.A.: gas phase analysis;
G.L.R.: gas liquid reactor; R: rotameter; P: manometer; Pu: pump

R-2-15-AAA rotameter (line I) or by constant flow units based on critical orifices. In line I, the carrier gas was passed through a temperature controlled chamber containing a permeation tube releasing $NO_2$ at a rate of 1.3 mg/h. The flow rate in line I was kept constant at 3 l/h. For $NO_2$ concentrations > 10 ppm, a stock cylinder containing 0.96% $NO_2$ in $N_2$ (Matheson, certified standard) was used. Line II was used for dilution,

this gas stream was saturated with water vapour using a bubbler located in a constant temperature bath. Ozone was produced in line III by the use of a modified Fischer model $O_3$ generator. The $NO_2$ and $O_3$ concentration could be adjusted by setting the proper flows through line II and/or line III. The total flow rate was always greater than 80 1/h. The $O_3$ concentration could be varied at constant $NO_2$ concentration by the use of mixtures of air and nitrogen in line III. The gas phase analysis of the $NO_2$ concentration was performed with a Monitor Labs model 8840 $NO_x$ analyzer. The $O_3$ concentration was measured by the chemiluminescent reaction with ethylene using a Bendix 8002 $O_3$ analyzer.

A part of the air-$NO_2$ or air-$NO_2$-$O_3$ mixture from the flow system was pumped through the gas-liquid reactor using a Charles Austen M361 pump in connection with a 0.9 mm capillary. The volumetric flow rate was 60 1/h ($\pm$ 3%) in all experiments. The pressure in the pumpline was measured with a mercurial manometer.
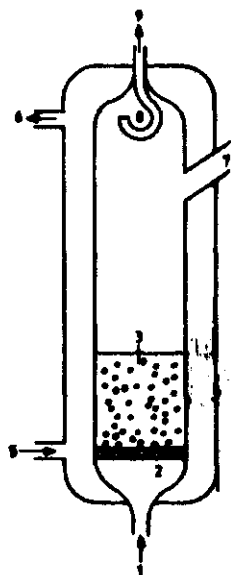


FIGURE 2    Gas-liquid reactor. (1) gas inlet; (2) disk-frit; (3) reagent
            water; (4) water jacket; (5, 6) thermostatted water in- and
            outlet; (7) in and outlet of reagent water; (8) provision to
            prevent loss of small water droplets; (9) gas outlet.

The gas-liquid reactor was an all-glass bubbler as shown in Figure 2. Temperature controlled water from a Colora WK 4 kryo-thermostat was cir-

culated through the water jacket in order to regulate and maintain a constant temperature (within ±0.1 K) in the reactor. In all experiments, the temperature was kept constant at 293 K. The gaseous reagents were introduced as finely divided bubbles through a fritted disk (frit porosity 2).

The water employed as a reagent and for humidification of the diluent gas was demineralized water which had been doubly distilled and further purified with active coal. Next, the water was filtered over a 5 μm membrane filter and degassed under vacuum. The water thus obtained had a pH value of 6.8 ± 0.1 as measured with a Radiometer PHM-83 pH meter. The conductivity of the reagent water was measured with a Philips PW 9504 conductivity meter and was found typically 1 μS/cm. For experiments at pH lower than 6.8, the reagent water was acidified with 85% $H_3PO_4$ (Merck p.a.)

The experiments were performed with the following standard procedure. The flow rate in each line was set at its proper value and the gas phase $NO_2$ and $O_3$ concentration were measured. A volume of 20 ml reagent water was pipetted in the gas-liquid reactor. At t=0 the three way valve (V2) was switched and the pump was started at the same time. The reagent gas mixture was brought into contact with the liquid for a well known reaction time. A run was stopped by simultaneously switching V2 and shutting of the pump. Next, the water was sampled for analysis. Kinetic information was obtained by repeating this procedure for a series of reaction times. Between the runs, the gas-liquid reactor was thoroughly cleaned and dried.

The analysis of the concentration of the ionic species formed by reaction (R2) (i.e. nitrite and nitrate) was performed using the isocratic HPLC method described by Gerritse (1979) and Leuenberger et al. (1980), which is based on UV detection at 210 nm. The HPLC equipment consisted of a Kipp model 414 LC pump and a Kratos Spectroflow 757 UV detector both connected to the analytical column by stainless steel 1/16 inch tubing. A Chrompack Iono-Spher A column was used. The temperature of the column was stabilized at 20 °C with a water jacket and temperature controlled water. The mobile phase consisted of 0.2 M $HPO_4{}^{2-}/H_2PO_4{}^-$-buffer (pH = 6.9). Before use, the eluens was filtered over a 5 μm membrane filter and degassed under vacuum.

Samples of 100 μl were injected using a Rheodyne model 7125 injector. The

chromatogram was registrated with a Spectra Physics 4270 integrator. An example of a chromatogram is given in Figure 3. The calibration was performed using standard solutions of NaNO$_2$ and KNO$_3$ (both Merck p.a.). The integrator output was found lineair in the range 0-100 µM. The detection limit was in the order of 0.1 µM. The standard deviation based on 5 sample injections was found to be 3% for $[NO_3^-]$ and about 5% for $[NO_2^-]$.
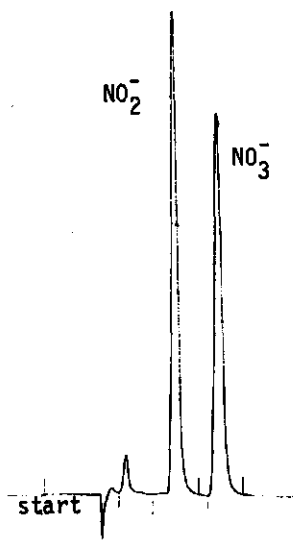


FIGURE 3.  Example of a ion-chromatogram for NO$_2^-$ and NO$_3^-$.


## 7.4.  RESULTS


### 7.4.1.  Interaction of NO$_2$(g) with H$_2$O(l)

A typical result of a series of experiments applying different reaction times is shown in the Figures 4 and 5.

The input concentration of NO$_2$ is 5.3 ppm corresponding to a NO$_2$ partial pressure ($p_{NO_2}$) of 5.3x10$^{-6}$ atm. We see that $[NO_2^-]$ as well as $[NO_3^-]$ appear to increase lineair with the reaction time. Such lineair relationships are found in all experiments with reaction times upto 180 minutes. The rate of formation of NO$_2^-$ (R(NO$_2^-$)) and NO$_3^-$ (R(NO$_3^-$)) is given by the slope of the concentration-time profiles.

The influence of pH (3.0 < pH < 7.0) is also indicated in the Figures 4 and 5. It can be seen that nitrate formation is independent of pH, whereas nitrite formation is not influenced at pH > 4.5. At pH = 3.0 less nitrite formation is observed. The dispersion of the data at constant reaction time but different pH is a measure of the accuracy of the experiments. From the Figures 4 and 5, the accuracy can be estimated to be in the order of 5 to 10%. If an experiment was repeated ten times using the same reaction conditions and at constant reaction time, a corresponding accuracy of 5% resulted.
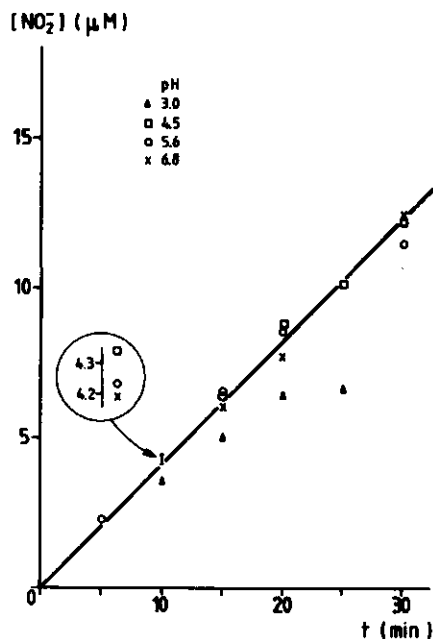


FIGURE 4. Nitrite formation as a function of time at various pH.
$P_{NO_2} = 5.3 \times 10^{-6}$ atm; $T = 293$ K.

Several sets of experiments have been performed to determine $R(NO_2^-)$ and $R(NO_3^-)$ as a function of the partial pressure of $NO_2$ with $1.35 \times 10^{-6} \leqslant p_{NO_2} \leqslant 4.5 \times 10^{-6}$ atm. In some experiments nitrogen has been used as the carrier gas. The results are summarized in Table I.

Note that at high $p_{NO_2}$ short reaction times were used. The concentrations of the products were always less then 20 $\mu M$. Thus, the decrease of $p_{NO_2}$ due to reaction was always less than 5%. Therefore, $p_{NO_2}$ can be considered as constant during the experiments.
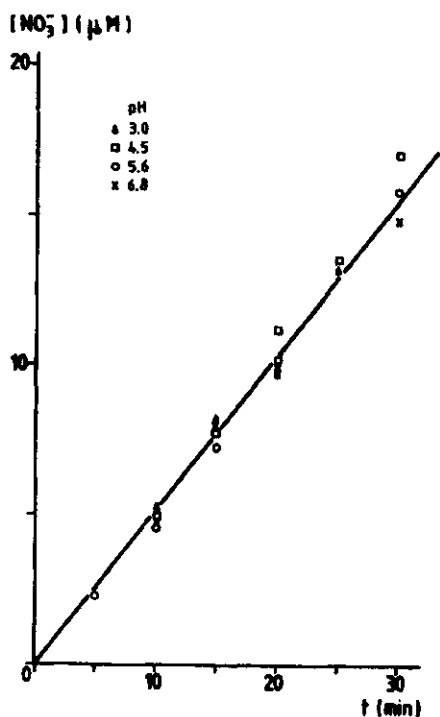


FIGURE 5.  Nitrate formation as a function of time at various pH. $p_{NO_2} = 5.3 \times 10^{-6}$ atm; $T = 293$ K.

TABLE I. The rate of nitrite and nitrate formation at various $p_{NO_2}$.
T = 293 K; pH = 6.8.

| $p_{NO_2}$ ($10^{-6}$ atm) | $R(NO_2^-)$ ($10^{-9}$ M.s$^{-1}$) | $R(NO_3^-)$ ($10^{-9}$ M.s$^{-1}$) | $R(NO_2^-)/R(NO_3^-)$ | $R(NO_3^-)-R(NO_2^-)$ ($10^{-9}$ M.s$^{-1}$) |
|---|---|---|---|---|
| 1.35 | 1.5 | 3.7 | 0.41 | 2.2 |
| 1.7 | 1.9 | 4.3 | 0.44 | 2.4 |
| 1.7[a] | 1.9 | 3.4 | 0.56 | 1.5 |
| 3.4 | 3.0 | 4.9 | 0.61 | 1.9 |
| 4.6 | 4.7 | 6.7 | 0.70 | 2.0 |
| 5.3 | 6.8 | 9.0 | 0.76 | 2.2 |
| 5.8 | 7.5 | 9.6 | 0.78 | 2.1 |
| 8.8 | 14 | 16 | 0.88 | 2 |
| 11.7 | 19 | 20 | 0.95 | 1 |
| 28[a] | 52 | 52 | 1.00 | 0 |
| 45[a] | 96 | 95 | 1.01 | -1 |

[a] Experiments using $N_2$ as the carrier gas

As can be expected, both $R(NO_2^-)$ and $R(NO_3^-)$ increase when $p_{NO_2}$ increases. Also indicated in Table I is the product stoichiometry defined as $R(NO_2^-)/R(NO_3^-)$. It can be seen that this product stoichiometry appears to deviate from the expected value of 1.0. Especially at low $p_{NO_2}$, relatively more $NO_3^-$ than $NO_2^-$ is formed, whereas at high $p_{NO_2}$ the product stoichiometry tends to a value of 1.0. In the last column of Table I, the difference between $R(NO_3^-)$ and $R(NO_2^-)$ is given. It seems that this difference is rather constant with an average value of about $2.1 \times 10^{-9}$ M.s$^{-1}$. Obviously, some extra $NO_3^-$ is formed at a constant rate, irrespective of the $NO_2$ partial pressure. For the experiments at $p_{NO_2} > 10^{-5}$ atm, nitrate formation cannot be distinguished within the limits of accuracy. Hence, $R(NO_3^-)-R(NO_2^-)$ differs from the value of $2 \times 10^{-9}$ M.s$^{-1}$, whereas the observed product stoichiometry is close to the expected value of 1.0.

## 7.4.2.   Interaction of $NO_2(g)$-$O_3(g)$ mixtures with $H_2O(l)$

The experiments have been performed using a gas mixture of air containing 5.3 ppm $NO_2$ and alternately 6.3, 3.3 and 1.0 ppm $O_3$. The concentration-time profiles are shown in the Figures 6 and 7.



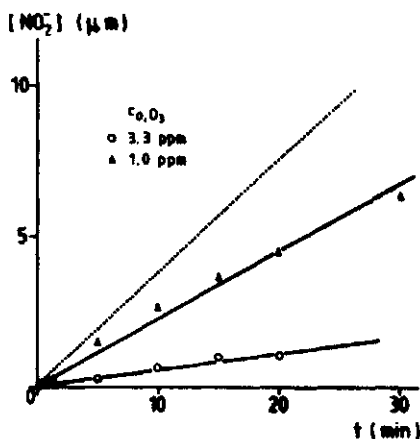FIGURE 6.   Nitrite formation as a function of time at various $p_{O_3}$.
$p_{NO_2}$ = 5.3 x $10^{-6}$ atm; T = 293 K.
($\cdots\cdots$) nitrite formation in absence of ozone.
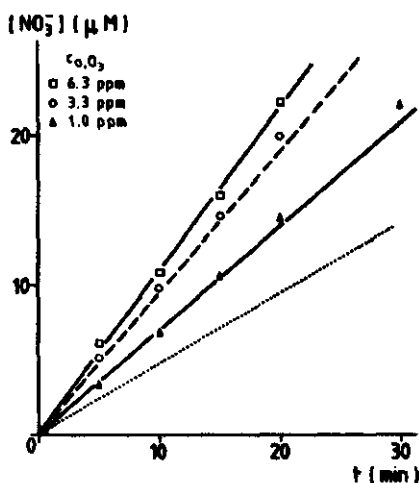


FIGURE 7.   Nitrate formation as a function of time at various $p_{O_3}$.
$p_{NO_2}$ = 5.3 x $10^{-6}$ atm; T = 293 K.
($\cdots\cdots$) nitrate formation in absence of ozone.
($-----$) sum of nitrite and nitrate formation in absence of $O_3$.

In the case of $c_{0,O_3}$ = 6.3 ppm, no $NO_2^-$ has been observed and the amount of $NO_3^-$ formed is clearly higher than the sum of $NO_2^-$ and $NO_3^-$ formed in the absence of $O_3$. When $c_{0,O_3}$ = 3.3 ppm, only traces of $NO_2^-$ have been detected and the $NO_3^-$ formation is less than at $c_{0,O_3}$ = 6.3 ppm. A considerable amount of $NO_2^-$ is formed at the lowest ozone partial pressure. This is accompanied with a nitrate formation that is clearly less than the nitrate formation at higher ozone partial pressures. Furthermore, it appears that the sum of $NO_2^-$ and $NO_3^-$ formation is approximately equal to the sum of $NO_2^-$ and $NO_3^-$ in absence of $O_3$.


## 7.5. DISCUSSION

### 7.5.1. Interaction of $NO_2(g)$ with $H_2O$

The results can be discussed referring to the so-called 'slow-reaction' model, which is summarized in paragraph 7.2.1. But, first some of the observed phenoma such as the pH dependence and the observed product stoichiometry have to be considered.

Any significant pH dependence is only observed at pH = 3.0 where less $NO_2^-$ is formed, whereas the $NO_3^-$ formation is unaffected. A simple quali-tative explanation is the following. At pH < 4, the formation of nitrous acid by the acid dissociation equilibrium

$$NO_2^- \quad + \quad H^+ \quad \rightleftharpoons \quad HNO_2(aq) \tag{R7}$$

becomes relevant ($pK_a$ = 3.2, Schwartz and White (1981)). The nitrous acid is in equilibrium with $NO(aq)$ and $NO_2(aq)$ according to
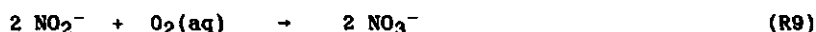
$$2\ HNO_2(aq) \quad \rightleftharpoons \quad NO(aq) \quad + \quad NO_2(aq) \quad + \quad H_2O \tag{R8}$$

In view of the low solubility of NO ($H_{NO}$ = $1.93 \times 10^{-3}$ $M.atm^{-1}$, Schwartz and White (1981)) and the absence of NO in the gas phase, it is likely that NO desorbs from the liquid phase. The NO desorption results in a $NO_2^-$ loss consistent with our observations at pH = 3.0.
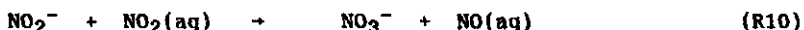
Another phenomenon to be considered is the lower-than-one product stoichiometry. According to reaction (R2) a product stoichiometry of one may be expected, which is also reported by Lee and Schwartz (1981a).

Probably, we have to deal with a side reaction. There are three possibili-
ties: (1) $NO_2^-$ loss followed by NO formation, (2) conversion of $NO_2^-$ into
$NO_3^-$ and (3) formation of $NO_3^-$ from $NO_2(g)$ or $NO_2(aq)$ by a reaction other
than (R2).

Any NO formation according to (R7) and (R8) is very unlikely at pH = 6.8.
Oxidation of $NO_2^-$ to $NO_3^-$ may occur by the reactions

$$2\ NO_2^-\ +\ O_2(aq)\quad\rightarrow\quad 2\ NO_3^- \tag{R9}$$

or

$$NO_2^-\ +\ NO_2(aq)\quad\rightarrow\quad NO_3^-\ +\ NO(aq) \tag{R10}$$

The kinetics of the oxidation of $NO_2^-$ by $O_2(aq)$ has been studied by
Damschen and Martin (1983). The rate constant reported is much too low to
cause any significant $NO_3^-$ formation. However, the rate of R(9) may be
enhanced by trace impurities in the water or because of the reaction taking
place on the surface of the glass vessel.

Reaction (R10) has not yet been studied and kinetic information is
currently not available.

In order to examine the role of $NO_2^-$, we have performed some experiments
using a $NaNO_2$ solution in stead of water. The $NO_2^-$ concentration of these
solutions was varied between 0.5 and 10 μM. Air as well as an air-$NO_2$ mix-
ture was allowed to flow through the $NO_2^-$ solution and the output gas was
analyzed for NO. With air, no $NO_2^-$ loss nor any $NO_3^-$ or NO formation was
observed. In the case of the $NO_2$-air mixture, no extra $NO_3^-$ nor NO for-
mation was found. Clearly, the lower-than-one product stoichiometry cannot
not be explained by a side reaction that involves $NO_2^-$.

Nitrate formation by a side reaction of $NO_2(g)$ or $NO_2(aq)$ remains as the
third possibility. Once more, the influence of trace impurities or surface
reactions is possible. An aqueous impurity can be excluded since the pro-
duct stoichiometry did not change when extra purified water was used.
Apparently, the best way to explain the observed product stoichiometry is
to assume a side reaction on the surface of the glass-liquid reactor.
Reactions on the surface of the disk-frit are particularly probable. The
order in $NO_2$ of this surface reaction must be lower than two since at high
$p_{NO_2}$ the side reaction is slow compared to the second-order reaction (R2).
In fact, it seems that the surface reaction is zero-order in $NO_2$ because

the difference between $R(NO_3^-)$ and $R(NO_2^-)$, i.e. the rate of the extra $NO_3^-$ formation, is not dependent on $p_{NO_2}$. This zero-order dependence on $p_{NO_2}$ can be explained referring to a surface reaction. When only a limited amount of active sites on the glass surface is available, saturation of these active sites rapidly occurs. In this case, not the amount of $NO_2$ determines the rate of artifact $NO_3^-$ formation, but the amount of active sites available.

The glass surface chemistry implies that the observed product stoichiometry will depend on the apparatus used. This may be an explanation for the fact that Lee and Schwartz (1981a) obtained a product stoichiometry of one. Interactions between glass surfaces and $NO_2$ are also known as an interference in the sampling of particulate nitrate with glass fiber filters. Spicer and Schumacher (1977) have shown that when glass fiber filters are exposed to $NO_2$ a considerable amount of nitrate is formed.

For the quantitative interpretation of the results, the 'slow reaction' model may be used. This model is outlined in paragraph 7.2.1. It is important to know whether $NO_2(g)$ or $NO_2(aq)$ reacts on the surface of the diskfrit. If $NO_2(g)$ reacts, $R(NO_2^-)$ or $R(NO_3^-)$ decreased with the rate of nitrate formation on the glass surface, i.e. $2.1x10^{-9}$ $M.s^{-1}$, must be used in the calculations. Moreover, the partial $NO_2$ pressure will be slightly lower, but mostly this effect can be neglected. In the case of surface reaction of $NO_2(aq)$, the steady-state equation (6) must be modified. However, this leads to erroneous results, especially at low $p_{NO_2}$. Therefore, we believe that $NO_2(g)$ rather than $NO_2(aq)$ reacts on the surface, which is not surprising in view of the numerous contacts between $NO_2(g)$ and the glass surface compared with those of $NO_2(aq)$.

Applying equation (8), the rate constant for reaction (R2) can be calculated, provided $\tau_m$ and $H_{NO_2}$ are known. A recommendation for the value of $H_{NO_2}$ is given by Schwartz and White (1982): $H_{NO_2} = 1x10^{-2}$ $M.atm^{-1}$. The characteristic time for convective mass transport ($\tau_m$) can be obtained from the experiments at $p_{NO_2}$ = $2.8x10^{-5}$ atm and $4.5x10^{-5}$ atm, assuming that at these partial pressures the rate of $NO_2$ uptake is controlled by convective mass transport, which follows from the criteria given by Lee and Schwartz (1981a). This means that $\tau_m$ can be obtained from equation (4) resulting in $\tau_m$ = $2.5 \pm 0.2$ s.

A $k_2$ value can be calculated from each $R(NO_2^-)$ and the corresponding $p_{NO_2}$ given in Table I. An average value of $k_2 = 2.7 \times 10^7$ M$^{-1}$.s$^{-1}$ is found with a standard deviation of about $1.4 \times 10^7$ M$^{-1}$.s$^{-1}$. This result may be compared with the value recommended by Schwartz and White (1982): $(7 \pm 3) \times 10^7$ M$^{-1}$.s$^{-1}$ in the temperature range 293 - 298 K. Our result is close to the lower limit of Schwartz and White, which means that it agrees reasonably well since our measurements were performed at 293 K.

These calculations can also be made using the $H_{NO_2}$ obtained in the laboratory study of Lee and Schwartz (1981a), notably: $H_{NO_2} = 7 \times 10^{-3}$ M.atm$^{-1}$ (298 K). Now we obtain $\tau_m = 1.8 \pm 0.2$ s and an average $k_2$ of $6.2 \times 10^7$ M$^{-1}$.s$^{-1}$; standard deviation $3.4 \times 10^7$ M$^{-1}$.s$^{-1}$. This result may be compared with the value reported by Lee and Schwartz (1981a) in their laboratory study: $( 10 \pm 1 ) \times 10^7$ M$^{-1}$.s$^{-1}$ at 298 K. Again our result is somewhat lower which may be due to the lower temperature (293 K).

From the high values of the standard deviation, it appears that there is a rather large scatter in the $k_2$ values obtained at various $p_{NO_2}$. This scatter can be understood, if we consider the result of the slow reaction model with respect to the accuracy of the variables in equation (8). The effect of a 30% change in $H_{NO_2}$ is already shown above. We have seen that the accuracy and reproducibility of $R(NO_2^-)$ is about 5 to 10%. This will also be the case for $\tau_m$ since it is derived from $R(NO_2^-)$. Table II sum-

TABLE II : Sensitivity analysis of the $k_2$ calculations.

| $p_{NO_2}$ (10$^{-6}$ atm) | $R(NO_2^-)$ (10$^{-9}$ M.s$^{-1}$) | $\tau_m$ (s) | $k_2$ (10$^7$ M$^{-1}$s$^{-1}$) |
|---|---|---|---|
| 5.3 | 6.8 | 2.5 | 1.9. |
| 5.3 | 6.2 | 2.5 | 1.3 |
| 5.3 | 7.4 | 2.5 | 2.6 |
| 5.3 | 6.8 | 2.7 | 2.6 |
| 5.3 | 6.8 | 2.3 | 1.4 |

marizes the results of a sensitivity analysis when $R(NO_2^-)$ and $\tau_m$ are varied between their limits. The experiment at $p_{NO_2} = 5.3 \times 10^{-6}$ atm is taken as the base case. The calculations are performed taking $H_{NO_2} = 1 \times 10^{-2}$ M.atm$^{-1}$.

The sensitivity of the calculated $k_2$ values is evident: a change of 10% in $R(NO_2^-)$ or $\tau_m$ leads to changes of approximately 30 to 50% in $k_2$.

## 7.5.2. Interaction of $NO_2(g)-O_3(g)$ mixtures with $H_2O$

We may begin the discussion with the experiments at $c_{o,O_3} = 1$ ppm. In this case, there is no enhancement of the rate of $NO_2$ uptake, which follows from the observation that the sum of the nitrite and nitrate formation rate at $c_{o,O_3} = 1$ ppm is equal to this sum in absence of $O_3$. The only effect of is a change of the product distribution, i.e. more $NO_3^-$ and less $NO_2^-$ is formed. This is caused by the oxidation of $NO_2^-$ according to:

$$NO_2^- + O_3(aq) \rightarrow NO_3^- + O_2(aq) \tag{R5}$$

This means that the results can be discussed using equation (12) given in paragraph 7.2.2.. With this equation the difference between the rate of nitrate and nitrite formation can be calculated as a function of the nitrite concentration, provided a realistic value for $k_5$ is assumed. Next, the nitrite concentration-time profile can be constructed since the sum of the rate of $NO_2^-$ and $NO_3^-$ formation is known. In Figure 8, some of these calculated plots are presented by the solid curves. The measured nitrite concentrations are also indicated in the Figure.

The best fit to the experimental data yields a $k_5$ value of $3.5 \times 10^5$ M$^{-1}$.s$^{-1}$. This result may be compared with the result of Damschen and Martin (1983), who report a $k_5$ value of $5 \times 10^5$ M$^{-1}$.s$^{-1}$ at 298 K. Penkett (1972) reports $k_5 = 1.6 \times 10^5$ M$^{-1}$.s$^{-1}$ at 283 K. The combination of these results implies an activation energy of about 14 kcal.mol$^{-1}$. Consequently, a value of about $3.3 \times 10^5$ M$^{-1}$.s$^{-1}$ may be expected at 293 K, which means that our result agrees fairly well with the literature data.

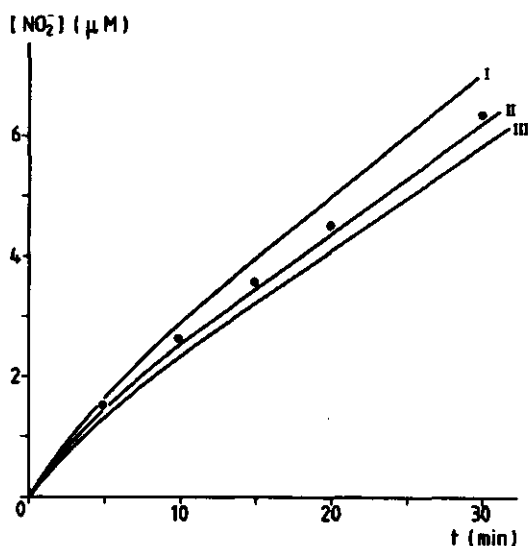FIGURE 8. The calculated $\left[NO_2^-\right]$-time profiles using equation (16) with $k_5 = 2 \times 10^5$ $M^{-1}.s^{-1}$ (I); $4 \times 10^5$ $M^{-1}.s^{-1}$(II) and $6 \times 10^5$ $M^{-1}$ $s^{-1}$ (III). (•) Experimental observations.

The experiments at higher $c_{o,O_3}$ exhibit the feature that the total amount of N-containing ionic species exceeds the amount formed in the absence of $O_3$. This indicates that the rate of $NO_2$ uptake is enhanced. Especially, the experiment performed at $c_{o,O_3} = 6.3$ ppm shows a substantial increase of 16%, appreciably larger than the accuracy of the measurement.

The reason for this behaviour may be twofold. It can be either a gas phase contribution or an aqueous phase reaction. The former refers to the gas phase $NO_2$-$O_3$ chemistry, which may lead to nitrate formation. The upper limit for the rate of gas phase nitrate formation is determined by twice the rate of the $NO_2$-$O_3$ reaction. Using the recommended rate constant of Baulch et al. (1982), $c_{o,O_3} = 6.3$ ppm and $c_{o,NO_2} = 5.3$ ppm, the upper limit for gas phase nitrate formation equals $2 \times 10^{-12}$ $mol.cm^{-3}.s^{-1}$. Since the volume where $NO_2$ and $O_3$ are in contact before entering the liquid is approximately 10 ml and the volume of the liquid is 20 ml, the maximum contribution to the aqueous nitrate formation is $1 \times 10^{-9}$ $M.s^{-1}$. This quantity is much smaller than the observed increase in nitrate formation rate, which equals $2.5 \times 10^{-8}$ $M.s^{-1}$. Therefore, a significant gas phase contribution to the nitrate formation may be excluded.

The second possibility is an aqueous phase reaction between $NO_2(aq)$ and $O_3(aq)$, which is likely to have the stoichiometry:

$$2\ NO_2(aq) + O_3(aq) + H_2O(1)\ \rightarrow\ 2\ NO_3^- + 2\ H^+ + O_2(aq) \qquad (R6)$$
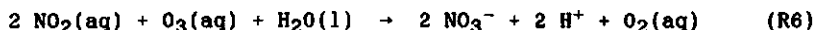
Schwartz and White (1981) have shown that from chemical thermodynamics, it may be concluded that the formation of the nitric acid product is strongly favoured. Kinetic information or information about the reaction mechanism is not available. Based on the present results, a value of the rate constant can be deduced. In order to evaluate this rate constant, the theory outlined in paragraph 7.2.2. is applied. This theory involves four equations, i.e. the equations (9), (14), (15) and (16). If a value of the reaction-order in $NO_2(aq)$ (n) is adopted, there are four unknown variables, i.e. $[NO_2(aq)]$, $[O_3(aq)]$, $[NO_2^-]$ and $k_6$. This set of 4 equations with 4 unknown parameters can be solved. Note that the rate of nitrate formation must be corrected for the artifact nitrate formation. This procedure leads to a $k_6$ value of $6.7 \times 10^6$ $M^{-1}.s^{-1}$ for a reaction first-order in $NO_2(aq)$ or to a $k_6$ value of $5.3 \times 10^{14}$ $M^{-2}.s^{-1}$ for a second-order reaction.

These values must be considered as rough estimates, regarding the uncertainity of the $k_2'$ value and the accuracy of the measurements. For example, sensitivity calculations for the first-order assumption show that $k_6$ may vary between $3.6 \times 10^6$ and $8 \times 10^6$ $M^{-1}.s^{-1}$ when $k_2$ is varied between $3.4 \times 10^7$ and $1.2 \times 10^7$ $M^{-1}.s^{-1}$. Deviations of the same size may be expected when other parameters such as $R''(NO_3^-)$, $H_{NO_2}$, $H_{O_3}$ etc. are varied between their uncertainity limits.

It is obvious that these rate constants are too small to cause any significant atmospheric nitrate formation by the $NO_2-O_3$ aqueous chemistry. In a cloud with a liquid water content of 1 $g/m^3$ and an ozone concentration of 50 ppb, the $NO_2$ conversion rate is about $10^{-3}$ % $h^{-1}$.

**GENERAL EVALUATION**

## 8.1. GENERAL DISCUSSION AND CONCLUSIONS

### 8.1.1. The gas phase $NO_2$-$O_3$ reaction system

In this section, some conclusions based on the results described in the chapters 4 and 6 are considered. Moreover, their importance in relation to atmospheric events is estimated.

An important conclusion is the reasonable agreement between the rate constants for the $NO_2$-$O_3$ reaction determined in this work and the rate constants reported in the current literature, although the reactant concentrations were at least one order of magnitude lower. It also appears that the rate constant is not affected by varying the relative humidity nor by the presence of certain sub-micron aerosol particles. Therefore, the present results support the generally accepted picture (as applied in the current models) that the $NO_2$-$O_3$ reaction pathway is initiated by the homogeneous gas phase, rate determining oxidation of $NO_2$ by $O_3$, after which equilibrium between $NO_2$, $NO_3$ and $N_2O_5$ is rapidly reached. However, the net result of the $NO_2$-$O_3$ chemistry depends on the reactivity of the reaction products $NO_3$ and $N_2O_5$. The actual atmospheric chemical processes for these compounds are not yet completely recognized. Moreover, accurate parameters needed to quantify the rate of the currently known processes are not available in sufficient detail.

In the present work, attention is paid to the reactivity of both $NO_3$ and $N_2O_5$. In most cases it is concluded that heterogeneous processes are involved.

In respect of the $NO_3$ reactivity, the heterogeneous $NO_3$ decomposition with subsequent formation of $NO_2$ is suggested to play an important role. Such a reaction is regularly used to interpret laboratory experiments, but it has not yet been introduced in model studies. Therefore, the definitive answer of the question, whether such a heterogeneous $NO_3$ removal is significant under representative atmospheric conditions, cannot be given.

In theory, this process may be the $NO_3$ sink needed to explain the $NO_3$ radical concentration profile observed during nights with relative humidities below 50 %. The typical features of these measurements are an average $NO_3$ lifetime of about 1 - 2 hours and a fairly constant value of the $NO_2$ concentration during the night (Platt et al., 1982). Qualitatively, these observations can be understood with a $NO_3$ removal by heterogeneous $NO_3$ to $NO_2$ conversion. The question is whether the rate of the removal process is sufficient to predict a $NO_3$ lifetime of 1 - 2 hours. Quantification involves an examination of the accommodation coefficient and of the total aerosol surface. In the chapters 4 and 6, we have estimated accommodation coefficients for the heterogeneous $NO_3$ to $NO_2$ conversion of the order of $6 \times 10^{-5}$ to $6.5 \times 10^{-4}$, allthough the values given in chapter 4 have to be considered as lower limits. For small aerosol particles of diameter 0.5 $\mu m$ and number concentration $10^4$ $cm^{-3}$, a first-order rate constant for $NO_3$ removal of $6.3 \times 10^{-5}$ $s^{-1}$ can be estimated, when an accommodation coefficient of $10^{-4}$ is employed. This first-order rate constant restricts the $NO_3$ lifetime to about four hours. This value is slightly higher than the observed values but in the right order of magnitude. Furthermore, we must note that the accommodation coefficients were determined on rather inert sufaces, such as Pyrex glass and NaCl. It seems reasonable that in the real atmosphere the accommodation coefficients are appreciably higher.

We may conclude that the heterogeneous $NO_3$ to $NO_2$ conversion is a potentially important removal process for $NO_3$. Therefore, this factor must be considered in describing or modelling the $NO_x$ chemistry in the nocturnal atmosphere.


Another process of crucial importance to the gas phase $NO_2-O_3$ chemistry is the hydrolysis of $N_2O_5$. In the current literature both homogeneous and heterogeneous $N_2O_5$ hydrolysis are considered as important $N_2O_5$ removal pathways. However, the quantification of the removal rate is still proble-

matic. In the chapters 4 and 6 of this thesis, we have addressed attention to this subject.

Regarding the homogeneous $N_2O_5$ hydrolysis, we have obtained an upper limit for its rate constant which is in fairly good agreement with the recent literature data. Using this upper limit, the $N_2O_5$ conversion rate (R.H. 50 %, T = 293 K) can be estimated to be approximately 40 %/h, which is slow compared to the rate of the thermal dissociation of $N_2O_5$. This implies that the homogeneous $N_2O_5$ removal competes with the various $NO_3$ removal processes.

It is evident that heterogeneous $N_2O_5$ hydrolysis is an important loss process for $N_2O_5$. The observation of heterogeneity is a common phenomenon in both laboratory and field studies. In order to quantify this process, it is necessary to know whether the heterogeneous $N_2O_5$ hydrolysis is surface-controlled or whether it is a bulk aqueous process.

In case of a surface-controlled $N_2O_5$ scavenging, we need to establish the accommodation coefficient. In chapter 4 we obtained values of $10^{-9}$ to $10^{-6}$, whereas in chapter 6 we found an accommodation coefficient of $10^{-5}$. This discrepancy raises questions about the validity of a surface-controlled scavenging. As an example, we may calculate the rate of $N_2O_5$ transfer when $\alpha = 10^{-5}$. For small aerosol particles (dp = 0.5 $\mu$m, N = $10^4$ cm$^{-3}$), a first-order rate constant of 4.8 x $10^{-6}$ s$^{-1}$, can be calculated. For in-cloud sca-venging with cloud droplets of diameter 20 $\mu$m and 100 droplets per cubic cm, this first-order rate constant is calculated to be 3.8 x $10^{-5}$ s$^{-1}$. These rate constants correspond with $N_2O_5$ conversion rates of 2 %/h and 14 %/h respectively, i.e. even slower than the homogeneous $N_2O_5$ hydrolysis. It may be clear that heterogeneous $N_2O_5$ removal by the surface-controlled mechanism is only effective in the atmosphere if the accommodation coef-ficient is considerably higher than found in this work.

Otherwise, the attachment of $N_2O_5$ to atmospheric liquid water can be considered as a bulk aqueous phase process. The reactive dissolution of $N_2O_5$ is characterized by the product of its Henry's law constant and the rate constant for $N_2O_5$ hydrolysis in the aqueous phase, for which we deduced a value of 2.4 x $10^2$ M atm$^{-1}$ s$^{-1}$ (chapter 6). This would agree with the results of chapter 4, when the liquid water content in the vessel during the experiments described in chapter 4 was between $10^{-6}$ and 6 x $10^{-6}$.

This result is in reasonable agreement with recent observations in our laboratory (Adema, 1986). Moreover, Adema found that the curve representing the relation between the liquid water content in the 67 l vessel and the relative humidity is of the same shape as the curve plotted in Figure 6 of chapter 4, i.e. the relation between the pseudo-first-order rate constant for $N_2O_5$ hydrolysis and the relative humidity. In view of this ascertainment and of the remarkable agreement between the observed reactive solubility of $N_2O_5$ and that of $N_2O_3$ and $N_2O_4$, we may conclude that a bulk aqueous phase process seems to be a realistic option to describe the heterogeneous $N_2O_5$ removal.

The atmospheric rate of this process can be evaluated assuming that there is no mass transport limitation. The amount of liquid water in a moderately dense cloud is about 1 $g/m^3$ (Pruppacher and Klett, 1978), corresponding with a liquid water content of $10^{-6}$. For such a cloud, the first-order $N_2O_5$ removal rate is calculated to be 6 x $10^{-3}$ $s^{-1}$ or a $N_2O_5$ conversion rate of 2160 %/h, comparable with the rate of thermal dissocation. For small aerosol particles, the liquid water content is much less ($10^{-10}$) and consequently the $N_2O_5$ conversion rate is considerably less (0.2 %/h).

The above means that in a cloud the $N_2O_5$ removal is fast compared with $NO_3$ removal processes, except for $NO_3$ photolysis and the $NO_3$-NO reaction provided sufficient NO is available. Since in most cases the NO concentration is too low at cloud level, a nocturnal cloud is the obvious atmospheric event for nitric acid formation by the $NO_2$-$O_3$ mechanism. Eventually, nitrate formation by this mechanism may be of importance in a dark cloud during day-time.

Recapitulating, we can describe nocturnal $NO_2$-$O_3$ system referring to Figure 1, in which the possible influence of organic species is neglected. The net result of the $NO_2$-$O_3$ chemistry will strongly depend on the actual atmospheric conditions. For example, if sufficient NO is available, the $NO_3$ depletion by reaction with NO dominates and no nitric acid formation occurs. The opposite extreme is relevant in a situation of relatively high liquid water content (cloud, fog), where the rapid $N_2O_5$ scavenging leads to significant nitric acid formation. In this case the $NO_2$ conversion rate at night is determined by the rate of the $NO_2$-$O_3$ reaction and can be as high as 25 %/h, i.e. considerably higher than the rate by photochemical processes.

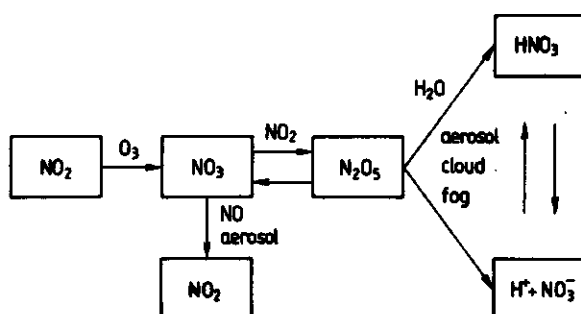FIGURE 1    Scheme of the nocturnal $NO_2$-$O_3$ system in absence
            of organic species.


In the absence of clouds or fog and at low NO concentration level, the
actual nitric acid production depends on the competition between $NO_3$ and
$N_2O_5$ removal processes.

   In conclusion, the present work confirms the current insights in the
atmospheric chemistry of $NO_2$-$O_3$. It provides more detailed knowledge about
some of the processes that play a role in the complex mechanism of noctur-
nal nitric acid formation. This information is valid for many represen-
tative atmospheric conditions and has to be considered in describing the
budgets of atmospheric nitrogen compounds.


8.1.2.   The aqueous phase $NO_2$-$O_3$ chemistry

   The aqueous phase chemistry has been described in chapter 7. The rate of
$NO_2$ uptake by liquid water appears to be in reasonable agreement with
recent laboratory studies. This implies that the nitrite and nitrate for-
mation by this aqueous phase mechanism may be considered insignificant for
typical atmospheric conditions, which is caused by the low physical disso-
lution of $NO_2$.

   The influence of $O_3$ is primarily the oxidation of nitrite to nitrate,
which has been recognized as an important atmospheric chemical process for
some time. Moreover, there is an indication for an aqueous phase reaction
between dissolved $NO_2$ and dissolved $O_3$. However, it is unlikely that this

process leads to significant nitrate production in atmospheric liquid water, because the observed rate is too low.

Evaluating the present knowledge, significant aqueous phase reactions of $NO_2$, leading to the formation of $NO_3^-$, have not been identified. However, up to now all kinetic studies on this subject have been performed using pure, liquid water. Atmospheric liquid water does not consist of pure, liquid water, but it may contain a large variety of dissolved species. These dissolved species may react with $NO_2$ and enhance its rate of uptake. For example, a reducing species is a possible reaction partner since $NO_2$ is a fairly strong oxidizing agent. Some recent experiments in our laboratory have qualitatively shown that the uptake of $NO_2$ is enhanced by $Fe^{2+}$ and $I^-$. Another possible influence of dissolved aqueous species is to act as a catalyst for the aqueous phase $NO_2$ disproportionation.

## 8.2. SOME SUGGESTIONS FOR FURTHER RESEARCH

Evaluating the results of the present study, it is inevitable to state that more detailed insight in the atmospheric chemistry of $NO_2-O_3$ systems is needed. Further research may be addressed to some of the subjects mentioned below.

In the case of laboratory experiments, the $NO_3$ depletion on aerosols of different chemical composure merits further investigations. Furthermore, the exact physical chemical nature of the $N_2O_5$ hydrolysis needs to be clarified. Especially, accurate values for the Henry's law constant of $N_2O_5$ and kinetic parameters of aqueous phase $N_2O_5$ reactions have to be determined. In order to obtain this information advantage may be taken from analogous laboratory studies concerning the reactive dissolution of $N_2O_3$ or $N_2O_4$. Also more laboratory work may be addressed to the aqueous phase chemistry of $NO_2$ and $NO_2-O_3$ mixtures, with emphasis on the chemistry in aqueous solutions characteristic for atmospheric liquid water.

Future field experiments are also needed. The determination of the ambient $N_2O_5$ concentration profiles during the night under different atmospheric conditions are crucial for a better understanding of the $NO_2-O_3$ chemistry. More field data on $NO_3$ concentration levels may also be useful, particularly when these experiments are accompanied with the determination of the concentration, size distribution and chemical composure of aerosol

particles.

It is obvious that new laboratory and field data lead to more model studies. Moreover, model sensitivity studies dealing with phenomena not yet fully understood, may provide more insight in the atmospheric chemistry of $NO_2$-$O_3$ systems.

# REFERENCES

Adema, E.H., 1979, Ozone interference in the determination of nitrogen dioxide by a modified manual Saltzman method, Anal. Chem., 51, 1002-1006.

Adema, E.H., en Ham, J. van (Red), 1983, 'Zure Regen - oorzaken, effecten en beleid', PUDOC, Wageningen.

Adema, E.H., 1986, Personal communication.

Agarwal, J.K., and Sem. G.J., 1980, Continuous flow, - single-particle - counting condensation nucleus counter, J. Aerosol. Sci., 11, 343-358.

Anderson, L.G., 1982, Fate of nitrogen dioxides in urban atmospheres, In : S.E. Schwartz (Ed.), 'Trace atmospheric constituents', Wiley, New York, pp. 371-409.

Anlauf, K.G., Fellin, P., Wiebe, H.A., Schiff, H.I., Mackay, G.I., Braman, R.S., and Gilbert. R., 1985, A comparison of three methods for measurement of atmospheric nitric acid and aerosol nitrate and ammonium, Atmos. Environ., 19, 325-333.

Appel, B.R., Kothny, E.L., Hoffer, E.M., Hidy, G.M., and Wesolowski, J.J., 1978, Sulfate and nitrate data from the California Aerosol Characterization Experiment (ACHEX), Environ. Sci. Technol., 12, 418-425.

Appel, B.R., Wall, S.M., Tokiwa, Y., and Haik, M., 1980, Simultaneous nitric acid, particulate nitrate and acidity measurements in ambient air, Atmos. Environ., 14, 549-554.

Appel, B.R., Tokiwa, Y., and Haik, M., 1981, Sampling of nitrates in ambient air, Atmos. Environ., 15, 283-289.

Asman, W.A.H., 1982, Wet deposition of $NO_x$, In : T. Schneider and L. Grant (Eds.), 'Air pollution by nitrogen oxides", Elsevier, Amsterdam, pp. 271-278.

Atkinson, R., Lloyd, A.C., and Winges, L., 1982, An updated chemical mechanism for hydrocarbon $NO_x/SO_2$ photo-oxidations suitable for inclusion in atmospheric simulation models, Atmos. Environ., 16, 1341-1355.

Atkinson, R., Plum, C.N., Carter, W.P., Winer, A.M., and Pitts, Jr., J.N., 1984, Rate constants for the gas phase reactions of $NO_3$ radicals with a series of organics in air at 298 ± 1 K, J. Phys. Chem., 88, 1210 - 1215.

Atkinson, R., Winer, A.M., and Pitts Jr., J.N., 1986, Estimation of night-time $N_2O_5$ concentrations from ambient $NO_2$ and $NO_3$ radical concentrations and the role of $N_2O_5$ in night-time chemistry, Atmos. Environ., 20, 331-339.

Attmanspacher, W., Hartmannsgruber, R., und Lang, P., 1984, Langzeittendenzen des Ozons der Atmosphäre auf Grund der 1967 begonnenen Ozonmessreihen am Meteorologischen Observatorium Hohenpeissenberg, Meteorol. Rdsch., 37, 193 - 199.

Ayers, G.P., and Gillett, R.W., 1984, Some observations on the acidity and composition of rainwater in Sydney, Australia, during the summer of 1980-81. J. Atmos. Chem., 2, 25-46.

Baulch, D.L., Cox, R.A., Crutzen, P.J., Hampson Jr., R.F., Kerr, J.A., Troe, J., and Watson, R.T., 1982, Evaluated kinetic and photochemical data for atmospheric chemistry : Supplement I, J. Phys. Chem. Ref. Data, 11, 328-495.

Becker, K.H., Schurath, V., and Seitz, H., 1974, Ozone-olefin reactions in the gas phase. 1. Rate constants and activation energies, Int. J. Chem. Kinet., 6, 725-739.

Beilke, S., 1983, Bildung von Säuren durch heterogene Reactionen, VDI-Berichte, 300, 35 - 42.

Beilke, S., and Elshout, A.J., (Eds.), 1983, 'Acid deposition'. D. Reidel, Dordrecht.

Besemer, A.C., Aalst, R.M. van, en Duijzer, J.H., 1984. In : H.S.M.A. Diederen en R. Guicherit (Red.), Fotochemische Luchtverontreiniging Aerosolen en Toxiciteit, CMP-rapport 84/31, hfdst. V.

Brewer, R.L., Gordon, R.J., Shepard, L.S., and Ellis, E.C., 1983, Chemistry of mist and fog from the Los Angeles urban area, Atmos. Environ., $\underline{17}$, 2267-2270.

Brink, H.M. ten, Mallant, R.K.A.M., and Vate, J.F. van de, 1982, The role of aerosol in air pollution chemistry, Proc. of the 5th International Clean Air Congress Buenos Aires Argentina, Volume I, pp. 358-364.

Brink, H.M. ten, Plomp, A., Spoelstra, H., and Vate, J.F. van de, 1983, A high-resolution electrical mobility aerosol spectrometer (MAS), J.Aerosol.Sci., $\underline{14}$, 589-597.

Bubenich, D.V., Record, F.A., and Kindya, R.J., 1983, Acid rain – an overview of the problem, Environmental Progress, $\underline{2}$, 15 – 32.

Buringh, E., 1980, Over het atmosferische gedrag en de emissie van sub-microne verkeersaerosolen, Ph. Thesis, Wageningen.

Burrows, J.P., Tyndall, G.S., and Moortgat, G.K., 1984, A Study of $N_2O_5$ and $NO_3$ chemistry in the photolysis of $N_2O_5$ mixtures, Proceedings of the 3rd European Symposium on physico-chemical behaviour of atmospheric pollu-tants, Varese, Italy, 10-12 April, 1984, pp. 240-248.

Cadle, S.H., 1985, Seasonal variations in nitric acid, nitrate, strong aerosol acidity and ammonia in an urban area, Atmos. Environ., $\underline{19}$, 181-188.

Calvert, J.G., Su, F., Bottenheim, J.W., and Strausz, O.P., 1978, Mechanism of the homogeneous oxidation of sulfur dioxide in the troposphere, Atmos. Environ., $\underline{12}$, 197 – 226.

Calvert, J.C., and Stockwell, W.R., 1983, Acid generation in the tropo-sphere by gas phase chemistry, Environ. Sci. Technol., $\underline{17}$, 429A-443A.

Carter, W.P.L., Lloyd, A.C., Sprung, J.L., and Pitts Jr., J.N., 1979, Computer modeling of smog chamber data : process in validation of a detailed mechanism for the photo-oxidation of propene and n-butane in photo-chemical smog, Int. J. Chem. Kinet., $\underline{11}$, 45-101.

Castillo, R.A., and Jiusto, J.E., 1983, Characteristics of non-precipitating stratiform clouds, In : H.R. Pruppacher, R.G. Semonin, and W.G.N. Slinn (Eds.) : 'Precipitation scavenging, Dry Deposition and Resuspension', Volume 1, Elsevier, Amsterdam, pp.115-122.

Chameides, W.L., and Davis, D.D., 1982, The free radical chemistry of cloud droplets and its impact upon the composition of rain, J. Geophys. Res., $\underline{87}$, 4863-4877.

Chameides, W.L., and Davis, D.D., 1983, The coupled gas-phase/aqueous phase free radical chemistry of a cloud, In : H.R. Pruppacher, R.G. Semonin, and W.G.N. Linn (Eds.), 'Precipitation Scavenging, Dry Deposition and Resuspension', Volume 1, Elsevier, Amsterdam, pp.431-443.

Clark, P.A., Fletcher, I.S., Kallend, A.S., McElroy, W.J., Marsh, A.R.W., and Webb, A.H., 1984, Observations of cloud chemistry during long-range transport of power plant plumes, Atmos. Environ., $\underline{18}$, 1849-1858.

Connell, P., and Johnston, H.S., 1979, The thermal dissociation of nitrogen pentoxide in molecular nitrogen, Geophys. Res. Lett., $\underline{6}$, 553-556.

Cox, R.A., 1974. Particle formation from homogeneous reactions of sulphur dioxide and nitrogen dioxide, Tellus, $\underline{26}$, 235-240.

Cox, R.A., 1982, Chemical transformation processes for $NO_x$ species in the atmosphere, In : T. Schneider and L. Grant (Eds.), 'Air pollution by nitrogen oxides', Elsevier, Amsterdam, pp. 249-261.

Cox, R.A., and Penkett, S.A., 1983, Formation of atmospheric acidity, In :
S. Beilke and A.J. Elshout (Eds.), 'Acid Deposition', D. Reidel,
Dordrecht, pp. 56-81.

Cox, R.A., and Coker, G.B., 1983, Kinetics of the reaction of nitrogen
dioxide with ozone, J. Atmos. Chem., $\underline{1}$, 53-63.

Crump, J.G., Flagan, R.C., and Seinfeld, J.H., 1983, Particle wall loss
rates in vessels, Aerosol Sci. and Technol., $\underline{2}$, 303 - 309.

Crump, J.G., and Seinfeld, J.H., 1981, Turbulent deposition and gravita-
tional sedimentation of an aerosol in a vessel of arbitrary shape, J.
Aerosol. Sci., $\underline{12}$, 405-415.

Crutzen, P.J., 1973, A discussion of the chemistry of some minor constituents
in the stratosphere and troposphere, Pure. Appl. Geophys., $\underline{106-108}$, 1385 -
1399.

Crutzen, P.J., 1985, The role of the tropics in atmospheric chemistry. Paper
presented at the United Nations International Conference on Climatic,
Biotic and Human Interactions in the humid tropics : Vegetation and
Climate Interactions in Amazonia, 26 February - 1 March, 1985, at the
Instituto de Pesquisas Espaciais - INPE, Sao José dos Campos, Brazil.

Damschen, D.E., and Martin, L.R., 1983, Aqueous aerosol oxidation of nitrous
acid by $O_2$,$O_3$ and $H_2O_2$, Atmos.Environ.,$\underline{17}$, 2005-2011.

Danckwerts, P.V., 1970, 'Gas-liquid reactions', McGraw-Hill, New-York.

Daum, P.H., Kelly, T.J., Schwartz, S.E., and Newman, L., 1984, Measurements
of the chemical composition of stratiform clouds, Atmos. Environ., $\underline{18}$,
2671-2684.

Davies, C.N., 1979, Coagulation of aerosols by Brownian motion, J. Aerosol.
Sci., $\underline{10}$, 151-161.

Davis, D.D., Prusazcyk, J., Dwyer, M., and Kim, P., 1974, A stop-flow
time-of-flight mass spectrometry kinetic study. Reaction of ozone with
nitrogen dioxide and sulfur dioxide, J. Phys. Chem., $\underline{78}$, 1775-1779.

Davis, L.I., Wang, C.G., Tang, X., Niki, H., and Weinstock, B., 1982,
Fluorescence measurements of OH at Niwot Ridge, 2nd Symp. on Comp. of
non-urban Tropos., 1982, Williamsburg, Am. Met. Soc. Boston, 319 - 323.

Diederen, H.S.M.A., 1984, Voorkomen, niveaus, karakterisering en inter-
acties van gasvormige verbindingen en aerosolen in de buitenlucht bij
verschillende meteorologische condities, In : H.S.M.A. Diederen en R.
Guicherit (Red.), 'Fotochemische luchtverontreiniging, aerosolen en toxi-
citeit', CMP-rapport 84/31, hfdst. II.

Drummond, J.W., Volz, A., and Ehhalt, D.H., 1985, An optimized chemilu-
minescence detector for tropospheric NO measurements, J. Atmos. Chem., $\underline{2}$,
287-306.

Durham, J.L., Overton, Jr., J.H., and Aneja, V.P., 1981, Influence of
gaseous nitric acid on sulfate production and acidity in rain, Atmos.
Environ., $\underline{15}$, 1059-1068.

Duuren, H. van, and Römer, F.G., 1982, On the results of the aerosol
measuring network for particulate sulphates and nitrates in the period
1979-1980 in the Netherlands, In : B. Versivo and H. Ott (Eds.),
'Physico-chemical behaviour of atmospheric pollutants', D. Reidel,
Dordrecht, pp. 596-601.

England, C., and Corcoran, W.H., 1974, Kinetics and mechanism of the gas
phase reaction of water vapor and nitrogen dioxide, Ind. Eng. Chem.
Fundam., $\underline{13}$, 373 - 384.

Ferm, M., Samuelsson, U., Sjödin, A., and Grennfelt, P., 1984, Long-
range transport of gaseous and particulate oxidized nitrogen compounds,
Atmos. Environ., $\underline{18}$, 1731-1735.

Fontijn, A., Sabadell, A.J., and Ronco, R.J., 1970, Homogeneous chemilumi-
nescent measurement of nitric oxide with ozone, Anal. Chem., 42, 575-579.

Ford, H.W., Doyle, G.J., and Endow, N., 1957, Rate constants at low
concentrations, I. Rate of reaction of ozone with nitrogen dioxide, J.
Chem. Phys., 26, 1336.

Forrest, J., Garber, R.W., and Newman, L., 1981, Conversion rates in power
plant plumes based on filter pack data : The coal-fired Cumberland plume,
Atmos. Environ., 15, 2273-2282.

Forrest, J., Spandau, D.J., Tanner, R.L., and Newman, L., 1982,
Determination of atmospheric nitrate and nitric acid employing a dif-
fusion denuder with a filter pack, Atmos. Environ., 16, 1473-1485.

Freyer, H.D., 1978, Seasonal trends of $NH_4^+$ and $NO_3^-$ nitrogen isotope
composition in rain collected at Jülich, Germany, Tellus, 30, 83-92.

Fuchs, N.A., 1964, The mechanics of aerosols, Pergamon Press, Oxford.

Fuchs, N.A., and Sutugin, A.G., 1970, The properties of highly dispersed
aerosol, in : G.M. Hidy and J.R., Brock (Eds.), 'The dynamics of aero-
colloidal systems', Pergamon Press, Oxford, pp. 105-134.

Gailey, P.C., McClenny, W.A., Braman, R.S., and Shelley, T.J., 1983,
A simple design for automation of the Tungsten (VI)-oxide technique for
measurement of $NH_3$ and $HNO_3$, Atmos. Environ., 17, 1517-1519.

Galloway, J.N., and Likens, G.E., 1981, Acid precipitation: the importance
of nitric acid, Atmos. Environ., 15, 1081-1085.

Georgii, H.W., und Schmitt, G., 1985, Methoden und Ergebnisse der Nebel-
analyse, Staub, 45, 260-264.

Gerritse, R.G., 1979, Rapid simultaneous determination of nitrate and
nitrite by high-performance liquid chromatography using ultraviolet
detection, J. Chromatogr., 171, 527-529.

Graham, R.A., and Johnston, H.S., 1974, Kinetics of gas-phase reaction
between ozone and nitrogen dioxide, J. Chem. Phys., 60, 4628-4629.

Graham, R.A., and Johnston, H.S., 1978, The photo-chemistry of $NO_3$ and the
kinetics of the $N_2O_5$-$O_3$ system, J. Phys. Chem., 82, 254-268.

Grosjean, D., 1983, Distribution of atmospheric nitrogeneous pollutants at
a Los Angeles area smog receptor site, Environ. Sci. Technol., 17, 13-19.

Grosjean, D., 1985, Wall loss of gaseous pollutants in outdoor teflon
chambers, Environ. Sci. Technol., 19, 1059-1065.

Harker, A.B., and Strauss, D.R., 1981, Kinetics of the heterogeneous
hydrolysis of dinitrogen pentoxide over the temperature range 214-263K,
Report No. FAA-EE-81-3, Rockwell International Science Center.

Hegg, D.A., Hobbs, P.V., and Radke, L.F., 1984, Measurements of the
scavenging of sulfate and nitrate in clouds, Atmos. Environ., 18, 1939-1946.

Heikes, B.G., and Thompson, A.M., 1983, Effects of heterogeneous processes
on $NO_3$, HONO, and $HNO_3$ chemistry in the troposphere, J. Geophys. Res.,
88, 10883-10895.

Heikes, B.G., 1984, Aqueous $H_2O_2$ production from $O_3$ in glass impingers,
Atmos.Environ., 18, 1433-1445.

Helas, G., Flanz, M., and Warneck, P., 1981, Improved $NO_x$ monitor for
measurements in tropospheric clean air regions, Int. J. Envir. Analyt.
Chem., 10, 155-166.

Herschbach, D.R., Johnston, H.S., Pitzer, K.S., and Powell, R.E., 1956,
Theoretical pre-exponentional factors of twelve biomolecular reactions,
J. Chem. Phys., 25, 736-741.

Hewitt, C.H., and Harrison, R.M., 1985, Tropospheric concentrations of
hydroxyl radical - a review, Atmos. Environ., 19, 545 - 554.

Holländer, W., Behnke, W., Koch, W., and Pohlmann, G., 1984, Design and

performance of an aerosol reactor for photochemical studies, In : B. Versino and G. Angelotti (Eds), 'Physico-chemical behaviour of atmonspheric pollutants', D. Reidel, Dordrecht, pp. 309-319.

Horvath, L., and Meszaros, E., 1984, The composition and acidity of precipitation in Hungary, Atmos. Environ., 18, 1843-1847.

Hughes, E.E., Rook, H.L., Deardorff, E.R., Margeson, J.H., and Fuerst, R.G., 1977, Performance of a $NO_2$ permeation device, Anal. Chem., 49, 1823-1829.

Huie, R.A., and Herron, J.T., 1974, the rate constant for the reaction $O_3 + NO_2 = O_2 + NO_3$ over the temperature range 259-362K, Chem. Phys. Lett., 27, 411-414.

Huygen, C., and Lanting, R.W., 1975, On the Saltzman factor, Atmos. Environ., 9, 1027-1029.

Jacob, D.J., Waldman, J.M., Munger, J.W., and Hoffmann, M.R., 1985, Chemical composition of fogwater collected along the California coast, Environ. Sci. Technol., 19, 730-736.

Jaffe, S., and Ford, H.W., 1967, The photolysis of nitrogen dioxide in the presence of nitric acid at 3660 Å and 25°, J. Phys. Chem., 71, 1832-1836.

Johnston, H.S., and Yost, D.M., 1949, The kinetics of the rapid gas reaction between ozone and nitrogen dioxide, J. Chem. Phys., 17, 386-392.

Jones, C.L., and Seinfeld, J.H., 1983, The oxidation of $NO_2$ to nitrate - day and night, Atmos. Environ., 17, 2370-2373.

Kaiser, E.W., and Wu, C.H., 1977, Measurement of the rate constant of the reaction of nitrous acid with nitric acid, J. Phys. Chem., 81, 187 - 190.

Kasting, J.F., and Ackerman, T.P., 1985, High atmospheric $NO_x$ levels and multiple photochemical steady states, J. Atmos. Chem., 3, 321-340.

Kelly, T.J., Tanner, R.L., Newman, L., Galvin, P.J., and Kadlecek, J.A., 1984, Trace gas and aerosol measurements at a remote site in the northeast U.S., Atmos. Environ., 18, 2565-2576.

Kircher, C.C., Margitan, J.J., and Sander, S.P., 1984, Pressure and temperature dependence of the reaction $NO_2 + NO_3 + M \rightarrow N_2O_5 + M$, J. Phys. Chem., 88, 4370-4375.

Kosak-Channing, L.F., and Helz, G.R., 1983, Solubility of ozone in aqueous solutions of 0-0.6 M ionic strength at 5-30 °C, Environ.Sci.Technol., 17, 145-149.

Lazrus, A.L., Haagenson, P.L., Kok, G.L., Huebert, B.J., Kreitzberg, C.W., Likens, G.E., Mohnen, V.A., Wilson, W.E., and Winchester, J.W., 1983, Acidity in air and water in a case of warm frontal precipitation, Atmos. Environ., 17, 581-591.

Lee, K.W., 1983, Change of particle size distribution during Brownian coagulation, J. Colloid. Interface Sci., 92, 315-326.

Lee, K.W., Chen, H., and Gieseke, J.A., 1984, Log-normally preserving size distribution for Brownian coagulation in the free-molecule regime, Aerosol Sci. Technol., 3, 53-62.

Lee, Y-N., and Schwartz, S.E., 1981a, Reaction kinetics of nitrogen dioxide with liquid water at low partial pressure, J. Phys. Chem., 85, 840-848.

Lee, Y-N., and Schwartz, S.E., 1981b, Evaluation of the rate of uptake of nitrogen dioxide by atmospheric and surface liquid water, J. Geophys. Res., 86, 11971-11983.

Lee, Y-N., and Schwartz, S.E., 1983, Kinetics of oxidation of aqueous sulfur (IV) by nitrogen dioxide, In : H.R. Pruppacher, R.G. Semonin, and W.G.N. Slinn, (Eds.), 'Precipitation Scavenging, Dry Deposition and Resuspension', Volume 1. Elsevier, Amsterdam, pp. 453-466.

Lee, Y-N., 1984, Atmospheric aqueous-phase reactions of nitrogen species, In : L. Newman (Ed.), 'Gas-liquid chemistry of natural waters', New York,

pp. 20-1 to 20-10.

Lee, Y-N, 1985, Chemical transformations in acid rain, Volume II: Investigation of kinetics and mechanism of aqueous-phase peroxide formation, Brookhaven National Laboratory, Upton, New York.

Leuenberger, U., Gauch, R., Rieder, K., and Baumgartner, 1980, Determination of nitrate and bromide in foodstuffs by high-performance liquid chromatography, J. Chromatogr., $\underline{202}$, 461-468.

Logan, J.A., Prather, M.J., Wofsy, S.C., and McElroy, M.B., 1981, Tropospheric chemistry : a global perspective, J. Geophys. Res., $\underline{86}$, 7210 - 7254.

Lindqvist, F., and Lanting, R.W., 1972, A modified permeation device for the preparation of trace gas mixtures, Atmos. Environ., $\underline{6}$, 943-946.

Liu, B.Y.H., Whitby, K.T., and Pui, D.Y.H., 1974, A portable electrical analyzer for size distribution measurement of submicron aerosols, J. Air. Pollut. Control. Assoc., $\underline{24}$, 1067-1072.

Liu, B.Y.H. and Pui, D.Y.H., 1974a, Equilibrium bipolar charge distribution of aerosols, J. Colloid Interface Sci., $\underline{49}$, 305-312.

Liu, B.Y.H., and Pui, D.Y.H., 1974b, Electrical neutralization of aerosols, J. Aerosol. Sci., $\underline{4}$, 465-472.

Liu. B.Y.H., and Pui, D.Y.H., 1975, On the performance of the electrical aerosol analyzer, J. Aerosol. Sci., $\underline{6}$, 249-264.

Liu, B.Y.H., and Lee, K.W., 1975, An aerosol generator of high stability, Amer. Ind. Hyg. J., $\underline{36}$, 861-865.

Liu, B.Y.H., Pui, D.Y.H., and Kapadia, A., 1976, Electrical aerosol analyzer : history, principle and data reduction, Part. Technol. Lab., pub. 303.

Liu, B.Y.H., and Kapadia, A., 1977, A computer data reduction program for the electrical aerosol analyzer, Part. Technol. Lab., pub. 325

Magnotta, F., and Johnston, H.S., 1980, Photodissociation quantum yields for $NO_3$ free radical, Geophys. Res. Lett., $\underline{7}$, 769-772.

Malko, M.W., and Troe, J., 1982, Analysis of the unimolecular reaction $N_2O_5 + M \rightleftharpoons NO_2 + NO_3 + M$, Int. J. Chem. Kinet., $\underline{14}$, 399-416.

Marsh, A.R.W., 1983, Studies of the acidity and chemical composition of clouds, In : S. Beilke and A.J. Elshout (Eds.) :'Acid Deposition', D. Reidel, Dordrecht, pp. 185-194.

Martin, A., 1984, Estimated washout coefficients for sulphur dioxide, nitric oxide, nitrogen dioxide and ozone, Atmos. Environ., $\underline{18}$, 1955-1961.

Martin, A., and Barber, F.R., 1984, Acid gases and acid rain monitored for over 5 years in rural east-central England, Atmos. Environ., $\underline{18}$, 1751-1724.

Matthews, R.D., Sawyer, R.F., and Schefer, R.W., 1977, Interferences in chemiluminescent measurement of NO and $NO_2$ emissions from combustion systems, Environ. Sci. Technol., $\underline{11}$, 1092-1096.

McMurry, P.H., and Grosjean, D., 1985, Gas and aerosol wall losses in teflon film smog chambers, Environ. Sci. Technol., $\underline{19}$, 1176-1182.

Meixner, F.X., Müller, K.P., Aheimer, G., and Höfken, K.D., 1985, Measurements of gaseous nitric acid and particulate nitrate, In : 'Pollutants cycles, transport modelling and field experiments', Bilthoven, Sept. 1985, pp. 108-119.

Meszaros. E., and Horvath, L., 1984, Concentration and dry deposition of atmospheric sulfur and nitrogen compounds in Hungary, Atmos. Environ., $\underline{18}$, 1725-1730.

Morris. Jr., E.D., and Niki, H., 1973, Reaction of dinitrogen pentoxide with water, J. Phys. Chem., $\underline{77}$, 1929-1932.

Myers, G.H., Silver, D.M., and Kaufman, F., 1966, Quenching of $NO_2$ fluorescence, J. Chem. Phys., 44, 718-723.

NEN 2040, 1982, Photometric determination of nitrogen dioxide (Saltzman method), NNI, Delft.

NEN 2042, 1982, Preparation of calibration gas mixtures by means of permeation tubes, NNI, Delft.

NEN 2045, 1981, The calibration of measuring methods for nitrogen monoxide, nitrogen dioxide and ozone by means of gas-phase titration, NNI, Delft.

NEN 2789, 1983, Photometric determination of ozone content with indogitin disulphonate, NNI, Delft.

Novakov, T., Chang, S.G., and Harker, A.B., 1974, Sulfate in pollution particulates : catalytic oxidation of $SO_2$ on carbon particles, Science, 186, 259 - 261.

Noxon, J.F., Norton, R.B., and Henderson, W.R., 1978, Observations of atmospheric $NO_3$, Geophys. Res. Lett., 5, 675-678.

Noxon, J.F., Norton, R.B., and Marovich, E., 1980, $NO_3$ in the troposphere, Geophys. Res. Lett., 7, 125-128.

NPR 2047, 1982, Preparation of low and constant ozone concentrations in air, NNI, Delft.

Okita, T., Morimoto, S., Izawa, M., and Konno, S., 1976, Measurement of gaseous and particulate nitrates in the atmosphere, Atmos. Environ., 10, 1085-1089.

Okuyama, K., Kousaka, Y., and Hosokawa, T., 1984, Turbulent and Brownian diffusive deposition and gravitational sedimentation of aerosol particles in a stirred tank. In: B.Y.H. Liu, D.Y.H. Pui, and H.J. Fissan (Eds), 'Aerosols', Elsevier, New York, pp. 857-860.

Penkett, S.A., 1972, Oxidation of $SO_2$ and other atmospheric gases by ozone in aqueous solution, Nature Phys. Sci., 240, 105-106.

Penkett, S.A., Jones, B.M.R., Brice, K.A., and Eggleton, A.E.J., 1979, The importance of atmospheric ozone and hydrogen peroxide in oxidising sulfur dioxide in cloud and rain water, Atmos. Environ., 13, 123 - 127.

Perner, D., Schmeltekopf, A., Winkler, R.H., Johnston, H.S., Calvert, J.G., Cantrell, C.A., and Stockwell, W.R., 1985, A laboratory and field study of the equilibrium $N_2O_5 \rightleftharpoons NO_3 + NO_2$, J. Geophys. Res., 90, 3807-3812.

Perry, R.H., and Chilton, C.H., 1973, Chemical Engineers Handbook, 5th Edn. Mc Graw-Hill, New York.

Peterson, T.W., and Seinfeld, J.H., 1980, Heterogeneous condensation and chemical reaction in droplets : Application to the heterogeneous atmospheric oxidation of $SO_2$, Adv. Environ. Sci. Technol., 10, 125-179.

Pitts Jr., J.N., Kummer, W.A., Steer, R.P., and Finlayson, B.J., 1972, The chemiluminescent reactions of ozone with olefins and organic sulfides. In : R.F. Gould (Ed.), 'Photochemical smog and ozone reactions', American Chemical Society Washington, pp. 246-254.

Platt, U., Perner, D., Winer, A.M., Harris, G.W., and Pitts, Jr., J.N., 1980, Detection of $NO_3$ in the polluted troposphere by differential optical absorption, Geophys. Res. Lett., 7, 89-92.

Platt, U., Perner, D., Schröder, J., Kessler, C., and Toenissen, A., 1981, The diurnal variation of $NO_3$, J. Geophys. Res., 86, 11965-11970.

Platt, U., Perner, D., and Kessler, C., 1982, The importance of $NO_3$ for the atmospheric $NO_x$ cycle from experimental observations. In : Proceedings of the 2nd Symposium : Composition of the non-urban troposphere, Williamsburg, May 1982, pp. 21-24.

Platt, U.F., Winer, A.M., Biermann, H.W., Atkinson, R., and Pitts, Jr., J.N., 1984, Measurement of nitrate radical concentrations in continental

air, Environ. Sci. Technol., 18, 365-369.

Platt, U., Perner, D., and Junkermann, W., 1985, The atmospheric life-time of nitrate radicals, In :'Pollutants cycles, transport modelling and field experiments', Bilthoven, Sept. 1985, pp. 82-88.

Pruppacher, H.R., and Klett, J.D., 1978, Microphysics of clouds and precipitation, D. Reidel, Dordrecht, pp. 158.

Römer, F.G., Viljeer, J.W., van den Beld, L., Slangewal, H.J., Veldkamp, A.A., and Reijnders, H.F.R., 1985, The chemical composition of cloud and rainwater. Results of preliminary measurements from an aircraft, Atmos. Environ., 19, 1847-1858.

Richards, L.W., 1983, Comments on 'the oxidation of $NO_2$ to nitrate day and night', Atmos. Environ., 17, 397-402.

Ridder, T.B., and Frantzen, A.J., 1983, Acid precipitation over the Netherlands, In : S. Beilke and A.J. Elshout (Eds.), 'Acid precipitation', D. Reidel, Dordrecht, pp. 123-128.

Russell, A.G., McRae, G.J., and Cass, G.R., 1985, The dynamics of nitric acid production and the fate of nitrogen oxides, Atmos. Environ., 19, 893-903.

Saltzman, B.E., 1954, Colorimetric micro-determination of nitrogen dioxide in the atmosphere, Anal. Chem., 26, 1949-1955.

Schwartz, S.E., and White, W.H., 1981, Solubility equilibria of the nitrogen oxides and oxyacids in dilute aqueous solution, Advan. Environ. Sci. Eng., 4, 1-45.

Schwartz, S.E., and Freiberg, J.E., 1981, Mass-transport limitation to the rate of reaction of gases in liquid droplets. Application to oxidation of $SO_2$ in aqueous solutions, Atmos. Environ., 15, 1129-1144.

Schwartz, S.E., and White, W.H., 1982, Kinetics of reactive dissolution of nitrogen oxides into aqueous solution, In : S.E. Schwartz (Ed.), 'Trace atmospheric constituents', Wiley, New York, pp. 1-116.

Seigneur, C., and Saxena, P., 1984, A study of atmospheric acid formation in different environments, Atmos. Environ., 18, 2109-2124.

Shaw, Jr., R.W., Stevens, R.K., Bowermaster, J., Tesch, J.W., and Tew, E., 1982, Measurements of atmospheric nitrate and nitric acid : the denuder difference experiment, Atmos. Environ., 16, 845-853.

Spicer, C.W., and Miller, D.F., 1976, Nitrogen balance in smog chamber studies, J. Air. Pollut. Control Assoc., 26, 45-50.

Spicer, C.W., and Schumacher, P.M., 1977, Interferences in sampling atmospheric particulate nitrate, Atmos. Environ., 11, 873-876.

Spicer, C.W., Howes, Jr., J.E., Bishop, T.A., Arnold, L.H., and Stevens, R.K., 1982, Nitric acid measurement methods : an intercomparison, Atmos. Environ., 16, 1487-1500.

Staehelin, J., and Hoigné, J., 1982, Decomposition of ozone in water: rate of initiation by hydroxide ions and hydrogenperoxide, Environ. Sci. Technol. , 16, 676-681.

Stedman, D.H., and Niki. H., 1973, Kinetics and mechanism of the photolysis of nitrogen dioxide in air, J. Phys. Chem., 77, 2604-2609.

Stockwell, W.R., and Calvert, J.G., 1983, The mechanism of $NO_3$ and HONO formation in the night-time chemistry of the urban atmosphere, J. Geophys. Res., 88, 6673-6682.

Streit, G.E., Wells, J.S., Fehsenfeld. F.C., and Howard, C.J., 1979, A tunable diode laser study of the reactions of nitric and nitrous acid : $HNO_3$ + NO and $HNO_2$ + $O_3$, J. Chem. Phys., 70, 3439 - 3443.

Svendrup, G.M., and Høv, O., 1984, Modeling study of the potential importance of heterogeneous surface reactions for $NO_x$ transformations in

plumes, Atmos. Environ., 18, 2753-2760.

Swedish Ministry of Agriculture, 1982, 'Acidification, today and tomorrow' - A Swedish study prepared for the 1982 Stockholm conference on the acidification of the environment, Swedish Ministry of Agriculture, Environment '82 Committee.

Tuazon, E.C., Atkinson, R., Plum, N., Winer, A.M., and Pitts, Jr., J.N., 1983, The reaction of gas phase $N_2O_5$ with water vapour, Geophys. Res. Lett., 10, 953-956.

Tuazon, E.C. Sanhueza, E., Atkinson, R., Carter, W.P.L., Winer, A.M., and Pitts, Jr., J.N., 1984, Direct determination of the equilibrium constant at 298K for the $NO_2 + NO_3 \rightleftharpoons N_2O_5$ reactions, J. Phys. Chem., 88, 3095-3098.

Vate, J.F. van de, Plomp, A., Jong, C. de, and Vrins, E.L.M., 1978, A battery-operated portable unit for electrostatic and impaction sampling of ambient aerosol for electron microscopy, Staub Reinhalt. Luft, 38, 53-64.

Vate, J.F. van de, 1980, Investigations into the dynamics of aerosols in enclosures as used for air pollution studies, Ph. D. Thesis, Agricultural University, Wageningen, pp. 24-30.

Verhees, P.W.C., and Adema, E.H., 1985, The $NO_2$-$O_3$ system at sub-ppm concentrations: Influence of Temperature and Relative Humidity, J. Atmos. Chem., 2, 387-403.

Viggiano, A.A., Davidson, J.A., Fehsenfeld, J.A., and Ferguson, E.E., 1981, Rate constants for the collisional dissociation of $N_2O_5$ by $N_2$, J. Chem. Phys., 74, 6113-6125.

VROM, 1985, 'Zure Regen' - voorlichtingsbrochure, Den Haag, april 1985.

Waldman, J.M., Munger, J.W., Jacob, D.J., Flagan, R.C., Morgan, J.J., and Hoffman, M.R., 1982, Chemical composition of acid fog, Science, 218, 677-679.

Waldman, J.M., Munger, J.W., Jacob, D.J., and Hoffman, M.R., 1983, Fog-water composition in southern California, In : H.R. Pruppacher, R.G. Semonin and W.G.N. Slinn, (Eds.) : 'Precipitation scavenging, Dry Deposition and Resuspension', Volume 1, Elsevier, Amsterdam, pp. 137-146.

Walter, H., 1973, Coagulation and size distribution of condensation aerosols, J. Aerosol. Sci., 4, 1-15.

Weinstock, B., Niki, H., and Chang, T.Y., 1980, Chemical factors affecting the hydroxyl radical concentration in the troposphere, Adv. Environ. Sci. Technol., 10, 221 - 258.

Whitby, K.T., Husar, R.B., and Liu, B.Y.H., 1972, The aerosol size distribution of Los Angeles smog, J. Colloid Interface Sci., 39, 177-204.

Whitby, K.T., Liu, B.Y.H., Husar, R.B., and Barsic, N.J., 1972, The Minnesota aerosol analyzing system used in the Los Angeles smog-project, In : G.W. Hidy (Ed.), 'Aerosols and atmospheric chemistry', Academic Press, New York, 189-217.

Willison, M.J., Clarke, A.G., and Zeki, E.M., 1985, Seasonal variation in atmospheric aerosol concentration and composition at urban and rural sites in northern England, Atmos. Environ., 19, 1081-1089.

Winer, A.M., Peters, J.W., Smith, J.P., and Pitts, Jr., J.N., 1974, Response of commercial chemiluminescent $NO$-$NO_2$ analyzers to other nitrogen-containing compounds, Environ. Sci. Technol., 8, 1118-1121.

Wu, C.H., Morris, Jr., E.D., and Niki, H., 1973, The reaction of nitrogen dioxide with ozone. J. Phys. Chem., 77, 2507-2511.

Zabielski, M.F., Seery, D.J., and Dodge, L.G., 1984, Influence of mass transport and quenching on nitric oxide chemiluminescent analysis, Environ. Sci. Technol., 18, 88-92.

# SUMMARY

In this dissertation a laboratory study dealing with the atmospheric chemistry of $NO_2$-$O_3$ systems is described. Knowledge of this system is relevant for a better understanding of a number of air pollution problems, particularly that of acid deposition.

In chapter 1 a short overview of atmospheric chemistry is given, in which the formation of oxidants, the $SO_2$ chemistry and the $NO_x$ chemistry are considered.

It appears that, in absence of light, interactions between $NO_2$ and $O_3$ may lead to the formation of nitric acid. After oxidation of $NO_2$ by $O_3$, the $NO_3$ radical is formed. Next, this radical can react in several ways. One of the possibilities is the reaction with $NO_2$ resulting in $N_2O_5$. The actual nitric acid formation is the $N_2O_5$ hydrolysis. In theory, this process can substantially contribute to the nitric acid formation in the atmosphere. Some gaps in the present knowledge are the exact mechanism and kinetics of the $N_2O_5$ hydrolysis and the $NO_3$ reactivity.

Chapter 2 contains a review of the recent literature. Subsequently, laboratory, field and model studies are considered. Without doubt, it can be concluded that the non-photochemical nitrate formation by the $NO_2$-$O_3$ system is recognized as an important atmospheric chemical process. The above-mentioned knowledge gaps are confirmed which, among other things, follows from measurements of the ambient $NO_3$ radical concentration profile. Regularly, it is suggested that heterogeneous processes of $NO_3$ or $N_2O_5$ removal are involved. The parameters needed to quantify such processes are currently unavailable.

After the general introduction and the literature review, the experimental methods applied in the present investigation are described. The construction of the employed laboratory equipment is given. The basic prin-

ciples of the techniques used for the generation and analysis of the reactants are listed.

In the chapters 4 to 7 the results are described and discussed. Chapter 4 treats the results of a study on the $NO_2-O_3$ chemistry at sub-ppm concentrations as well as the influence of temperature and relative humidity (R.H.). The experiments are performed using the standard techniques for measurement and calibration of $NO_2$ and $O_3$

If we consider the stoichiometry of the reaction system at R.H. < 0.1%, it appears that it deviates from the theoretical value of two. Obviously a side-reaction, that regenerates $NO_2$, consumes extra $O_3$ or both, is involved. Since the stoichiometry significantly differs in reaction vessels of different size (other variables constant), we have to deal with a wall reaction. Further analysis of the results combined with literature data leads to the interpretation that the low stoichiometry is caused by the heterogeneous $NO_3$ decay on the vessel wall with regeneration of $NO_2$. With this reaction mechanism, kinetic parameters can be obtained from the mass-balance of every component. The rate constant of the $NO_2-O_3$ reaction appears to agree reasonably well with literature values.

The influence of R.H. results in an increase of the stoichiometry caused by $N_2O_5$ hydrolysis. The kinetics of the $NO_2-O_3$ reaction remains unchanged. The kinetics of the $N_2O_5$ hydrolysis can be described with its pseudo-first-order rate constant. This rate constant is not directly proportional to the R.H., which is an indication that the $N_2O_5$ hydrolysis -at least in part- occurs heterogeneously at the wall of the reaction vessel.

In the atmosphere, aerosol particles are involved in these heterogeneous processes. Before studying the $NO_2-O_3$-aerosol chemistry, the dynamical behaviour of aerosol particles in the reaction vessels is considered. The results are given in chapter 5. The differences in the particle number concentration and in the particle size distribution of the feed and steady state aerosol have been measured. It appears that these differences are caused by coagulation and wall deposition processes.

The influence of aerosol particles on the $NO_2-O_3$ chemistry is the subject of chapter 6. 'Dry' aerosol (NaCl; R.H.=15%) and 'wet' aerosol (MgCl$_2$; R.H.=78%) are distinguished. In case of a 'dry' aerosol a small decrease in the stoichiometry is observed. This can be interpreted as a $NO_3$ decay on the aerosol surface. In case of 'wet' aerosol $NO_3$ decay as well as $N_2O_5$

hydrolysis is important. This follows from the nearly constant stoichio-metry and the nitrate formation in the aerosol.

The kinetics of the $NO_2$-$O_3$ reaction do not change in the presence of aerosol particles. Moreover, the rate constants of the heterogeneous reactions can be obtained. From these the so-called 'accommodation coefficient' can be deduced. This coefficient indicates what part of the gas-aerosol collisions really leads to reaction and characterizes the rate of the heterogeneous reaction. The heterogeneous $N_2O_5$ hydrolysis can also be understood as a bulk aqueous phase process. The product of Henry's law constant and the rate constant of the aqueous phase hydrolysis can be found. It appears that for $N_2O_5$ this product is in fairly good agreement with the product for $N_2O_3$ and $N_2O_4$.

In chapter 7 the aqueous phase chemistry of $NO_2$ and $O_3$ is considered. It is investigated using a gas-liquid contact reactor and analysis of the nitrite and nitrate formation. The results of the interaction between $NO_2$ and liquid water are in agreement with the current literature. The influence of $O_3$ is restricted to the oxidation of nitrite. From the results it can be deduced that aqueous phase $NO_2$-$O_3$ reactions do not significantly contribute to atmospheric nitrate formation.

Finally, a general evaluation is given in chapter 8. It can be concluded that this investigation confirms the present insights in the atmospheric chemistry of $NO_2$ and $O_3$ and that new insights in the reactivity of $NO_3$ and $N_2O_5$ are obtained.

**SAMENVATTING**

In dit proefschrift wordt een laboratorium onderzoek naar de atmosferische chemie van $NO_2$-$O_3$ systemen beschreven. Kennis van dit systeem is van groot belang voor een beter begrip van tal van luchtverontreinigingsproblemen met name dat van de zure depositie.

In hoofdstuk 1 wordt een kort overzicht gegeven van de atmosferische chemie, waarbij wordt ingegaan op de vorming van oxidantia, de $SO_2$ chemie en de $NO_x$ chemie.

Duidelijk wordt dat, in afwezigheid van licht, interacties tussen $NO_2$ en $O_3$ kunnen leiden tot de vorming van salpeterzuur. Bij de oxidatie van $NO_2$ door $O_3$ vormt zich het $NO_3$ radicaal. Dit radicaal kan op een aantal manieren verder reageren onder meer met $NO_2$, waarbij het salpeterzuuranhydride $N_2O_5$ wordt gevormd. De feitelijke vorming van $HNO_3$ is de hydrolyse van $N_2O_5$. In theorie kan dit proces wezenlijk bijdragen tot salpeterzuurvorming in de atmosfeer. Kennislacunes die opgevuld moeten worden, zijn met name het mechanisme en de kinetiek van de $N_2O_5$ hydrolyse en de reactiviteit van $NO_3$.

Hoofdstuk 2 geeft een overzicht van de recente literatuur. Achtereenvolgens worden laboratorium-, veld- en model studies besproken. Zonder meer kan geconcludeerd worden dat de niet-fotochemische route voor nitraat vorming via het $NO_2$-$O_3$ systeem onderkend wordt als een relevant atmosfeer chemisch proces. De bovengenoemde kennislacunes worden bevestigd; dit blijkt onder meer uit de in het veld gemeten profielen van de $NO_3$ radicaal concentratie. Regelmatig wordt gesuggereerd dat heterogene verwijderingsprocessen voor $NO_3$ of $N_2O_5$ een rol spelen. De parameters die nodig zijn om dergelijke processen te kwantificeren ontbreken echter.

Na de algemene inleiding en de literatuurbespreking worden in hoofdstuk 3 de in dit onderzoek toegepaste experimentele methoden beschreven. De opbouw van de gebruikte laboratorium opstelling wordt gegeven. De

basisprincipes van de technieken voor de generatie en analyse van de reactanten worden opgesomd.

In de hoofdstukken 4 t/m 7 worden de resultaten besproken en bediscussieerd. Hoofdstuk 4 behandelt de resultaten van een studie naar de $NO_2$-$O_3$ chemie bij sub-ppm concentraties alsmede de invloed van de temperatuur en de relatieve vochtigheid (R.V.). De experimenten zijn uitgevoerd in een flow systeem met daarin opgenomen een glazen bolvormig reactievat uitgesloten van licht. De generatie en analyse van de reactanten vindt plaats met de standaard technieken voor meting en ijking van $NO_2$ en $O_3$.

Beschouwen we de stoechiometrie in het reactiesysteem bij R.V. < 0,1%, dan blijkt dat deze afwijkt van de theoretische waarde van twee. Dit wijst op een nevenreactie die $NO_2$ terugvormt, extra $O_3$ afbreekt of beide. Daar de stoechiometrie significant verschilt in reactievaten van verschillende grootte (overige variabelen constant) is er sprake van een wandreactie. Verdere analyse van de resultaten gecombineerd met literatuurgegevens resulteert in de interpretatie dat de lage stoechiometrie veroorzaakt wordt door een heterogene afbraak van $NO_3$ aan de wand van het reactievat, waarbij $NO_2$ wordt teruggevormd. Gegeven dit mechanisme kunnen kinetische gegevens verkregen worden uitgaande van de massabalans voor iedere component. De reactiesnelheidsconstante van de $NO_2$-$O_3$ reactie en haar temperatuurafhankelijkheid blijkt redelijk overeen te komen met literatuur gegevens.

De invloed van de R.V. krijgt gestalte in een verhoging van de stoechiometrie als gevolg van de $N_2O_5$ hydrolyse. De kinetiek van de $NO_2$-$O_3$ reactie blijft onveranderd, die van de $N_2O_5$ hydrolyse kan beschreven worden met de pseudo-eerste-orde reactiesnelheidsconstante. Deze blijkt niet rechtevenredig met de R.V., hetgeen een indicatie is dat de $N_2O_5$ hydrolyse - althans gedeeltelijk - heterogeen aan de wand plaatsvindt.

In de atmosfeer zijn bij dergelijke heterogene processen aerosol deeltjes betrokken. Alvorens de $NO_2$-$O_3$-aerosol chemie te onderzoeken is aandacht besteed aan het dynamisch gedrag van aerosol deeltjes in het reactievat. De uitkomsten zijn weergegeven in hoofdstuk 5. De verschillen in de deeltjesaantalconcentratie en in de deeltjesgrootteverdeling van het aerosol voor en na het reactievat zijn gemeten. Het blijkt dat deze verschillen veroorzaakt worden door coagulatie en wandverliezen ten gevolge van diffusie en electrostatische depositie.

De invloed van de aerosol deeltjes op de $NO_2$-$O_3$ chemie wordt beschouwd in hoofdstuk 6. Er is onderscheid gemaakt tussen 'droog' aerosol (NaCl; R.V.=15%) en 'nat' aerosol ($MgCl_2$; R.V.=78%). In geval van een 'droog' aerosol wordt een kleine afname van de stoechiometrie waargenomen, mits voldoende oppervlak aanwezig. Dit kan worden geïnterpreteerd als een $NO_3$ afbraak aan het aerosol oppervlak. Bij 'nat' aerosol is behalve $NO_3$ afbraak ook de $N_2O_5$ hydrolyse van belang. Dit blijkt uit de stoechiometrie die vrijwel constant blijft en uit de nitraat vorming in het aerosol.

De kinetiek van de $NO_2$-$O_3$ reactie verandert niet ten gevolge van de aanwezigheid van aerosol deeltjes. Verder worden reactiesnelheidsconstanten van de heterogene reacties aan het aerosol bepaald. Hieruit kan de zogenaamde 'accommodatie coëfficiënt' worden gehaald. Deze coëfficiënt geeft aan welk gedeelte van de gas-aerosol botsingen daadwerkelijk tot reactie leidt en karakteriseert daarmee de snelheid van de heterogene reactie. De heterogene $N_2O_5$ hydrolyse kan ook opgevat worden als een bulk waterfase proces. In dat geval kan het product van de Henry constante en de reactiesnelheidsconstante voor de waterfase hydrolyse bepaald worden. Het blijkt dat dit product voor $N_2O_5$ nagenoeg overeenkomt met die van $N_2O_3$ en $N_2O_4$.

In hoofdstuk 7 is de waterfase chemie van $NO_2$ en $O_3$ aan de orde. Deze wordt onderzocht met behulp van een gas-vloeistof contact reactor en analyse van de nitriet en nitraat vorming. De resultaten van de interactie van $NO_2$ met vloeibaar water is in overeenstemming met de literatuur. De invloed van $O_3$ beperkt zich tot de oxidatie van nitriet. Uit de resultaten kan afgeleid worden dat waterfase $NO_2$-$O_3$ interacties geen significante bijdrage leveren tot de nitraat vorming in de atmosfeer.

Het proefschrift wordt afgesloten met een algemene evaluatie in hoofdstuk 8. Geconcludeerd wordt dat dit onderzoek de huidige inzichten in de atmosferische chemie van $NO_2$-$O_3$ bevestigt en dat nieuwe inzichten in de reactiviteit van $NO_3$ en $N_2O_5$ zijn verkregen.

**CURRICULUM VITAE**

Pieter Verhees werd geboren op 19 december 1958 te Helmond. Hij bezocht het Dr. Knippenbergcollege aldaar en behaalde het diploma Atheneum B in juni 1977. In datzelfde jaar begon hij met de studie van de Scheikunde aan de Rijksuniversiteit te Utrecht. Op 30 juni 1980 behaalde hij het kan-didaatsexamen en op 1 november 1982 het doctoraalexamen met als hoofdvak Anorganische Chemie en als bijvak de Fysische- en Colloïdchemie.

Van 1 november 1982 tot 30 juni 1986 werd hij door de Stichting Technische Wetenschappen in staat gesteld om bij de Vakgroep Luchthygiëne en -verontreiniging van de Landbouw Hogeschool te Wageningen het onderzoek, beschreven in dit proefschrift, uit te voeren. Vanaf 1 september 1986 is hij als wetenschappelijk medewerker in dienst van de N.V. Philips te Eindhoven.

Pieter Verhees was born on 19 December 1958 in Helmond, where he attended the Dr. Knippenbergcollege. He obtained his Atheneum B certificate in June 1977. In that year he started his chemistry study at the State University of Utrecht. On 30 June 1980 he obtained his B.A. examination and on 1 November 1982 his Masters degree with majors in Inorganic, Physical and Colloid Chemistry.

From 1 November 1982 to 30 June 1986, the dutch Technology Foundation enabled him to perform the investigation described in this thesis at the Department of Air Pollution of the Agricultural University Wageningen. Since 1 September 1986, he is employed at N.V. Philips Eindhoven.